Development of Electroactive Polymers and Its Applications

Zhang, Yiyang

(Degree)
博士（工学）

(Date of Degree)
2018-03-25

(Date of Publication)
2019-03-01

(Resource Type)
doctoral thesis

(Report Number)
甲第7205号

(URL)
https://hdl.handle.net/20.500.14094/D1007205

Doctor Thesis

Development of Electroactive Polymers and Its Applications
電気活性ポリマーの開発及び応用

2018.1

Graduate School of System Informatics, Kobe University

Yiyang Zhang

張　亦暘

Abstract

Electroactive polymers, or EAPs, are the polymers which can change their shapes under applied electric field. The most common applications of this material are in actuators, sensors, and generator. Dielectric elastomers (DE), as an artificial muscle with the highest potential, are attracting attentions for its large strain, fast response, light weight, low modulus, reliability and high energy density, which have been widely employed in biomimetics and micro-robotics.

In spite of the advantages of dielectric elastomers, some main technical issues must be solved before applying to extensive fields. We focused on balancing the permittivity and modulus to improve the electrostriction properties of the material, and a method to control the modulus of composite was indicated to design the polymer. High permittivity ceramic particles calcium copper titanate(CCTO) were introduced as fillers to the polymer matrix, and modifications to the surface of CCTO have been carried out.

A Polyaniline (PANI) / styrene-ethylene-butylene-styrene block polymer (SEBS) conductive elastomer was developed for the electrodes of dielectric elastomer actuator. The materials showed a high conductivity at the large strain with a stabilized signal output. The conductive elastomer was combined with the prepared dielectric elastomer to fabricate a capacitive strain sensor and proved a promising material for flexible

sensors.

We synthesized high permittivity particle calcium copper titanate (CCTO) via a thermal treatment method and flux method. Silicone elastomer filled with CCTO was employed to fabricate high dielectric constant DE. Aggregation of particles was observed while increasing the filling amount of CCTO. By modifying the surface of CCTO with polymer, the particles will disperse better in elastomer matrix, which leads to a lower modulus. Core-shell structured calcium copper titanate@polyaniline (CCTO@PANI) was synthesized using a simple procedure involving in-situ polymerization of aniline in aqueous hydrochloric acid solution. The silicone elastomer (PDMS) filled with self-prepared CCTO@PANI composites had high dielectric constant, low dielectric loss, and actuated strains which was greatly improved at low electric field. Meanwhile, the elastic modulus of CCTO@PANI/PDMS composites was increased slightly only with a good flexibility. Compared to pure silicone elastomer (8.94%), the CCTO/PDMS and CCTO@PANI/PDMS (The weight ratio of CCTO and aniline was 10) composites exhibited a greater actuated strain of 10.95 % and 13.24 % at a low electric field and filling content of 10 V/μm, respectively.

The permittivity of composites would greatly increase near percolation threshold. Polyaniline (PANI) is a kind of typical conductive polymers and can be used as fillers to

synthesis conductive polymer. Compared to inorganic fillers, PANI have better compatibility with organic matrix and less modulus so the composite would not lose flexibility. We synthesized a dielectric elastomer using organic soluble PANI and PDMS through solution blending method.

The electrode is a main issue that limits the performance of DEs. Carbon grease will become unreliable due to the solvent evaporation, causing increasing resistance after stretched. Conductive polymer can be used as electrode, but CNT based conductive polymer usually can only endure a strain of 5%. Thus we prepared a conductive elastomer using PANI and SEBS via solution blending method. This is the first conductive elastomer that can maintain conductivity while elongated to 600% strain in the world. The conductivity of this material was 8.0 S/m, and elongation could reach 600% with a tensile strength of 15MPa. Within 0-100% elongation range, the material's resistance showed linear increasing, and could be applied as a large-scale strain sensor.

We realized that the dielectric elastomers could also be applied as dielectric layers of capacitance sensors. By combining CCTO/SEBS with PANI/SEBS with a thermoforming process, we manufactured a capacitance strain sensor, which have stabilized capacitance variety range at different conditions with high durability. A capacitive stretchable strain sensor with easy process and low cost was finally designed.

Contents

Chapter 1 Introduction

1.1 Dielectric elastomers

An actuator is a component of a machine that transforms inputting energy into mechanical movement and is responsible for moving or controlling a mechanism or system[1]. Artificial muscles are a type of actuator simulated animal muscles. Traditional artificial muscles including piezoelectric type, hydraulic type, pneumatic type and shape memory alloys, have a complicated mechanism in transforming energy at low power and small deformation range. Since a lot of problems on size, weight, shape and response time need to be solved, the researchers committed to looking for new replacement materials applied for micro robots[2], portable devices, flexible electronic equipment[3,4].

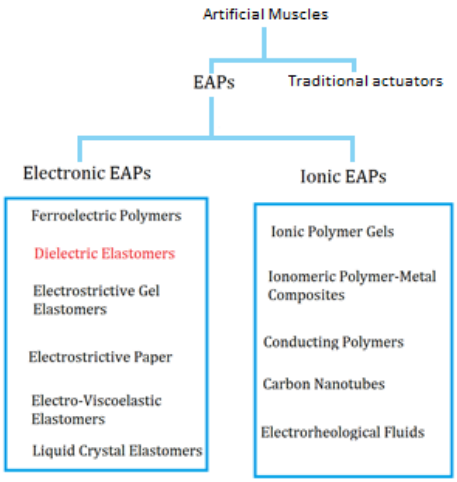

Fig. 1-1 Classification of EAPs

Electrically Activated Polymers (EAPs), as new type of flexible actuator, are being applied to electromechanical actuating and sensing fields. Among which, dielectric elastomers (DEs), as shown in Fig. 1-1, are new rising material as energy harvester and actuating material[5-8]. They are attracting attentions for the large strain, fast response, light weight, low modulus, reliability and high energy density [9-14]. As an electroactive polymer with the highest potential, DEs have been widely employed in artificial muscles, biomimetics, and micro-robotics as actuators, sensors, and generators [15-22].

1.1.1 Dielectric elastomer actuators

Dielectric elastomer actuators (DEAs) have caused great concern since R.Pelrine et.al reported their work in 1998[23]. DEAs are formed of a membrane of DE sandwiched between two flexible electrodes. Applied with voltage on the electrodes, the DEA will receive the electric field pressure from surface electrostatics, “Maxwell pressure” [24]. Due to the incompressible property of robber, the DE membrane will horizontally expand under Maxwell pressure. Normally, the dielectric membrane is made of silicones or acrylics, and electrodes are made of carbon powder/grease or metallic paint [25].

Dielectric elastomers are the most promising technology in soft actuators [26-28]. They have a simple structure as shown in Fig. 1-2. The closely contacted electrodes are able

to synchronously stretch or contract. As voltage is applied, membrane is stretched and electrical energy is transformed into mechanical energy. When the voltage is off, the membrane resumes former shape. Dielectric elastomer can also work in an opposite direction as sensors, transforming mechanical energy into electrical signal.

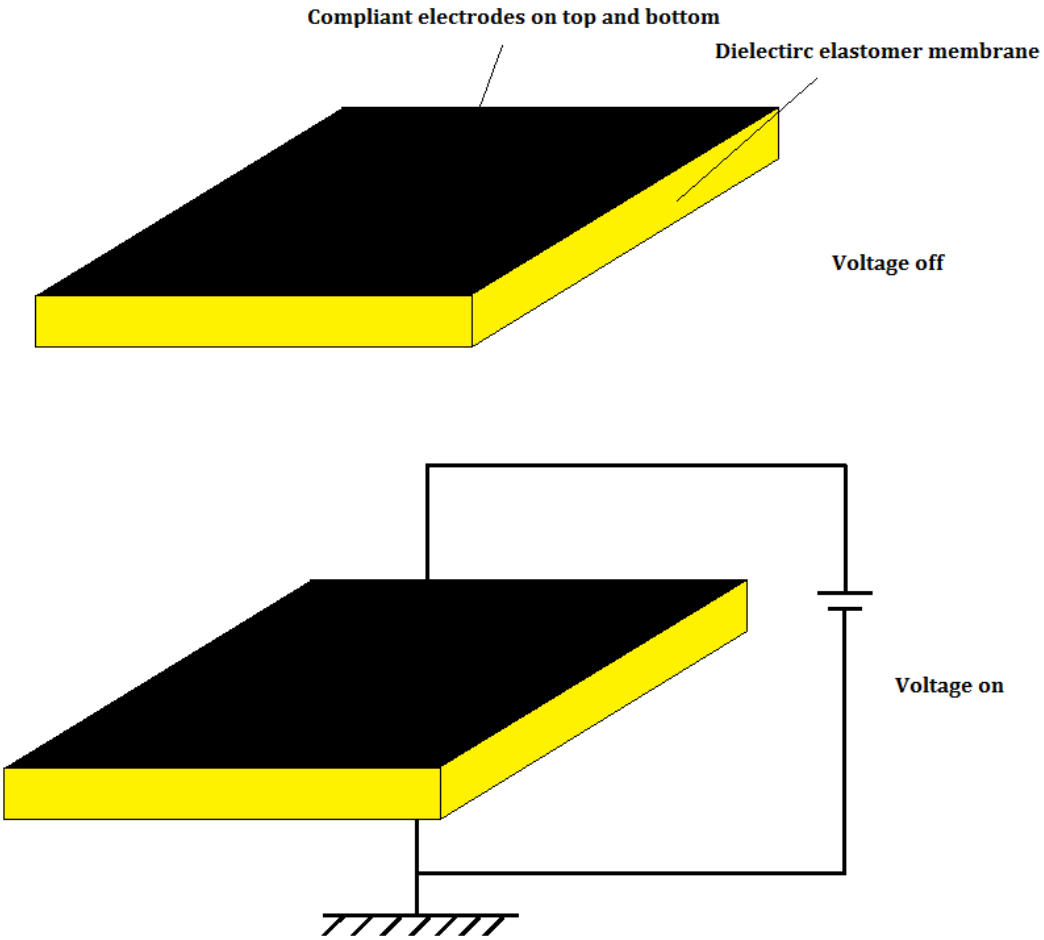

Fig. 1-2 Schematic diagram of dielectric elastomer's electrostrictive strain

In actuating mode, the sandwich structure is working as a variable capacitance, and usually drove by a high voltage of 500V to 10kV. The electric charge is accumulated on the electrode and electrostatic charge caused the Maxwell pressure, which can be

approximated by:

$$p = \varepsilon_0 \varepsilon_r E^2$$

Where P is Maxwell pressure on the material; ε_0 is the vacuum permittivity (8.854pF/m); ε_r is the relative permittivity. For small strain, the young's modulus of elastomer remains constant, and the vertical deformation S_z could be expressed as:

$$S_z = -\frac{p}{Y} = -\frac{\varepsilon_0 \varepsilon_r E^2}{Y}$$

It is obvious that the electrostriction of dielectric elastomer depends on ratio of ε_r /Y, which means the actuating strains are proportional to the relative permittivity of material and inversely proportional to the young's modulus. Therefore, the key to improve the actuating properties of dielectric elastomer is to increase the relative permittivity while reduce young's modulus to a certain level. A lot of researches have been carried out around this subject recently.

1.1.2 Preparing process of dielectric elastomers

Since the pioneering work has been reported by R.Pelrine et.al, many researchers have made effects to probe the application of DEs [23]. Early studies have been carried on about elastomer matrix and curing agents, and methods of improving electromechanical response of DEs through pre-stretch have been reported [29-31]. According to Li's work, pre-stretch can even stabilize the DE's actuating behavior while

increasing the breakdown voltage of DEs [32]. Suo developed a theory about DE's actuating principle and studied the unstable mechanism caused by breakdown of DEs at high voltage [33-37]. Furthermore, they also developed an energy harvesting system made of DEs which utilized the opposite electrostriction mechanism.

In spite of the advantages of dielectric elastomers, some main technical issues must be resolved before applying to extensive fields. The driving voltage of dielectric elastomer is a high voltage of 10-30 V/μm, and which restricted the application of DEs, especially in biologic and medical field. The actuating properties are depending on the comprehensive performance of DEs and researches have been focused on studies of DE matrix materials, filler particles of DE composites, and corresponding composite and modifying methods.

Some papers reported that using a small amount of carbon nanotube (CNT) as the filler of DEs[38] could increase the permittivity of DEs significantly, while the elastic modulus's increasing was not obvious thus these materials have a high electromechanical response[39,40]. The permittivity of composite will increase greatly near percolation threshold, that's why DEs using CNT fillers can achieve a high permittivity with a small filling amount. A challenge of this kind of DEs is the aggregation of CNTs in the system due to Van der Waals forces. A lot of works have be

carried on to improve the dispersion of CNTs such as ultrasonic treatments and functionalization of CNT. However, there is still a critical problem about the CNT-based DEs that is the low breakdown voltage of the materials. Some of the materials even have a lower breakdown voltage than driving voltage [41].

The common methods to overcome the disadvantages of DEs are to fill the material with high dielectric constant particles. Zhang's group controlled the dielectric properties of DEs through various methods such as cross-linking density adjustment, introducing plasticizer, grafting short chain groups in matrix, and obtained DEs could generate large strain in a relatively low electric field[42-44]. Some researchers studied the effect of filling high permittivity particles into DEs to improve the dielectric constant of composites[45-47]. Dang's team studied the process of composites of $BaTiO_3$, carbon black and silicone, they mitigated the impact of modulus increasing caused by $BaTiO_3$[48,49]. F.Carpi et. al used TiO2 as filler, and enhanced the permittivity of DE while the modulus of material increased slightly[50-52]. Nuchmapa's group prepared a natural rubber/ Al_2O_3 composite which can perform an obvious bending in a electric field of 200V/mm[53]. However, the massive use of fillers will result in various adverse effects. For example, filling high dielectric constant particles like $BaTiO_3$ will improve the dielectric constant of system greatly, but the young's modulus will increase

simultaneously which affected electrostriction properties [54-56]. The filling amount of high permittivity particles must be limited to maintain a low modulus.

1.1.3 Application of dielectric elastomers

Currently, the studies about structures of DEs have aroused general concern, and the applications are mainly planar actuators based on huge planar electroactive expansion. Besides, some common applications are actuators designed according to the thickness changes of DEs, and some have specialized structures using pre-stretch process to store energy.

There is no doubt that DEs have notable planar strains, but they are not the most suitable for the bionic devices and artificial muscles applications. The movements of muscles usually involve linear stretch and planar shape changing with high degrees of freedom. Besides, the pre-stretch process needed the DEs to be fixed on the frames and which made the independence structure of DEAs very difficult. Thus, the main issues about DEA's applications are transforming planar expansion into actuation strains with expected action.

Dubowsky.S et.al reported a solution with the robot arm they designed in 2006[57]. Every single unit are made of a linear stable component with only one expansion direction allowed, which transformed planar expansion into linear extension. When the

horizontal expansion generated enough force, the whole device will be trigger into stretching mode. Lochmatter.P et al. proposed a shell bending actuator through combining DEA with mechanical structure [58]. As the DE side is stimulated, a bending of the system could be observed.

Stacking DEs is another proposed design of DEA. A vertical contractible actuator stacking DEAs was designed to enhance the thickness changes. G.Kovacs et al published a cylinder device made of VHB acrylics from 3M Company [59]. Every layer was divided by electrodes connected to alternately positive and negative power supply. This device showed a 30% decreased length after applied voltage. F.Carpi et.al made stacked DEA using folding and spiral structures [60], both devices showed more convenience manufacturing process of stacked DEAs.

G.Kofod et.al proposed an approach called self-organization and energy minimization for creating complex structures with embedded actuation in planar manufacturing steps[61]. This device used stored energy generated by pre-stretch like a spiral torsion spring. In relaxation mode, they bend to seek the energy minimized condition, and stretch to planar mode when electrically stimulated. This design can generate a considerable output power and perform a preset action.

1.2 Flexible electrodes materials

DEAs need flexible electrodes [62] to hold the static charge applying electrostatic pressure, and maintain conductivity during stretched in order to let the charges evenly distributed on the electrodes. An ignorable stiffness is also needed to ensure they are not obstructing deformations. Carbon grease [11], graphite and carbon powders, serrated metal electrodes[10], corrugated metal electrodes[63], electrolyte solution[64] are reported to be suitable options.

Carbon greases are the most common flexible conductive material. They are made of carbon black particles dispersing in grease. Carbon greases have excellent conductivity even in a large strain, and are easy to apply to the surface of polymers for its conglutination, with a minimized effect on electrostriction properties of DEs.

The main problem about these electrode materials is their durability, which made them vulnerable to strains after a short time. Conductive elastomers can be also applied as electrodes of DEs. Generally, they were synthesized by adding conductive materials, especially carbon-based materials, into polymer matrix. However, the conductive polymers achieved by this method suffer a short strain range and long responding time normally[65]. Polyanilines (PANIs)[66], as typical conductive polymers, are drawing great attention for their conductivity, easy preparation and low cost. PANIs were also used as

fillers to synthesis conductive elastomer composites using the mechanical blending method[67-69], but the large strain range and stable conductivity could not be achieved simultaneously.

1.3 Stretchable strain sensors

Another application of dielectric elastomers are materials for strain sensors, which could be applied as soft robots, wearable devices, movements monitoring and virtual reality technologies due to its durability, linear sensing and rapid response [70-74]. Among which, the stretchable strain sensors are drawing attention for their ability of outputting signal while large strain [75,76]. The stretchable strain sensors could be divided into resistance sensors and capacitive sensors by the sensing mechanism. The resistance sensors are usually fabricated by polymers filled with conductive fillers. The resistance changes during the stretch are decided by both the micro structural deformation and the function between strain and resistance [77].

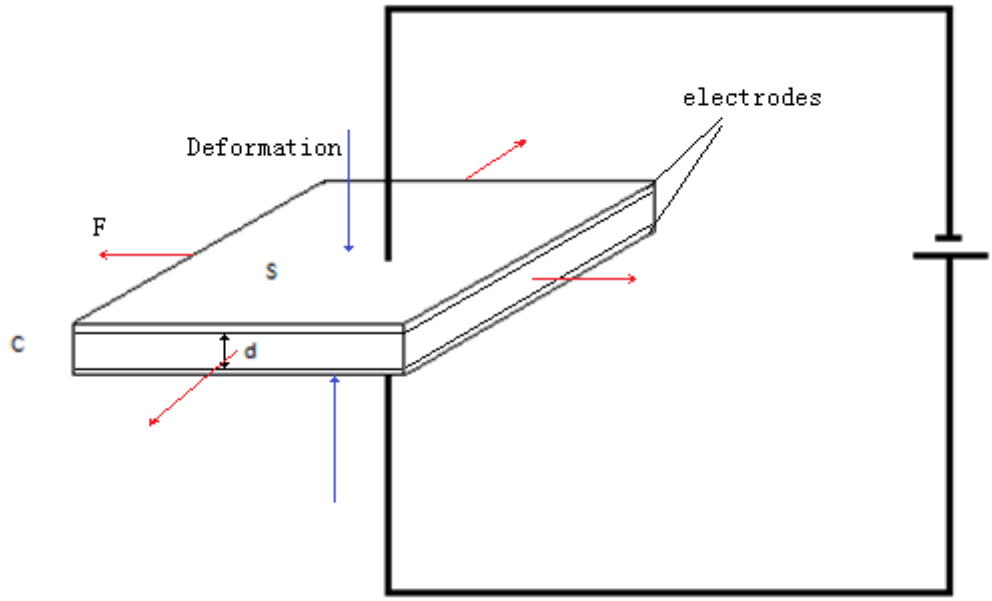

Fig.1-3 Schematic diagram of capacitive strain sensors

Capacitive strain sensors were formed with a dielectric layer sandwiched between a pair of stretchable electrodes (Fig.1-3), the capacitance change are determined by the permittivity and thickness of dielectric layer [70, 78, 79].

As the definition formula of capacitor, we have:

$$C=Q/U$$

Where C is the capacitance, Q is electric charge, and U is potential difference. The capacitance of a certain capacitor could be calculated by:

$$C = \frac{\varepsilon S}{d}$$

Where ε is the permittivity of dielectric layer, S is is the area of electrodes, d is the distance between two electrodes. As the shape of capacitor changes, the S and d will

change, capacitance will also change with strain, the capacitor will start to charge or discharge, current will flow in the circuit, then we have a signal output. For ideal elastomer, the volume of capacitance do not change, so we have $\Delta S \Delta d = 1$, then the capacitance change can be described as a function of strain.

Compared with resistance sensors, the capacitive strain sensors showed linear relationship between strain and capacitance, with fine hysteresis properties [80, 81].

The problem of existing stretchable strain sensors designed for large strains is the electrodes (for capacitive type) or conductive filler (for resistance type) is prepared by long-chain CNTs. The employing of CNTs made the cost of these materials raised to a very high level. If we switch the filler to organic conductive material PANI we can get a highly dispersed all-organic conductive composite, with high elongation at break and low cost.

1.4 Research purposes

Dielectric elastomers, as the core component of artificial muscles, designers are aiming composites with high ε/Y ratio. However, higher permittivity means larger filling amount of particles, which lead to higher modulus. Thus, the focus of researches nowadays becomes balancing the permittivity and modulus, but there are some issues still existing: (1) Large filling amount of ceramic particles will increase modulus,

limiting the electrostriction property of DEA; (2) Conductive fillers such as CNT and graphene can enhance the permittivity of composites obviously but they lead to a low breakdown voltage and high processing difficulty; (3) Using flexible polar materials as fillers to improve the dielectric property of DEs have no significant effect; (4) The problems about flexible electrodes of DEAs remained unsolved which limited the application of DEAs. Regarding on the issues mentioned, following aspects are studied in this paper:

(1) In order to understand the relation between structure and properties of materials, we need to analyze the morphology of particles mixed in silicone matrix. We designed a experiment to fill the silicone elastomer with different CCTO particles and discussed the effect of phase stated of filling particles.

(2) Since the employ of high permittivity particles will increase the modulus of composites, filling amount must be limited. Surface modification with organic materials could improve the compatibility of inorganic particles and organic matrix. To solve this problem, we synthesized core-shell structured calcium copper titanate@polyaniline (CCTO@PANI) using a simple procedure involving in-situ polymerization of aniline in aqueous hydrochloric acid solution.

(3) As a result of greatly enhanced permittivity near critical percolation

concentration, dielectric materials could be prepared by filling very small amount of conductive materials. A dielectric elastomer has been synthesized using organic soluble PANI and PDMS through solution blending method.

(4) The electrode is a main issue that limits the performance of DEs. Carbon grease will become unreliable for the solvent evaporation, causing increasing resistance after stretched. Conductive polymer can be applied as electrode, but CNT based conductive polymer usually very expensive. Thus we prepared a conductive elastomer using polyaniline (PANI) and styrene-ethylene-butylene- styrene block polymer (SEBS) via solution blending method.

(5) The dielectric elastomer could also be applied as dielectric layers of capacitance sensors. Since the existing capacitance strain sensors are employing long-chain CNT based materials, the cost are very high. By combining CCTO/SEBS with PANI/SEBS with a thermoforming process, we manufactured a new kind of capacitance strain sensor. The sensors have stabilized capacitance variety range at different conditions with high reproducibility and low cost.

1.5 Composition of the paper

The structure of this paper is as follows

Chapter 2 stated the basic knowledges about dielectric materials, polarization and

conductive materials.

In Chapter 3, we stated the designing and fabrication of PDMS based dielectric elastomer. The electrostrictive strain tests were also carried out.

In Chapter 4, a conductive elastomer using PANI and SEBS was prepared via solution blending method with both high conductivity and elasticity. Experiments about testing the electrostatic properties were carried out for the applications in sensors.

In Chapter 5, a capacitive strain sensor using CCTO/SEBS as dielectric layer and PAN/SEBS as electrodes was designed and manufactured by thermoforming process. The composite was showing promising properties for applications as stretchable strain sensors.

Chapter 6 is a summary of the paper and stated the conclusions.

Chapter.2 Basic knowledge

2.1 Dielectric materials

2.1.1 Dielectric

Dielectric property is the storing and dissipation ability of static energy of dielectric materials in electric fields. When applied with an electric field, electric charges cannot flow freely in the dielectric materials, for the dielectric materials are not conductive, but the bounded electric charges in the dielectric materials are displacing partially, causing the macro electrical behavior in the dielectric material. This phenomenon is called dielectric polarization [82].

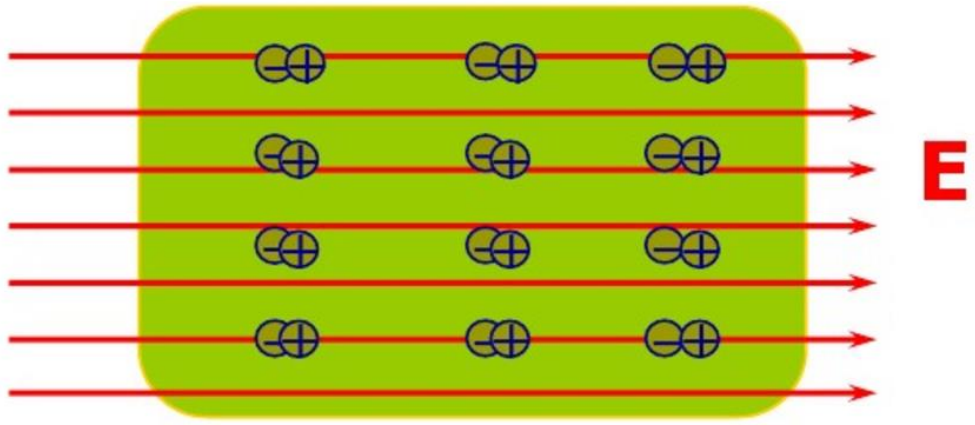

Fig. 2-1 Polarized dielectric material in an electric field

Because of dielectric polarization, positive charges are tends to displace towards the direction of electric fields, and negative charges for the opposite direction. This phenomenon created an inner electric field to weaken the electric field applied. If the

polar molecules of dielectric materials are connected with weak bounds, the molecules will also orient to align to the field[83].

2.1.2 Dielectric polarization

In dielectric model, materials are formed by atoms. The atoms are made up of two parts: surrounding electron clouds with negative charge and the nuclear with positive point charge at the center. When applied with electric field, the balance point was deviated from its former position, this phenomenon could be defined as dipole. A vector quantity, dipole moment, M, is used to characterize dipole. The relationship between the electric field E and M can be characterized by function F[84]

$$M=F(E)$$

Dipolar polarization is a polarization caused by polar molecules orientating in electric field. The polar molecules consist unbalanced which means, the charge center of positive charge and negative charge does not coincide, for example NH_4 or HCl. The gathering of these dipoles forms a dipolar polarization[84].

Ionic polarization is polarization caused by the deformation of electron cloud of positive and negative ions affecting each other in ionic compounds. In ionic compounds, the electron charges around one atom tend to be positive or negative. When these atoms were deviated from former position due to the vibrations of molecular, the charge

centers of the atoms were also displaced. As a result, the charge center of the molecular is also displaced, causing ionic polarization [84].

The dielectric property of a material is a collaborative effect of the above polarizations. For example the dielectric property of barium titanate is caused by the ionic polarization of Ti^{4+} and electron polarization of one O^{2-} molecular [85].

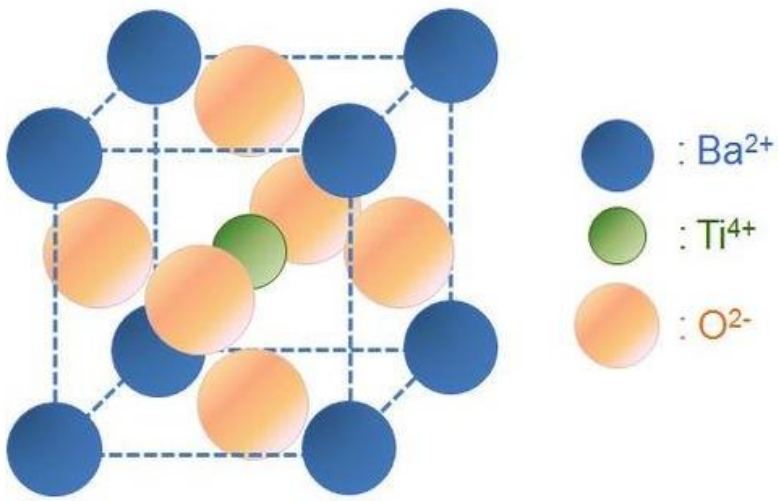

Figure 2-2 Structure of barium titanate

In our researches, we chose a ceramic particle with very high permittivity called CCTO as filler (Fig.2-3). The permittivity of CCTO could exceed 10^4 at room temperature (Fig.2-4).

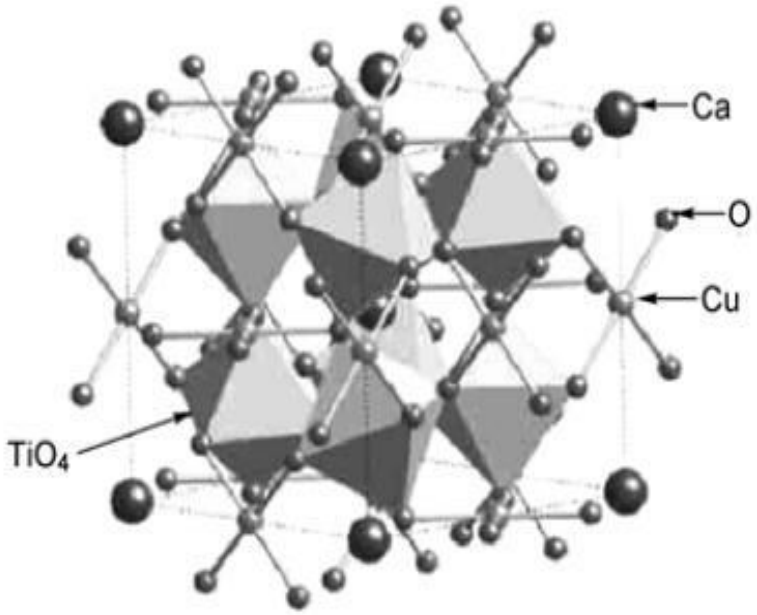

Fig.2-3 Crystal structure of CCTO[77]

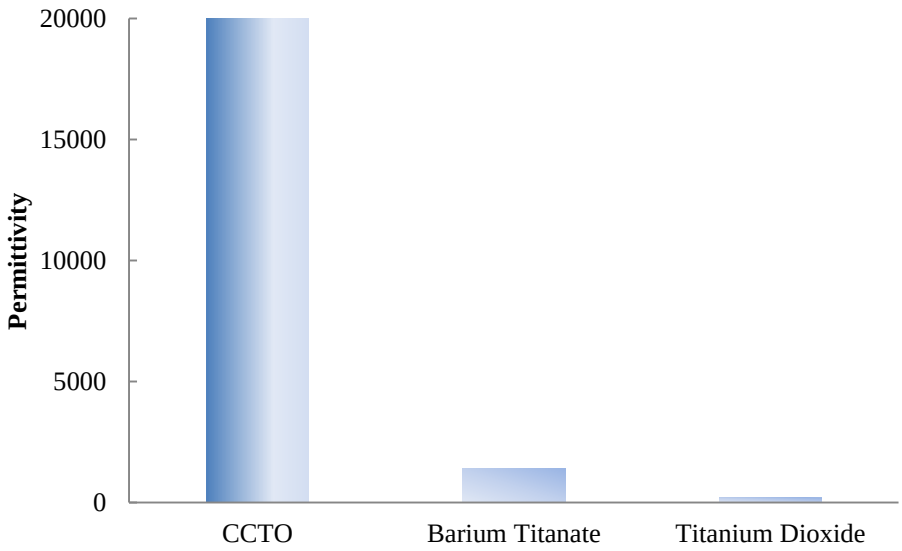

Fig.2-4 Permittivity of CCTO compared with $BaTiO_3$ and TiO_2

The CCTO shows a strong nonlinear relationship between voltage and current at room temperature and the breakdown voltages are 1525 and 775 V/cm for 2 kinds of CCTO samples. When the voltages exceed the breakdown values, the current values are beyond

the limit of the experimental setup (20mA) [86].

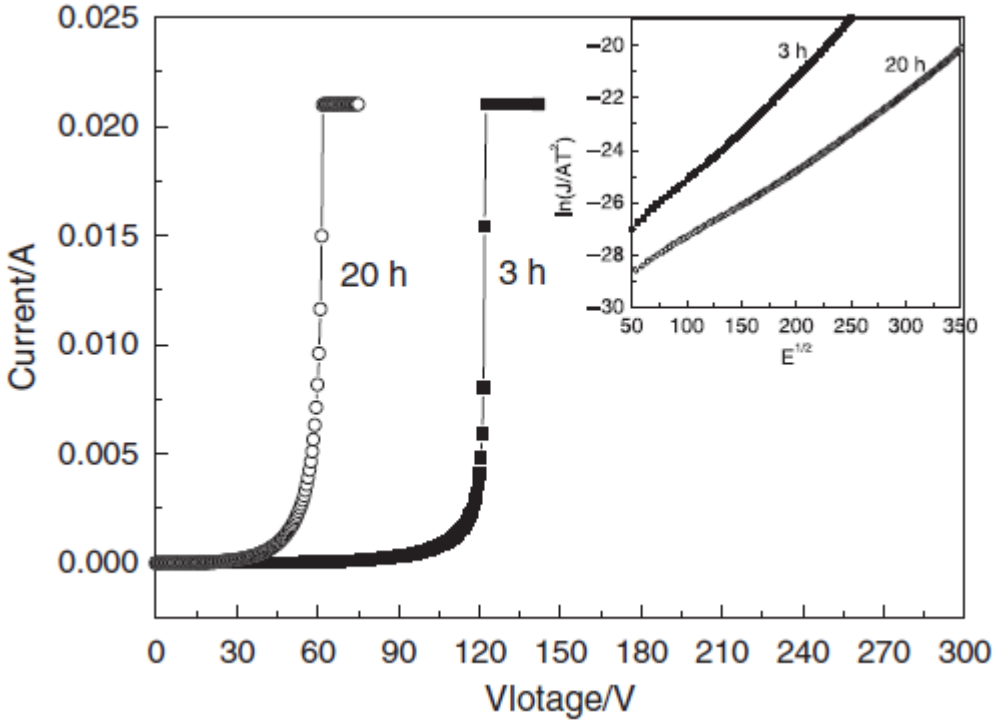

Fig.2-5 Plots of current versus voltage for the 3h and 20h sintered samples (at 1050°C).[86]

2.1.4 The matrix material of dielectric elastomers

In 1990s and early 21st century, researcher test various elastomers that could be applied as dielectric elastomer actuator, including silicone rubber [87], polyurethane[88-91], thermoplastic materials[92,93] and acrylics[94]. Amongst these materials, VHB series acrylic elastomers produced by 3M Company seem to have the highest electrostriction strain. Its reported that the electrostriction strains of VHB4910 membranes have reached 380% under a high pre-stretch [95]. The VHB acrylics have a high energy density of 3.4

MJ/m^3, and a permittivity of about 4.2-4.7. However, these membranes are showing a very obvious viscoelastic property [96], and the glass transition temperature of which is about -20^oC[97]. Thus, the elasticity and tg need to be improved to be suitable for further application.

Silicone rubber showed another option for dielectric elastomer matrix [13]. They are showing less viscoelasticity [98] with a tg of -100^oC, which made them adapt to applications in higher frequency and lower temperature [99]. The silicon rubber's permittivity is 2.8 and they are able to achieve an electrostriction strain of 100% under pre-stretch [100], which is much less than VHB acrylics though.

2.2 Percolation theory

Percolation theory is the formation of long-range connectivity in random systems. Below the percolation threshold p_c, the matrix is formed with clusters of isolated nodes, continuous phase does not exist; while above it, the clusters of nodes will be connected to the whole network. The conductivity of composite material could be described by this model. When below p_c, the material shows no conductivity, above it, the material is conductive. [101]

For a regular matrix, we define two nodes is connected by bonds by probability p or not occupied by probability 1-p. We assume there is a percolation threshold, p_c, when

$p>p_c$, isolated nodes will be connected to the whole network. For the description of the electrical percolation, we assume the conductive component have a conductivity σ_m. And the dielectric component with conductivity σ_d as non-occupied bonds. [101] If the dielectric component is insulated material, we have σ_d =0. If the percolation threshold is approached from above:

$$\sigma_{dc}(p) \propto \sigma_m (p - p_c)^t$$

The exponent t is one of the two critical exponents for electrical percolation. Below p_c the material shows no conductivity [101]

The dielectric constant also shows a critical behavior near the percolation threshold[98].

$$\varepsilon(p) = \frac{\varepsilon_d}{|p - p_c|^s}$$

Where ε_d corresponds to non-occupied bonds. s is another one of the two critical exponents for electrical percolation. [101]

This phenomenon could be used to prepare electroactive polymer by filling small amount of conductive fillers.

2.3 Raw Materials

2.3.1 Base materials

Poly (dimethyl siloxane) (PDMS Fig.2-6-a) (RTV-3483) used as matrix in chapter 3 were purchased from Dow Corning Corporation. Aniline monomer (Fig.2-6-b) was

obtained from Sinopharm Chemical Reagent Co., Ltd. of China. SEBS (YH501T,Fig.2-7) used as matrix in chapter 4 and 5 was provided by China Petroleum & Chemical Corporation of Baling Company.

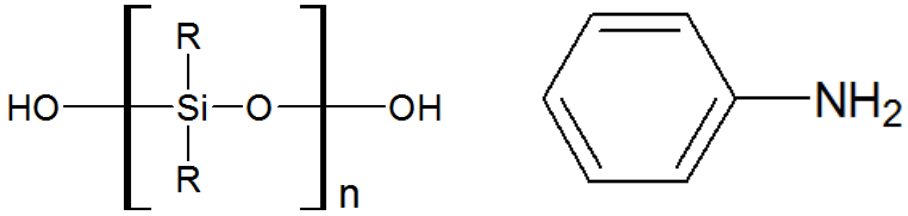

a **b**

Fig.2-6 Structure of PDMS(a) and aniline (b)

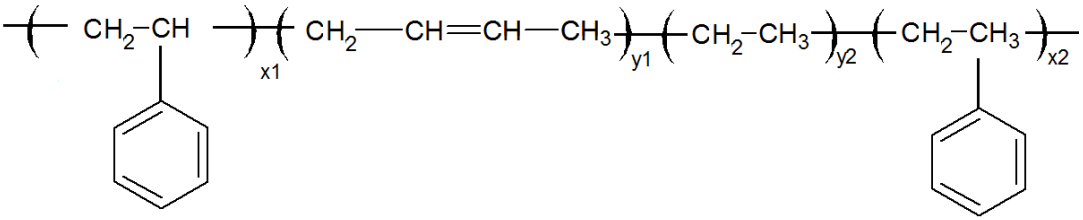

Fig.2-7 Structure of SEBS

2.3.2 Initiator

Ammonium persulfate (APS Fig.2-8) used as initiator for PANI were obtained from Sinopharm Chemical Reagent Co., Ltd. of China.

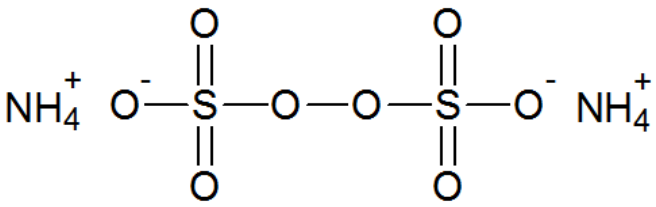

Fig.2-8 Structure of APS

2.3.3 Surface modifier

3-aminopropyltriethoxysilane(APTES fig.2-9-a) and polyvinylpyrrolidone(PVP 30 kDa,

fig.2-9-b), used to modify the surface of CCTO in chapter 2, were obtained from Sinopharm Chemical Reagent Co., Ltd. of China.

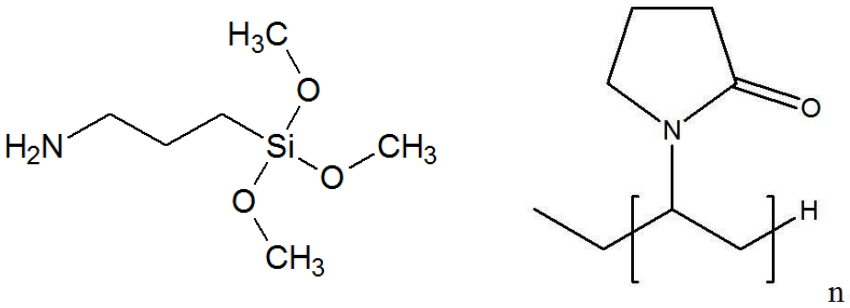

a **b**

Fig.2-9 Structure of APTES(a) and PVP(b)

2.3.4 Components with active hydrogen

We used hydrochloric acid (HCl) as active hydrogen component for PANI in chapter 3, and Dodecyl benzenesulfonic acid (DBSA Fig.2-10) in chapter 4 and 5.

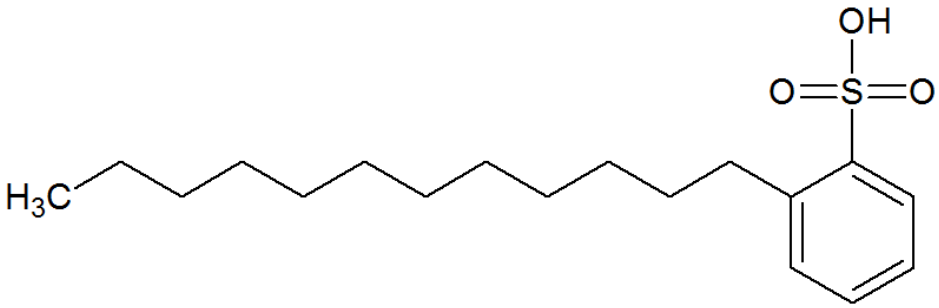

Fig.2-10 Sturcture of DBSA

2.3.5 Filling material

4 kinds of CCTO with different particle size was used as inorganic fillers.

300nm	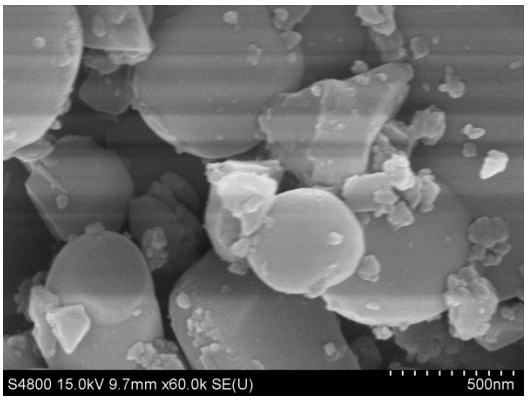

1μm	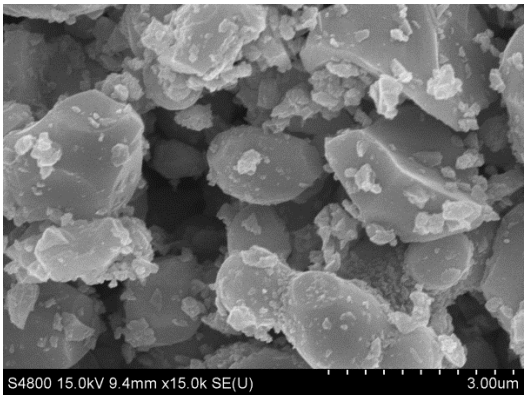
10μm	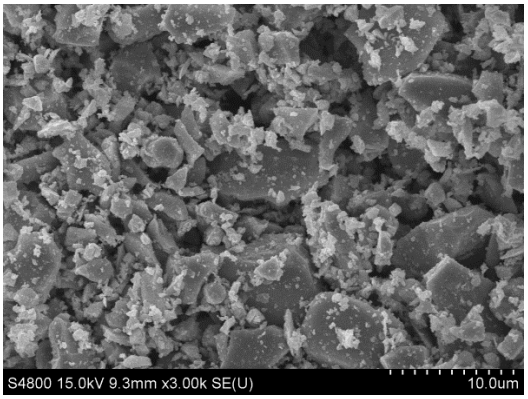
60μm	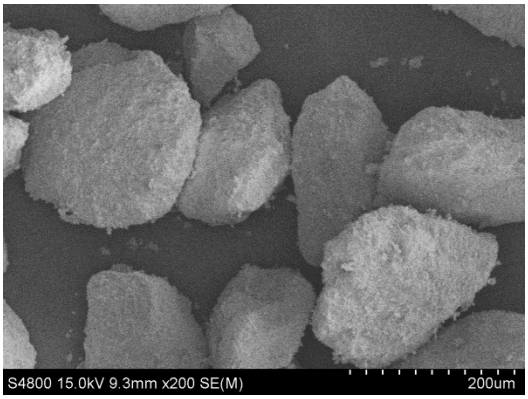
Jiangsu WuXi Kai-Star Electro-optic Materials Co.,Ltd, China	

Chapter.3 Development and characterizing of PDMS based dielectric elastomers

3.1 Introduction

Dielectric elastomers (DE) are attracting attentions for its large strain, fast response, light weight, low modulus, reliability and high energy density [102,103]. As an electroactive polymer with the highest potential, DEs have been widely employed in artificial muscles, biomimetics, and micro-robotics as actuator, sensor, and generator [10,28,104].

Dielectric elastomer actuator (DEA) is formed of a membrane of DE sandwiched between two flexible electrodes. Applied with voltage on the electrodes, the DEA will strain due to the electric field pressure from surface electrostatics, “Maxwell pressure”, the thickness strain of a DEA can be approximated by:

$$Sz = -P/Y = -\varepsilon_0 \varepsilon_r E^2/Y \quad (1)$$

Where P is Maxwell pressure on the material, Y is Young’s modulus, ε_0 is the vacuum permittivity, ε_r is the relative permittivity.

Researchers have been working on improving the dielectric property of DEs. Z.G. Suo proposed a theory coupled large deformation and electric potential, and described nonlinear and nonequilibrium behavior of DEs [51]. Filling silicone with TiO2 particles

can improve the permittivity of material with lower Young's modulus have been reported by several groups [70,105]. D. Yang etc. fabricated a DE with high dielectric strain by filling various types of TiO2 and they also found that the size of TiO2 particles influenced the dielectric strain greatly [60]. We chose various types of the high permittivity particle calcium copper titanate(CCTO) with different sizes as filler, and poly(dimethyl siloxane) PDMS as matrix to prepare DEs, and analyze the influences by particle size[106-108].Because the actuation strain are in a small range and causing a large measurement error, we decided to measure the capacitance of samples to evaluate the dielectric property of DE, and the relationship between capacitance C and dielectric constant is given by

$$C = \frac{\varepsilon_0 \varepsilon_r S}{d} \tag{2}$$

Where S is area of the electrical conductor, d is thickness of the insulator layer. The size of particle fillers only affects the Young's modulus, while the permittivity of composite material is determined by the permittivity and volume fraction of the filler.

One effective method to improve ε/Y of DEs is to introduce more filling and higher dielectric constant ceramics into the elastomer matrix [109]. However, it is difficult to balance these two incompatible key properties through filling more ceramics. Therefore, in order to get a large ratio of dielectric constant to elastic modulus (k/Y), the dielectric

constant of the filling materials must be improved further.

Due to their synergic properties, particularly, conducting polymer/ceramics composites due to the hyper-electronic polarization are developed for various technological applications such as capacitors, energy storage, and charge storage devices, etc [110]. Polyaniline (PANI) is one of the most attractive conducting polymers extensively studied due to its low cost, easy process ability, environmental stability and good electrical conductivity[112-114]. Therefore, PANI could be effectively employed to combine giant dielectric CCTO particles in order to achieve improved electrical and dielectric properties[115]. It is challenging and very important for the development of new generation dielectric elastomers.

Silicone elastomer has high flexibility, elasticity, and stability over a wide range of temperatures. Its dielectric loss and viscoelastic loss are independent of temperature and frequency. Besides, it has high filling capacity as well as electric breakdown strength. So, silicone elastomer is preferentially used as the matrix for DEs [116-118].

We obtained CCTO@PANI composites a simple in-situ surface polymerization method, and introduced into the silicone elastomer [114]. Meanwhile, we aimed to design and develop CCTO@PANI/PDMS composites with balanced dielectric constant and modulus by addition of higher dielectric constant materials. The microstructure,

mechanical and dielectric properties of the composites, the relationship between microstructure and dielectric properties, and the underlying mechanism were investigated.

In the progress of developing CCTO@PANI/PDMS, we found that filling of dispersed particles increases the modulus of composites greatly, which limited our final product reaching an ideal electroactive property. There is a contradiction that the high phase content of dielectric fillings will lead to an increment in the modulus of the composite material for the dielectric phase acts as the physical crosslinker for the elastomer matrix. How to solve this problem is a pursuit in this field. We have theoretically analyzed how to control the phase content and morphology in the matrix to get a balance in the soft matrix and high content of dielectric phase at first, then CCTO ultrafine powders with different particle sizes have been selected to certificate the theoretical results by nano-nomination method. The results could provide a hint to develop DE composites with the desired electro-deformation.

$$\varepsilon(p) = \frac{\varepsilon_d}{|p-p_c|^s} \tag{3}$$

This equation describes the greatly increasing permittivity of composite near percolation threshold [101]. Where $\varepsilon(p)$ is the permittivity near critical percolation concentration p_c, p is stand for the concentration and ε_d is the permittivity of matrix.

We decided to make use of this enhancement of permittivity.

Polyaniline (PANI) is a kind of typical conductive polymers and can be used as fillers to synthesis conductive polymer. Compared to inorganic fillers, PANI have better compatibility with organic matrix and less modulus so the composite would not lose flexibility. In this work, we present a dielectric elastomer using organic soluble PANI and PDMS through solution blending method.

3.2 Methods

3.2.1 Material

Three types of calcium copper titanate with different particle sizes (300nm-, 1μm-, 10μm- and 60μm-) were obtained from Jiangsu WuXi Kai-Star Electro-optic Materials Co.,Ltd, China. $H_2C_2O_4 \cdot H_2O$, $Ca(NO_3)_2 \cdot 4H_2O$, $Cu(NO_3)_2 \cdot 3H_2O$, $Ti(OC_4H_9)_4$, $Mg(NO_3)_2 \cdot 6H_2O$, tetrahydrofuran, and absolute ethanol were provided by Sinopharm Chemical Reagent, China. Poly (dimethyl siloxane) (PDMS) (RTV-3483), matching curing agent (RTV-3083) and compliant electrode materials (Molykote HP-800 Grease) were purchased from Dow Corning Corporation. Polypropylene glycol (Specification: PPG-400) was supplied by Jiangsu Haian petrol Chemical Plant of China. Aniline, hydrochloric acid, 3-aminopropyltriethoxysilane(APTES), ammonium persulfate(APS), polyvinylpyrrolidone(PVP, 30 kDa), ethanol and tetrahydrofuran (they were all

analytical grade) were obtained from Sinopharm Chemical Reagent Co., Ltd. of China.

3.2.2 Synthesis of CCTO/PDMS

There is many method of mixing filler into rubber matrix. The traditional way of rubber processing is mechanical blend through a two-roll mixer. A dielectric elastomer prepared with CCTO and PDMS composite via mechanical blend method was reported[119] but the result was not very ideal. The filling particles in composites obtained by this method cannot fully disperse in the matrix. Thus we intend to use another suspension blending method to get better dispersed filling particles.

The CCTO particles were initially mixed with PDMS, and tetrahydrofuran as solvent at room temperature by stirring for 20 min. Subsequently, curing agent was blended with the composites further to get suspension. Then, the suspension of CCTO/PDMS composite was poured into a self-manufacture PTFE mold and heated in an oven at 30 ºC for 24h. Finally, the thickness of the composites was controlled to be 0.5 mm.

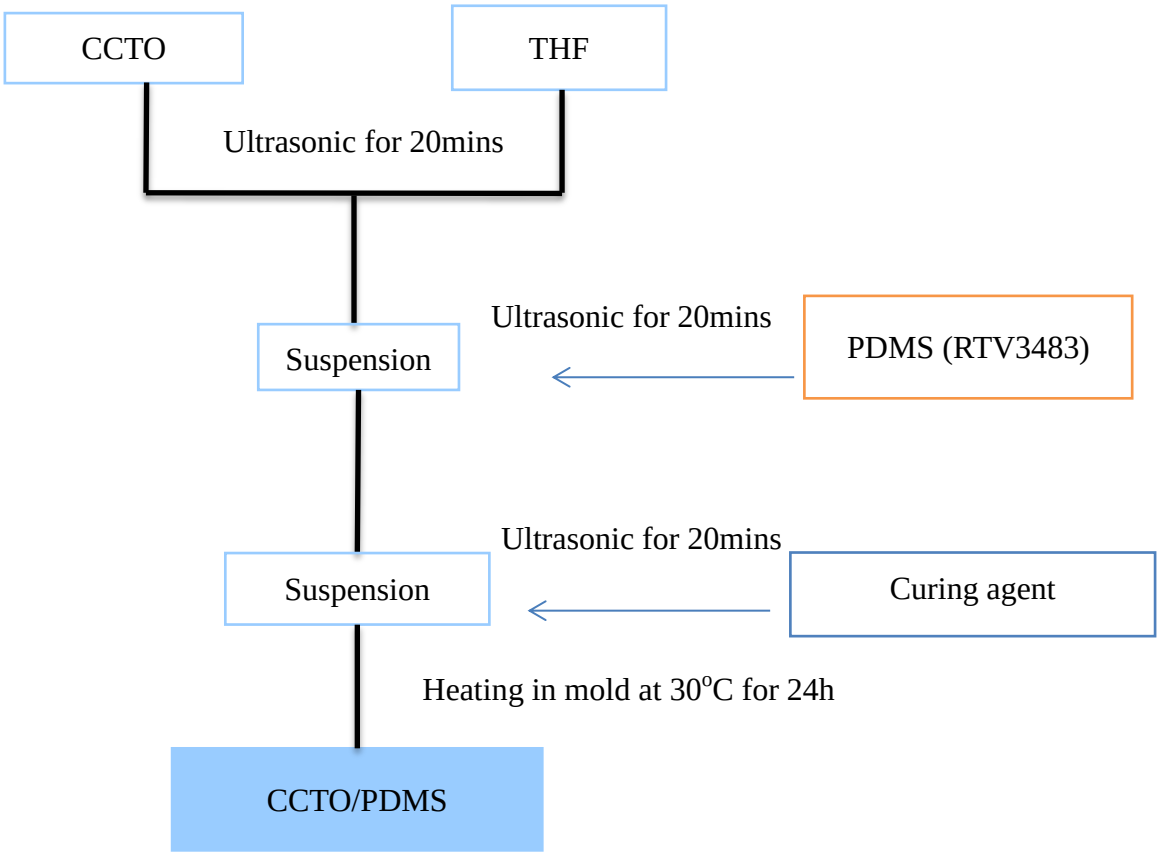

Fig.3-1 Synthesis of CCTO/PDMS

3.2.3 Synthesis of CCTO@PANI/PDMS composites by in-situ polymerization method

PANI could be effectively employed to combine giant dielectric CCTO particles in order to achieve improved electrical and dielectric properties[114]. In order to improve the coating rate of PANI, we modified the CCTO particles with APTES first to obtain a amine-functioned CCTO (NH_2-CCTO)[120], then PVP was grafted to $-NH_2$. Since the CCTO directly modified with PANI was clay-like layer structure[114], we introduced PVP to build up a core-shell structure for PANI to polymerize on. Polyaniline was

finally polymerized on the surface of PVP, this method gave us a core-shell CCTO@PANI particle coated with thicker shell structure.

CCTO (10 g) and APTES (10 g) were dispersed in anhydrous ethanol (45g) to obtain a mixture solution and sonicated for 10 min. The solution was refluxed for 5 h under dry N_2. The obtained CCTO particles were filtered and then washed with anhydrous ethanol. Finally, the product was dried in vacuum at 60 °C for 24 h, a dark powder (NH_2-CCTO) was obtained[120].

The different weights of aniline were used to prepare the CCTO@PANI particles as listed in the Table 3-1. Taking S3 for example, PVP (1 g) was dissolved in 500 mL hydrochloric acid (1 mol/L), and then the NH_2-CCTO particles (10 g) were added. The mixture was then ultrasonically dispersed, and aniline (1 g) was added into the mixture with vigorous stirring. Afterward, the mixture was mechanically stirred for 30 min at 20 °C. Then the solution of hydrochloric acid (250mL) and APS (3.68 g) was added into the above mixture instantly to start the oxidative polymerization. The reaction was performed under mechanical stirring for 5 h. The resulting precipitates were washed with deionized water and ethanol several times. Finally, the product was dried in vacuum at 60 °C for 24 h to obtain of the desired CCTO@PANI composite as a dark powder[114].

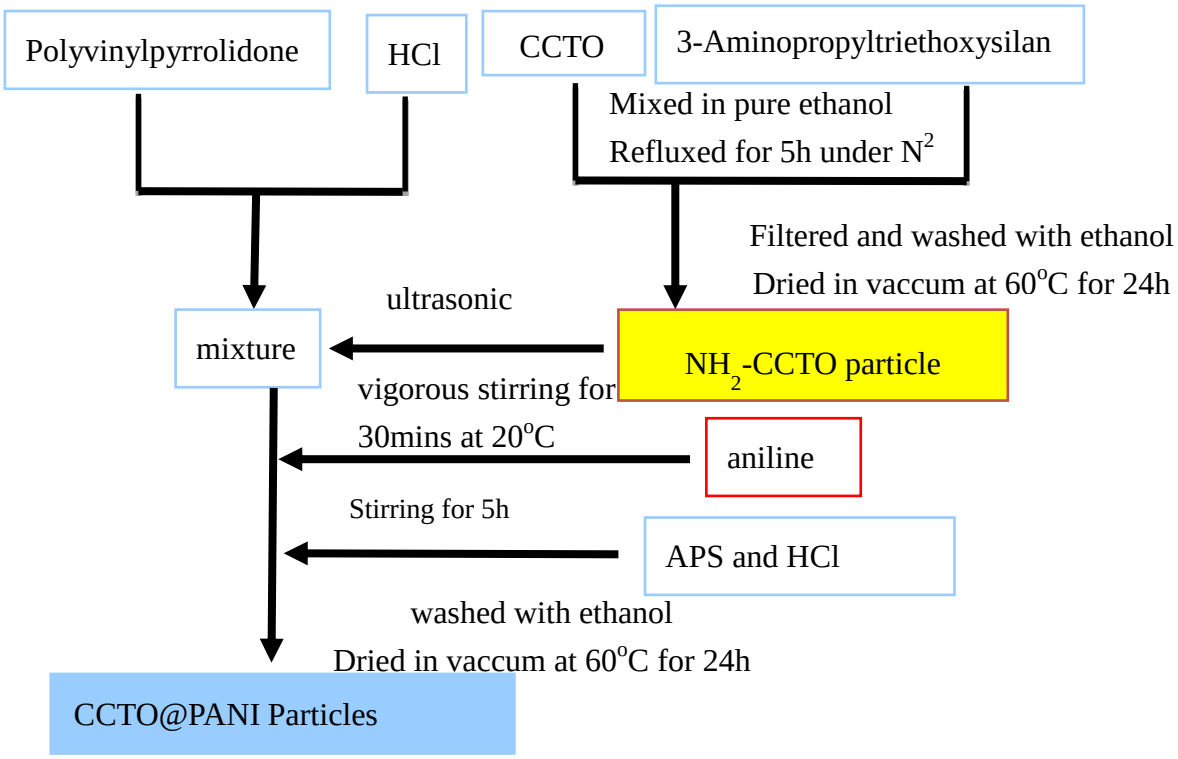

Fig.3-2 Synthesis of CCTO@PANI Particles

Table 3-1 The relational information of the synthesis and characterization of the pure silicone elastomer, CCTO/PDMS and CCTO@PANI/PDMS composites.

Sample number	Aniline of raw materials (g)	Composites	Y(MPa) 1-20%	Dielectric constant ε_r at 50 Hz	Actuated strain at 10V/μm(%)
S1	-	Pure silicone elastomer	0.25	3.21	8.94
S2	-	CCTO/PDMS	0.27	3.65	10.95
S3	1	CCTO@PANI/PDMS	0.29	4.60	13.24
S4	3	CCTO@PANI/PDMS	0.31	3.93	10.18
S5	5	CCTO@PANI/PDMS	0.27	3.91	10.95

0.18g CCTO or CCTO@PANI was dispersed in 18g tetrahydrofuran by sonication for 20 min. Then, a well-dispersed solution was mixed adequately with 18g PDMS and 0.9g curing agent for 20min to obtain a uniform suspension. Subsequently, the above suspension was poured into a self-manufacture PTFE mold and heated in an oven at 30 ºC for 24h. After this curing process, the samples with a thickness of 0.5 mm were easily removed from the mold.

3.2.4 Preparation of PANI-PDMS dielectric elastomers.

5.59 g of aniline monomer was added into the emulsion prepared from 200 ml of water mixed with 36.28 g of DBSA and 50 ml of toluene in a cooling bath maintained at 2 ^{o}C for 1 h. 9.13 g of APS dissolved in 50 ml of water was dripped into the polymerization bath for a period of 1 h, and maintained stirring at 0-5 ^{o}C for 17 h[121]. After polymerization was completed, 200 ml of toluene and 200g of acetone was poured into the emulsion and stirred for 1h. The solution was separated into 501.68 g of water layer and 198.36 g of oil layer after being left standing for 1h. The oil layer was vacuum filtrated to remove insoluble and obtained 196.25 g of clarified green oil layer, with a solid content of 4.38%.

Take an example of filling rate at 0.2 wt%, we mixed 0.15 g of dodecylbenzenesulfonic acid modified polyaniline in toluene solution, 3.3 g of PDMS and 0.17 g of curing agent for 20 mins, obtaining a homogeneous solution of PANI/PDMS, then poured the above solution into self-made Polytetrafluoroethylene mold and heated at 30 ^{o}C for 24h. After fully cured, the sample was removed from mold and PANI/PDMS composite with a thickness of 0.5mm was obtained.

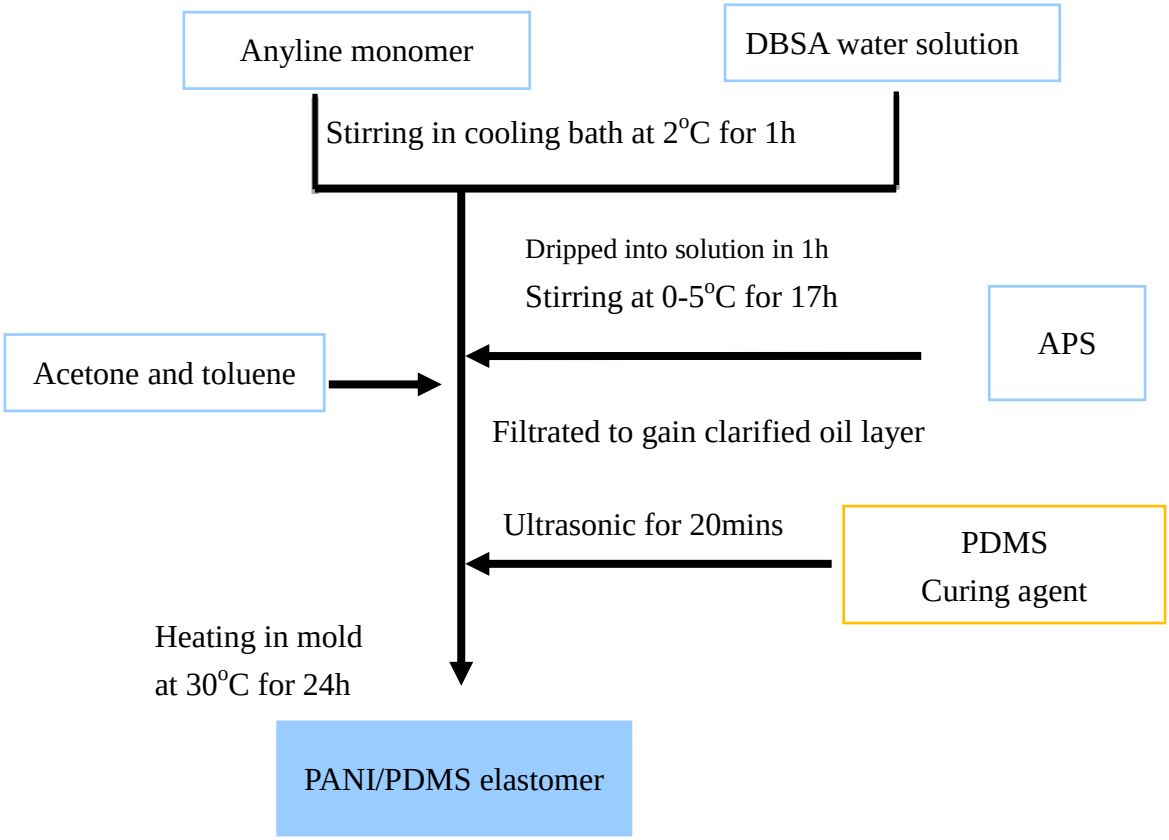

Fig.3-3 Synthesis of PANI/PDMS elastomer

3.2.5 Characterization

The CCTO@PANI particles and CCTO@PANI/PDMS composites were characterized by FTIR (German Bruker Tensor 27), STEM (USA Tecnai G2 F30 S-TWIN), FESEM (Japan Hitachi S-4800 FESEM), DMA (Q800, TA, USA). Element mapping at atomic resolution have been obtained by EELS spectrum imaging (SI) in the STEM mode. The specialized routines under Gatan Digital Micrograph have been used for image and spectral data processing. The dielectric properties of the composites were obtained using a dielectric spectrometer (Novocontrol Technologies, Germany) at room

temperature. The compliant electrode material for dielectric elastomers was conductive grease coating each side of the DEs. The actuated plane strain of the dielectric elastomer was measured under a high voltage supplied by an intelligent DC high voltage generator. During actuation, the images were captured by a commercial camera. Capacitance measurements were performed by using the UC2876 Precision LCR meter with a 1V a.c. signal.

3.3 Result and Discussion

3.3.1 Theory about the effect of particle phase morphology

Initially, We chose various types of the high permittivity particle calcium copper titanate(CCTO) with different sizes as filler, and poly(dimethyl siloxane) PDMS as matrix to prepare DEs, and analyze the influences by particle size.

The permittivity of composite material is determined mainly by the permittivity and volume fraction of the filler. We have several models [122,123] to describe composite's permittivity such as Lichtenecker Model (eq.4), Bruggeman Model (eq.5), Maxwell-Garnett Model (eq.6), etc.

$$log\varepsilon_{eff} = (1-f)log\varepsilon_1 + flog\varepsilon_2 \tag{4}$$

$$\varepsilon_{eff} = \varepsilon_2 + 3f\varepsilon_2 \frac{\varepsilon_1-\varepsilon_2}{\varepsilon_1+3f\varepsilon_2-f(\varepsilon_1-\varepsilon_2)} \tag{5}$$

$$\frac{\varepsilon_{eff}-\varepsilon_1}{\varepsilon_{eff}-\varepsilon_2} = (1-f)\left(\frac{\varepsilon_1}{\varepsilon_2}\right)^{\frac{1}{3}} \tag{6}$$

The ε_{eff} stands for the efficient permittivity of composites, the f stands for the volume fraction of filler. ε_1 and ε_2 stands for the permittivity of filling particles and matrix, respectively.

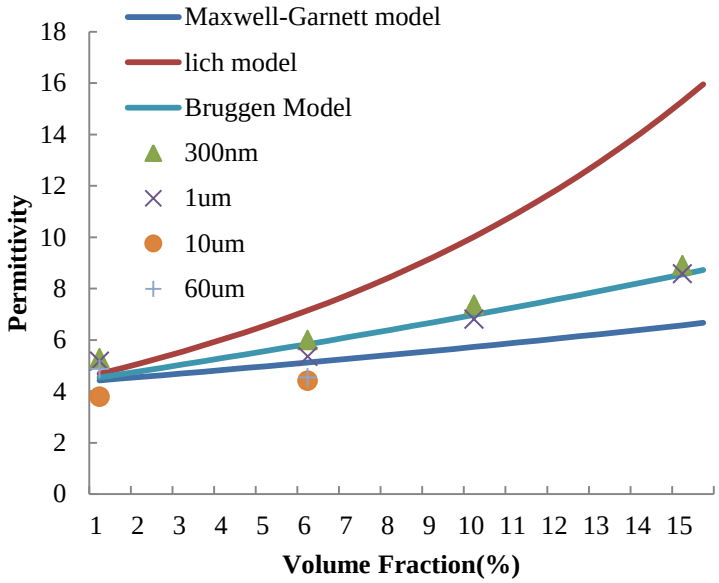

Fig.3-4 The permittivity of different kinds of samples compared with theoretical value calculated by three kinds of models

We compared the permittivity of samples filled with 4 kinds of particles(Fig3-4) and the permittivity of samples filled with particles sizes of 10 and 60 μm was very low due to precipitation. The samples filled with smaller particles showed similar values to Bruggeman model. The model was designed to describe the properties of ceramics and metal materials but our results still fit the model well. Due to the low permittivity of major component, the efficient permittivity of composite did not increase obviously at

low volume fraction.

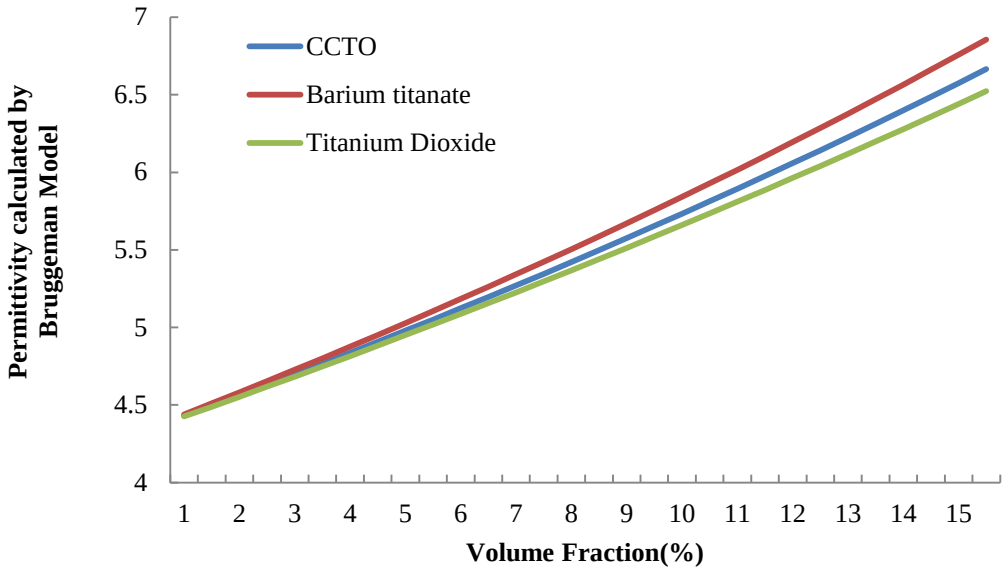

Fig.3-5 The theoretical permittivity calculated by three kinds of filling particles

If we replace ε_1 by the permittivity of $BaTiO_3$ and TiO_2, which is about 1400 and 120, we can easily observe that at low filling amount of dielectric particles, the efficient permittivity of composites do not affect by the high permittivity of dielectric particles very much(Fig.3-5).

In the former researches, we found some interesting phenomena that phase morphology also affects the dielectric properties of composites. Referring to the dielectric inorganic materials, the dielectric constant was found to be a function of the diameter of particles and wires or the thickness of films, which could be described a simple thermos dynamic model presented by M. Tian, et al.[124], with the following formula:

$$\frac{\varepsilon(D)-\varepsilon(\infty)}{\varepsilon(\infty)-1}=2\left\{\exp\left(-\frac{(\alpha-1)}{(D/D_0-1)}\right)-1\right\} \tag{6}$$

Where α is a function of surrounding conditions of low-dimensional and D_0 denotes acritical diameter at which almost all atoms of a low-dimensional material are located on its surface. This equation is effective with the particle size ranging from $2D_0$ to bulk materials.

There are two cases: 0<α<1 and α>1. In the case of 0<α<1, the dielectric constant increased as the particle size decreased. Otherwise, the dielectric constant decreased as the particle size decreased. The dielectric constant as a function of the particle size were calculated with D_0 of 5 nm and $\varepsilon(\infty)$ of 50000 and illustrated in Fig.3-6.

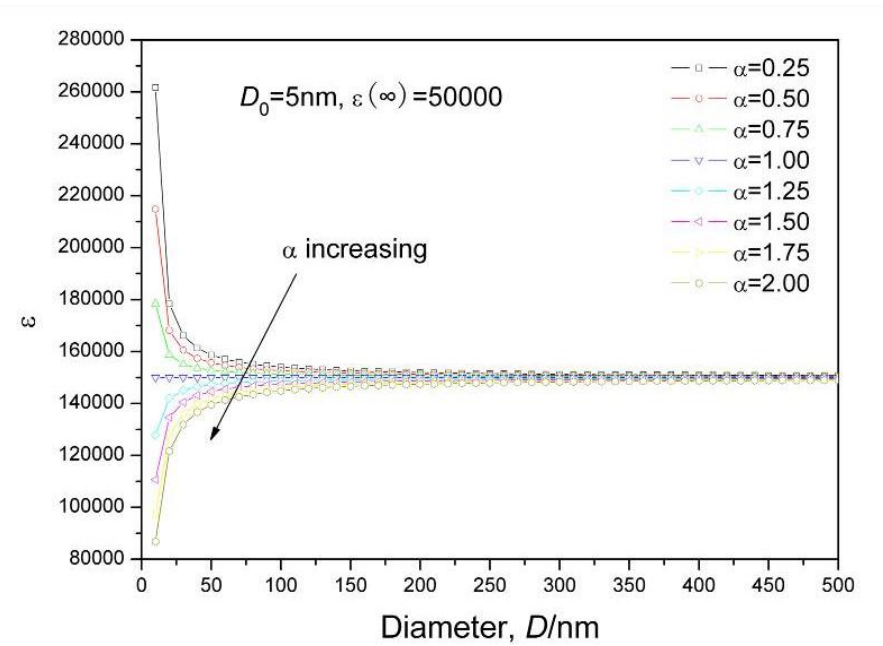

Fig.3-6 The dielectric constant as a function of the particle size

Quite a lot of dielectric materials agree the changing trend as 0<α<1. For example, CCTO, one kind of dielectric materials supposed to be characterized of huge dielectric

constant. The dielectric constant of CCTO powders with different average particle sizes were measured and shown in Fig.3-7.

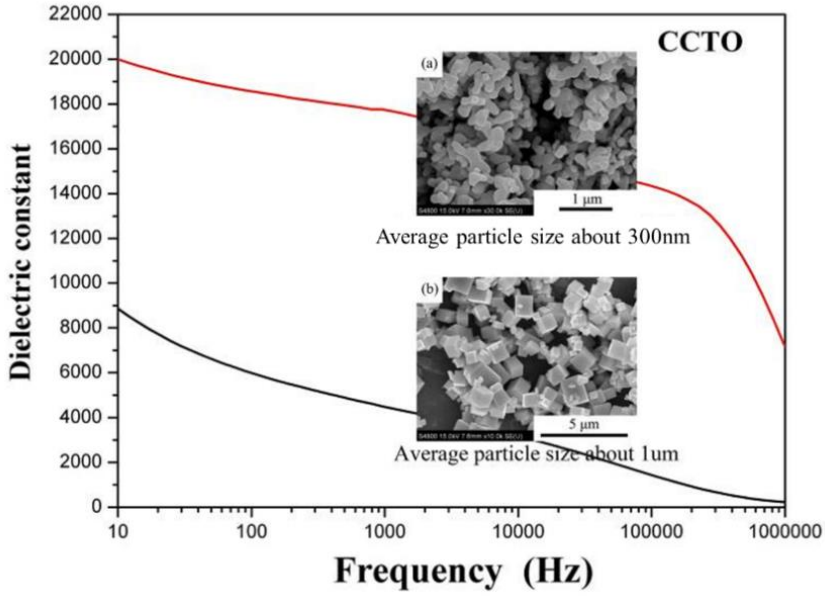

Fig.3-7 The dielectric constant as a function of the particle size

Turning to the DEs fabricated by inorganic and organic compositing, the driving force, *p*, related to the applied voltage, *U*, dielectric constant, ε, and the thickness of the DEs particular to the direction of the applied electric field:

$$p = \varepsilon \times \varepsilon_0 \left(\frac{U}{\delta} \right)^2 \tag{7}$$

The resulted electro-deformation, *S*,could be described as:

$$\mathrm{S} = -p / Y \tag{8}$$

Where Y is the Young's modulus.

Considering that most of the elastomer matrix of DEs is chemically crosslinked,

the Young's modulus must be ascribed to the contribution of physical crosslinking. Obviously, the physical crosslinking density is mainly determined by the interfacial interaction and the number of the phase crosslinking points. With a similar surface state and different particle sizes, the physical crosslinking density could be as a linear function of the total surface area of the particles. From this perspective, the Young's modulus would take the following description:

$$\mathrm{Y} = \frac{\mathrm{km}}{\rho D} \tag{9}$$

Where *m* and ρ are the weight and density of inorganic particles as the filling phase, respectively. D is the diameter of filling particles and k is a parameter describe the effect of crosslinking.

From the equation from 3 to 6, the qualitative relationships of the characteristic parameters including dielectric constant, driving force, Young's modulus, and electro-deformation with the particle size were analyzed and listed in Table 3-2.From the qualitative analysis, it is obvious to see that:

(1) In the case of α>1, the dielectric inorganic particles with larger particle size approaches to a higher dielectric constant. The physical crosslinking density decreases by a homogenous distribution of dielectric inorganic particles with larger spaces between particles. Therefore, the DEs will take a stronger driving force, lower Young's

modulus and higher electro-deformation.

Table.3-2 The characteristic parameters of DEs as a function of particle size

Characteristic parameters	As a function of particle size F(D)	α>1	0<α<1
Dielectric constant ε	$\frac{\varepsilon(D)-\varepsilon(\infty)}{\varepsilon(\infty)-1}=2\left\{\exp\left(-\frac{(\alpha-1)}{(D/D_0-1)}\right)-1\right\}$	$D\downarrow \rightarrow \varepsilon\downarrow$	$D\downarrow \rightarrow \varepsilon\uparrow$
Young's Modulus Y	$Y\propto 1/Q\propto 1/ND^2$	$D\downarrow \rightarrow Y\uparrow$	$D\downarrow \rightarrow Y\uparrow$
Electro-deformation S	$S=-\varepsilon_0\varepsilon_r E^2/Y$	$D\downarrow \rightarrow \varepsilon\downarrow,\ Y\uparrow$ $\rightarrow S\downarrow$	$D\downarrow \rightarrow \varepsilon\uparrow,\ Y\uparrow$ $\rightarrow S\downarrow$ or $S\uparrow$

(2) For our case, 0<α<1, the dielectric inorganic particles with a smaller particle size are favored to enhance dielectric constant, but it leads to the increment in the Young's modulus if there is no special phase micro-structure. Therefore, the electro-deformation may decrease or increase in view of the enhanced driving force and increasing Young's modulus.(Fig.3-8-a) To refine the electro-deformation effect, the phase micro-structures with aggregates consisting of nano powders (Fig.3-8-b).

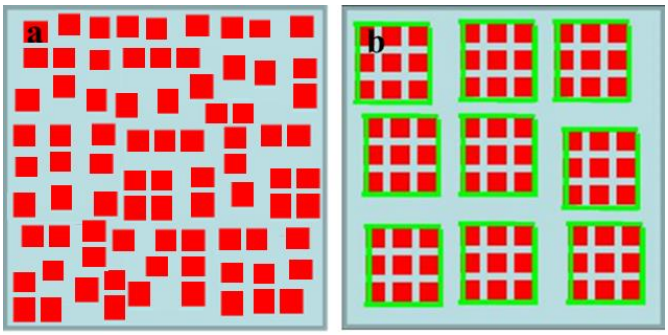

Fig.3-8 The designed phase micro-structures of DEs to enhanced electro-deformation effect (a. α>1; b. 0<α<1)

In the theoretical analysis, the tunable Young's modulus and the high dielectric constant of the inorganic fillings will provide a way to control the phase morphology to achieve ab electro-deformation.

The huge dielectric CCTO ultrafine powders with different average particle sizes of 300 nm and 1 μm were used as the fillings to blend with silicon elastomer matrix to fabricate DE composites with the same weight ratio. The SEM images of the DE composites (as shown in Fig.3-9) indicated a relatively homogeneous distribution of CCTO particles in the silicon elastomer matrix. As the particle size decreased, there was a slight agglomeration due to the higher specific surface area (Fig.3-9-b). If the CCTO particles were modified with –NH2 first, they will disperse better in the matrix(Fig.3-9-a).

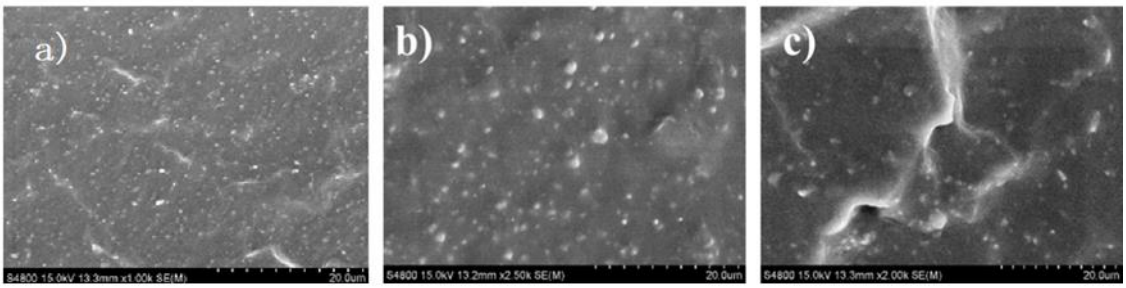

Fig.3-9 The SEM images of DEs with different CCTO powders

(a. 300nm dispersed; b. 300nm agglomerated; c. 1μm)

With nanoindentation method, the statistical modulus of the as-fabricated DE composites was shown in Fig.3-10. We were unable to determine the particle borders of

the sample filled with dispersed 300nm particles, for the 300nm particles were too small for our nano-indentation, thus, the results of samples filled with dispersed 300nm particles were not listed. From the statistical modulus, it was found that after blending with the CCTO dielectric phase, the modulus of the fabricated composites increased. The value of the neat elastomer matrix was about 6 MPa. With the same phase content of CCTO, the modulus showed a lower value as using CCTO with the average particle size of 300 nm comparing to that of the composites fabricated by using CCTO with the average particle size of 1 μm as the fillings. It was very interesting. For the particles with the smaller particle size would provide more physical crosslinking points, the higher modulus was expected. Therefore, the CCTO powders with the particle size of 300nm may form some sophisticated structures due to the agglomeration.

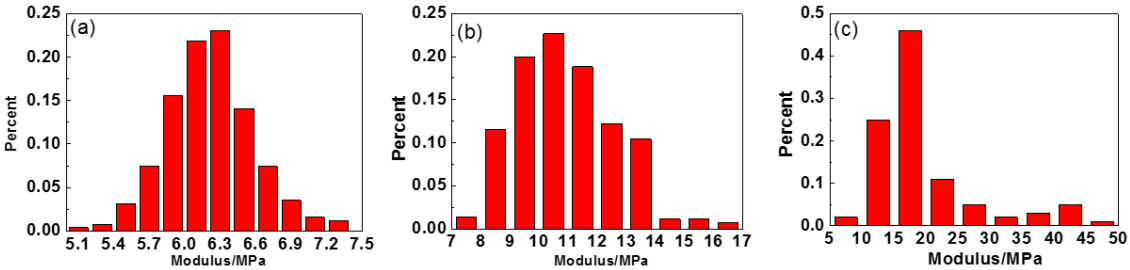

Fig.3-10 The statistical modulus of DEs with different CCTO powders

(a. neat; b. 300nm agglomorated; c. 1μm)

To make it clearer, the modulus mapping was carried out in a micro-domain. The results were demonstrated in Fig.3-11. From the modulus mapping, it was obvious that the CCTO/PDMS composites with the CCTO particle size of 300 nm showed a

relatively homogeneity in the modulus, while the CCTO particle size of 1 μm led to differences in the different micro-domains. This indicated that the CCTO with smaller particle sizes of 300 nm did not make great contribution to the increment in modulus even there was slight agglomeration as shown in SEM results. It gave a softer composite and the higher electro-deformation was expected. Such a result gave a hint to control the particle morphology to tune the electro-deformation of DEs.

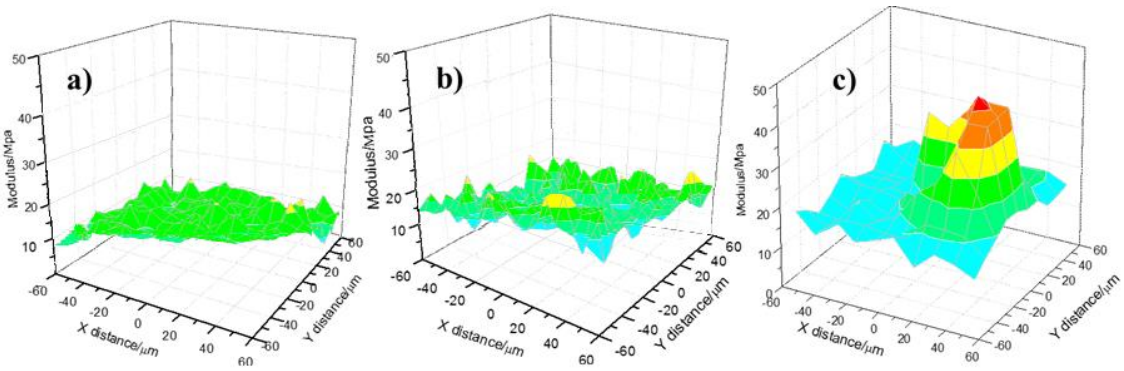

Fig.3-11 The modulus distribution of DEs with different CCTO powders in micro-domains (a. neat; b. 300nm agglomorated; c. 1μm)

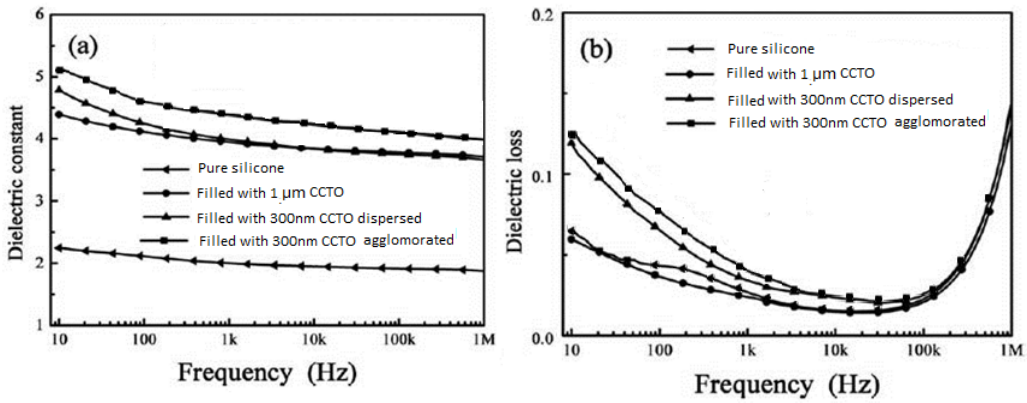

Fig.3-12 The dielectric properties of samples filled with different CCTO particles

In Figure.3-12 we can see that the dielectric constant was greatly improved after filling

small amount of CCTO particles. The permittivity was dropping before 100Hz then tend to be decreasing smoothly, we suppose that the dipole polarization was dropping with frequency, and surface polarization was hardly effected by frequency changes. The samples filled with 300nm CCTO showed higher permittivity, we assume that it is for the smaller particles have larger surface area, which leaded to higher interfacial polarization.

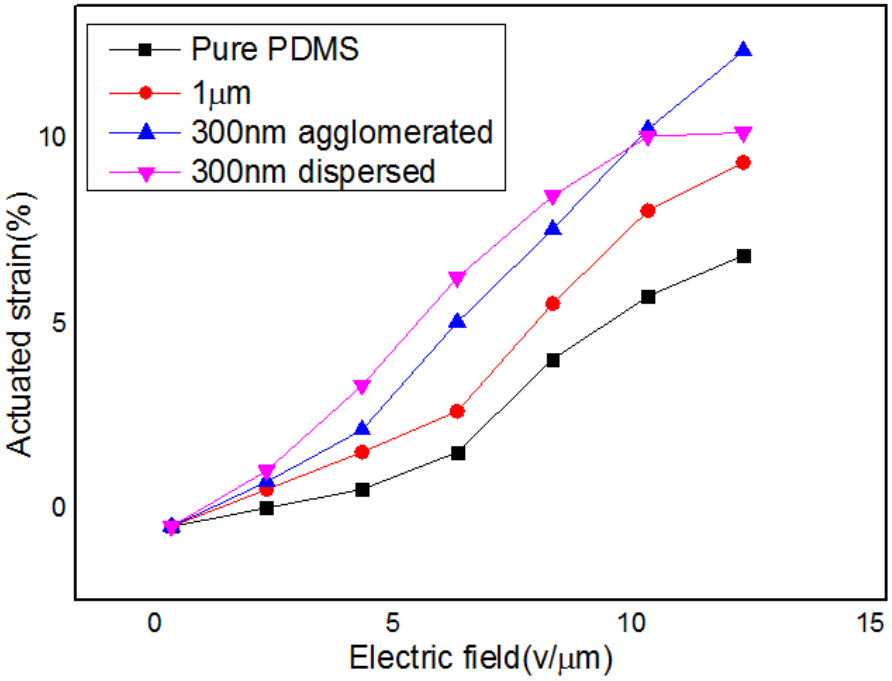

Fig.3-13 Electrostrictive of DEs with different CCTO powders

Table.3-3 The dielectric and mechanic properties of DEs filled with different kinds of particles

Characteristic parameters	Pure PDMS	Dispersed 300nm	Agglomerated 300nm	1μm
Dielectric constant ε	2.15	5.13	4.89	4.41
Young's Modulus Y at 0-20% strain (MPa)	0.28	0.42	0.32	0.40
ε/Y	7.78	12.21	15.28	11.02
Strain at 12V/μm	5.7	10.2	12.5	8.5

Dielectric and mechanical properties of the composites was listed on table.3-3. The electro deformation characteristics of the fabricated composites (as shown in Fig.3-13) agreed with the nanoindentation results and the ε/*Y* values calculated. The fabricated DE with the CCTO particle size of 300 nm showed a better electric response with the largest deformation about 15% under the electric field of 16V/μm while this value was about 12% as the CCTO particle size of 1 μm. The sample filled with well dispersed CCTO showed a higher electroactive strain at low electric field but with a lower strain range at high voltage. It was believed that the higher dielectric parameter and lower modulus made contributions together to this.

3.3.2 Properties of core-shell structured CCTO@PANI/PDMS dielectric elastomers

FESEM inspection is conducted to characterize the size and shape of the commercial

CCTO particles and CCTO@PANI composites, as shown in Fig. 3-14. It can be seen from Fig. 3-14(a) that the size of CCTO particles is about 3 μm with well dispersion. Fig. 3-14 (b) depicts the FESEM images of CCTO@PANI composites without any visible agglomerates and morphology changes, and almost all CCTO particles are embedded in the PANI. In addition, fine grains of CCTO surrounded by numerous of PANI can be observed. After being coated, a continuous overlayer of PANI polymers is successfully produced on the surface of CCTO particles. However, with the increase of the weight of aniline during preparing CCTO@PANI composites, the agglomerates of particles become more serious because many polymerization reactions did not occur on the surface of the particles, as shown in Fig. 3-14 (c) and Fig. 3-14 (d).

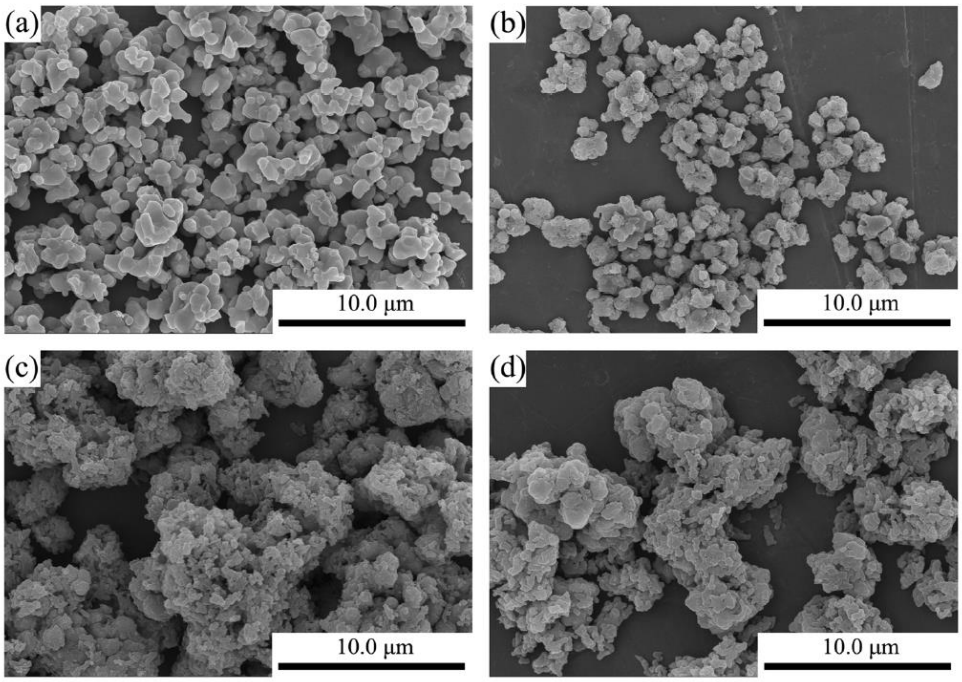

Fig.3-14 FESEM pictures of a:CCTO and CCTO@PANI particles, b: S3, c: S4, d:S5.

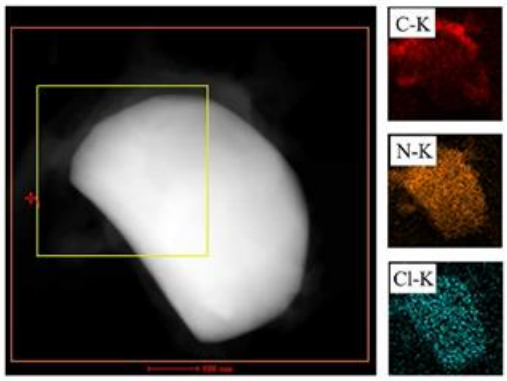

Fig.3-15 element mapping of CCTO@PANI composite (S3).

Fig. 3-15 shows the STEM imaging and dual-EDS X-ray mappings for chemically resolved structural characterization and element dispersion of CCTO@PANI composites (S3). The individual elemental maps of C, N and Cl are presented in red, orange and green, respectively. It is demonstrated that PANI is uniformly coated on the surface of CCTO particles.

Fig. 3-16 shows the FESEM micrographs of the fractured surfaces of CCTO/PDMS and CCTO@PANI/PDMS composites (S2, S3). CCTO and CCTO@PANI particles are well dispersed in the silicone elastomer without any visible agglomerates. Compared to CCTO/PDMS composites, the compatibility between CCTO@PANI and silicone is better, as indicated by the smooth fractured surfaces and the presence of bonded rubber on the fillers.

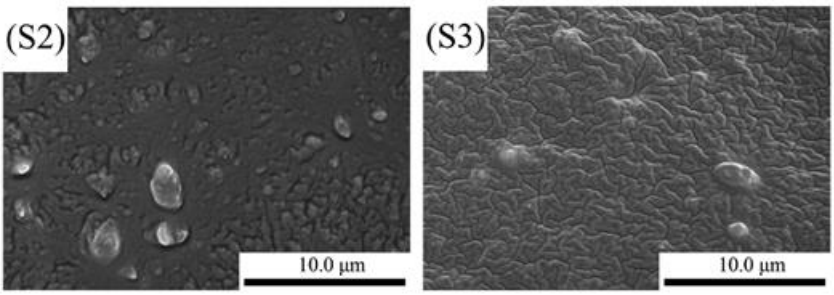

Fig.3-16 FESEM micrographs of the fractured surfaces of CCTO/PDMS composite (S2) and CCTO@PANI/PDMS composite (S3).

Fig. 3-17 shows the tensile stress-strain curves of pure silicone elastomer, CCTO/PDMS and CCTO@PANI/PDMS composites (S1- S3). Pure silicone elastomer used in this study shows a very low elastic modulus (0.25 MPa). The Y of CCTO/PDMS and CCTO@PANI/PDMS composites are up slightly (see Table 3-1), respectively, and the tensile strength of the composites shows the same tendency. It ensures the good mechanical strength and thus facilitating the practical application of DEs.

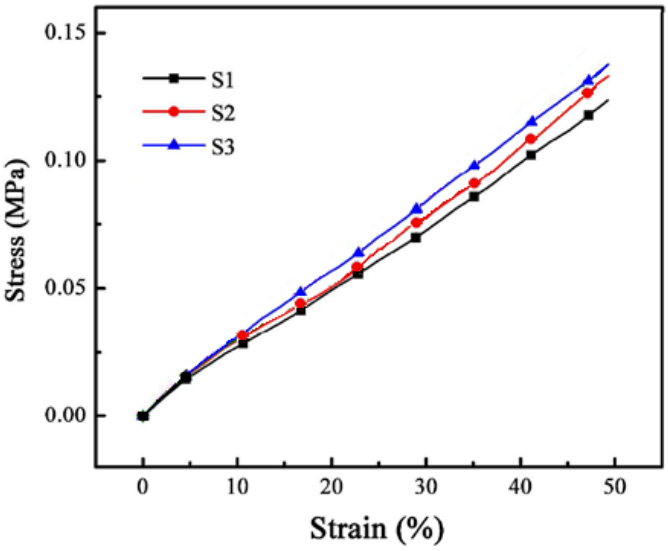

Fig.3-17 Stress-Strain curves of pure silicone elastomer (S1), CCTO/PDMS composite

(S2) and CCTO@PANI/PDMS composite (S3).

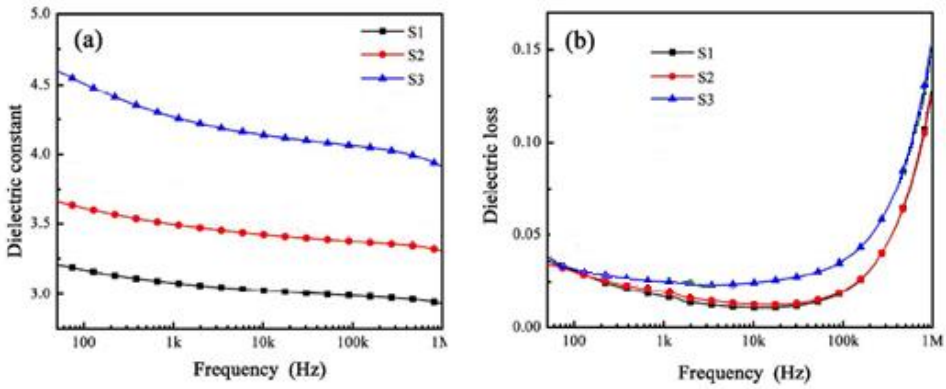

Fig.3-18 Frequency dependence of dielectric constant (a) and the dependence of the dielectric loss (b) of pure silicone elastomer (S1), CCTO/PDMS composites (S2) and CCTO@PANI/PDMS composites S3

Fig.3-18 displays the room temperature relative dielectric constant (ε_r) and loss tangent (tan δ) of pure silicone elastomer, CCTO/PDMS and CCTO@PANI/PDMS composites (S1- S5) in the frequency range of 10 Hz to 10^6 Hz. The detailed values of dielectric constant at 50 Hz are summarized at table 1. We can observe that the dielectric constant of S3 at 50 Hz obviously increases from 3.21 for pure silicone elastomer to 4.60, fortunately, the dielectric loss has slight change. However, the dielectric constant of S4 and S5 coating with more PANI is lower due to the agglomerates of CCTO@PANI composites, which will reduce the effect of the electronic polarization and polaron delocalization.

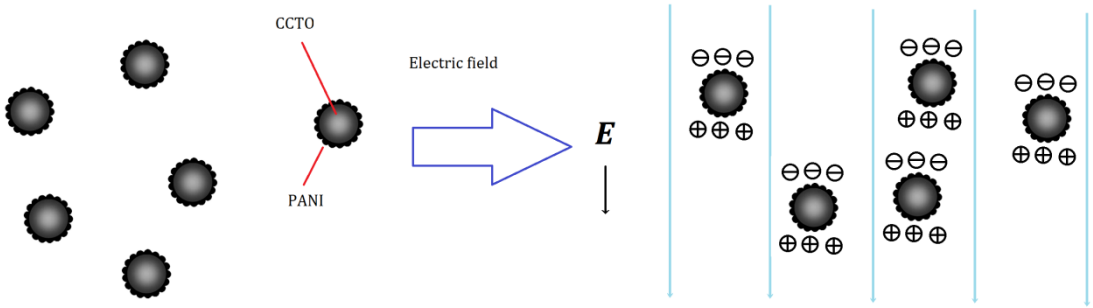

Fig.3-19 Schematic representation of the mechanism of the hyper-electronic polarization and a strong polaron delocalization of CCTO@PANI particles under the electric field.

CCTO@PANI/PDMS composites exhibited higher dielectric constants than that of pure silicone elastomer and CCTO/PDMS composites. It may be correlated to the hyper-electronic polarization and a strong polaron delocalization [114]. Furthermore, the CCTO particles surrounded by the network of PANI acting as nano-dielectric domains yielded high dielectric constants via the interfacial/Maxwell Wagner type of polarization mechanism, as shown in Fig.3-19.

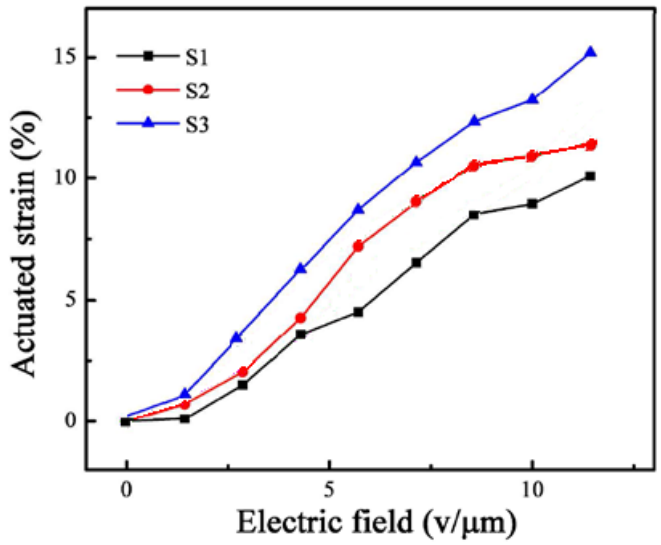

Fig.3-20 Actuation strain of pure silicone elastomer (S1), CCTO/PDMS composites (S2) and CCTO@PANI/PDMS composites S3.

Fig.3-20 shows the actuated strains of pure silicone elastomer, CCTO/PDMS and CCTO@PANI/PDMS composites S1- S3 as a function of electric field. With the increase in the electric field, the actuated strain of all the samples increases. The values of the actuated strains at 10 V/μm are summarized in Table 1. The actuated strain of CCTO/PDMS and CCTO@PANI/PDMS composites at the same electric field is much higher than that of pure silicone elastomer. For example, the actuated strain at 10 V/μm obviously increases from 8.94% for pure silicone elastomer to 10.95% and 13.24% for the composite with 1 wt. % of CCTO (S2) and CCTO@PANI (S3), respectively. Here, it should be noted that the actuated strain tests were performed by using circular membrane actuators without prestrain.

3.3.3 Properties of PANI-PDMS electroactive polymers

This greatly increasing permittivity of composite near percolation threshold has been reported. We could achieve EAP with high electroactive strain by filling small amount of conductive materials in rubber matrix. Polyaniline is a kind of typical conductive polymers and can be used as fillers to synthesis conductive polymer. Compared to inorganic fillers, PANI have better compatibility with organic matrix and less modulus so the composite would not lose flexibility. Some researchers prepared polymer with high dielectric constant using PANI as filler via a in situ polymerization or mechanical blending method, but the synthesis was complicated and filling amount was restricted. Organic soluble PANIs could be prepared in toluene solution. A dielectric elastomer using organic soluble PANI and PDMS through solution blending method was prepared.

Fig.3-21 shows the Raman spectra of PANI-PDMS dielectric elastomer. The peak at 1590 cm^{-1} shows the characteristic absorbing vibration of a quinone structure N=Q=N. As the filling amount of polyaniline increases, the quinone characteristic peaks are significantly enhanced. The peak at 1499 cm^{-1} is caused by the characteristic absorbing vibration benzene structure N-B-N. The characteristic peak of quinone structure and benzene structure in polyaniline are weakened after doping. The peaks at 1379 cm^{-1} and 1302 cm^{-1} are caused by aromatic amine Ar-N, and peaks at 830 cm^{-1} and 1161 cm^{-1} are

bending vibration characteristic absorption band of outer and inner ring of benzene ring. From the result of Raman spectra, we assume that the PANI-PDMS composite was successfully synthesized.

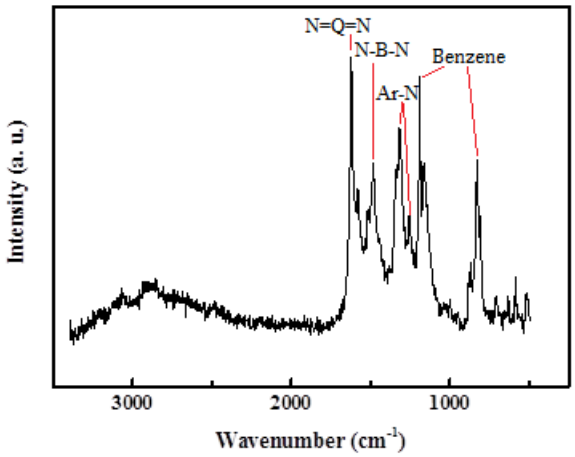

Fig.3-21 Raman spectra of PANI-PDMS

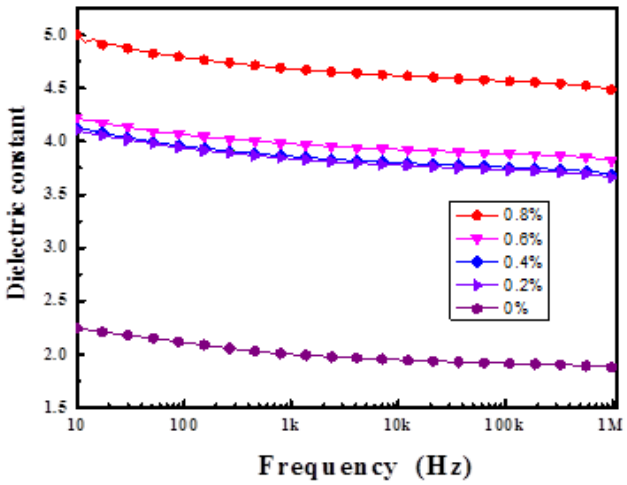

Fig.3-22 The permittivity of pure silicone and PANI/PDMS of different filling amount

Fig 3-22 is the permittivity of pure silicone and PANI/PDMS of different filling amount. As shown in the figure, the dielectric constants of composites increase at different levels. When the filling amount reaches 0.8 wt.%, the dielectric constant of PANI/PDMS composite is 4.82, which is 2.24 times of pure silicone. The reason of increasing dielectric constant of PANI/PDMS is due to the dipole polarization in matrix network and electron polarization in conductive polyaniline. According to the Maxwell-Wagner polarization theory, a great amount of charges accumulated on the surface between PANI and PDMS in an external electric field, forming numerous micro capacitors in parallel. Thence, interface polarization can enhance the permittivity of dielectric elastomer significantly. As the filling amount of conductive polyaniline increases, more micro capacitors formed in the system and dielectric properties of material are improved.

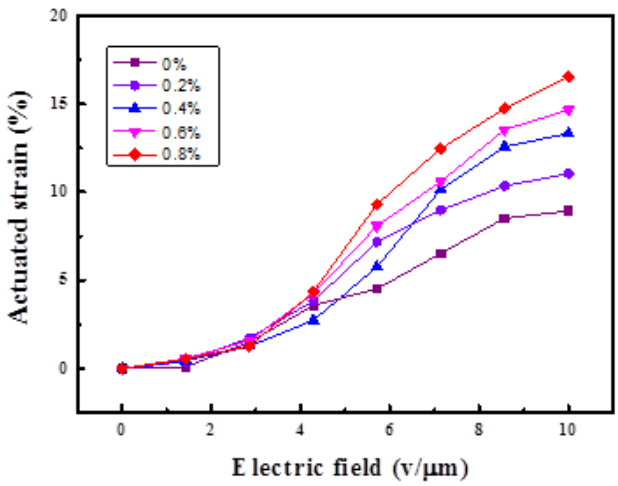

Fig.3-23 The actuated strain of PANI/PDMS of different filling amount

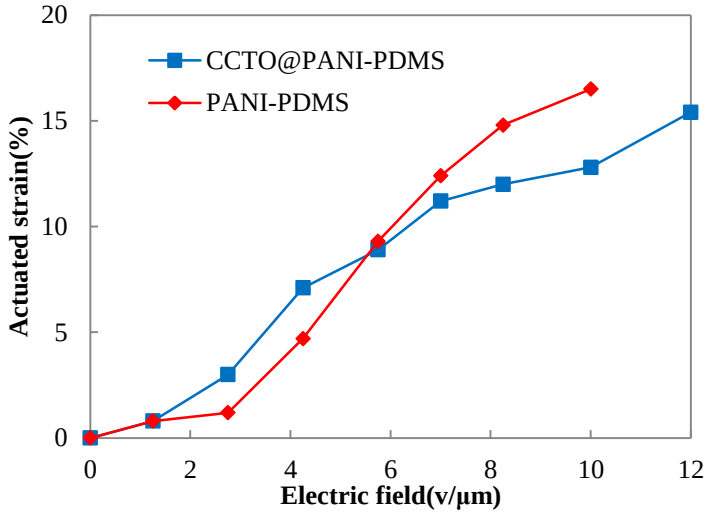

Fig.3-24 The electroactive strain compared with PDMS filled with CCTO@PANI

Fig.3-23 shows the electrostriction strain curve of pure silicone and PANI/PDMS of different filling amount in electric field. The actuated strains of all samples are increasing as the electric field grew, and the actuated strains of PANI/PDMS composites are obviously larger than pure silicone. For example, the actuated strain of pure silicone at 10V/μm is 8.52%, and the actuated strain of 0.8w.t % PANI/PDMS is 16.57% at the same electric field, the enhancement of dielectric constant is reflected intuitively through actuating property. The actuated strain was also compared with the CCTO@PANI-PDMS material fabricated by our group earlier [107], showing higher electrostriction at lower voltage (Fig.3-24). The PANI/PDMS dielectric elastomer showed a high actuating property in low electricity fields, and could be applied to fields with specialized requirements such as biological and medical science.

Table.3-4 Comparing with other silicone-based dielectric elastomers

Filler	Dispersion method	Content	Particle size	ε	Y[MPa]	Thickness[μm]	Actuation strain[%]
$BaTiO_3$[128]	Two-roll mixer	100 phr	100nm	5	0.15	n.a.	13.5@35V/μm
CCTO[119]	Two-roll mixer	20 wt.%	5μm	5.2	0.38	100	6@25V/μm
$BaTiO_3$[129]	Suspension	20 vol%	<3μm	7.5	0.2	250	8@8.5V/μm
CCTO@PANI	Suspension	1 phr	300nm	4.6	0.29	500	15@12V/μm
PANI	Solution blend	0.8wt%	-	4.8	0.2	500	16.5@10V/μm

In table 3-4 we compared two kinds of PDMS based DEAs with other materials reported. Clearly we have improved the actuation strain of DEAs at lower electric field with less content of fillers. In order to make the figure.3-25 clearer, the value was adjusted to a similar range. We can see more clearly in fig. 3-25 that the ε/Y is the determine parameter of the dielectric elastomer, which is deciding the maximum actuation strain. Breakdown voltage is also very important that the material cannot work

if the breakdown voltage is lower than driving voltage. The 3M VHB acrylic seems to be a perfect dielectric elastomer but the low rebound resilience ratio and viscoelasticity is limiting its applications. Thus our material successfully achieved high electroactive strain at relatively low electric field while maintaining high good properties.

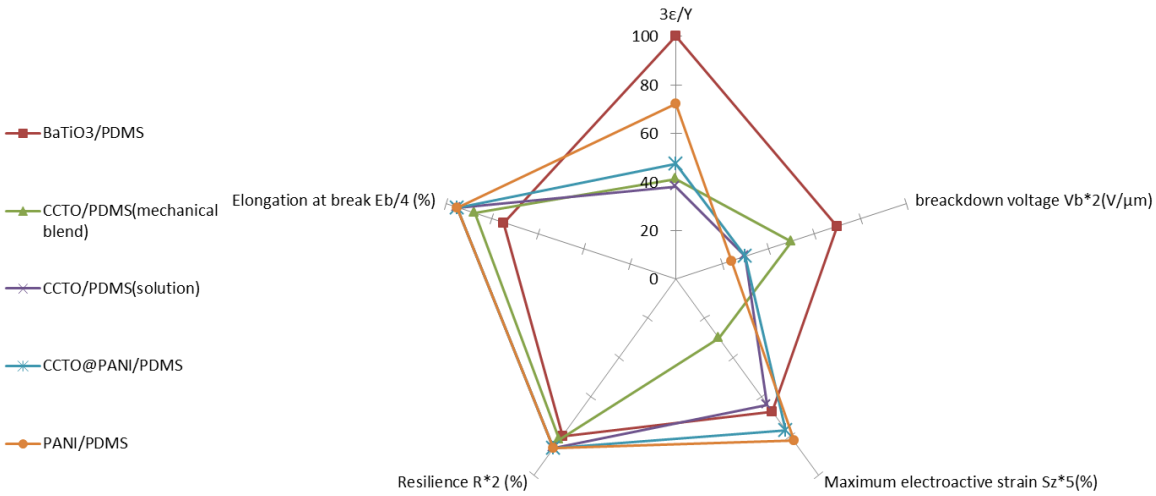

Fig 3.25 The major parameters of dielectric elastomers compared with reported materials

3.4 Conclusions

The strategies for designing dielectric elastomers with larger electro-deformations have been probed based on the theoretical calculation and experimental results. The CCTO with smaller particle sizes showed a larger dielectric parameter. With smaller CCTO particle as the fillings, the fabricated elastomer composite would approach to a low modulus by a proper CCTO phase morphology in the matrix. The result provided

aneffective way to design CCTO/PDMS composite as a dielectric elastomer with a higher electro-deformation.

CCTO@PANI/PDMS dielectric composites (S3) with high dielectric constant and greatly improved actuated strain at low electric field have been prepared by filling tiny dielectric CCTO@PANI particles. The CCTO@PANI/PDMS composites have much higher actuated strain than pure silicone elastomer and CCTO/PDMS composites due to the hyper-electronic polarization and a strong polaron delocalization. This study provides a simple and effective method for the improvement of actuated strain at low electric field through coating conductive materials onto the surface of the giant dielectric constant CCTO particles, facilitating the wide application of dielectric materials.

A dielectric elastomer has been synthesized using organic soluble PANI and PDMS through solution blending method. The dielectric constant of PANI/PDMS composite reached 4.82 with a filling amount of 0.8 wt.%, which was 2.24 times of pure silicone, due to the dipole polarization in matrix network and electron polarization in conductive polyaniline. The actuated strain of 0.8w.t % PANI/PDMS was 16.57% compared to 8.52% of pure silicone at an electric field of 10V/μm.

A dielectric elastomer has been synthesized using organic soluble PANI and PDMS

through solution blending method. The dielectric constant of PANI/PDMS composite reached 4.82 with a filling amount of 0.8 wt.%, which was 2.24 times of pure silicone, due to the dipole polarization in matrix network and electron polarization in conductive polyaniline. The actuated strain of 0.8w.t % PANI/PDMS was 16.57% compared to 8.52% of pure silicone at an electric field of 10V/μm, and could be applied to fields with specialized requirements such as biological and medical science.

Chapter.4 Development and characterizing of PANI/SEBS conductive polymer via solution blending method

4.1 Introduction

The electrode is a main issue that limits the performance of DEs. Carbon grease will become unreliable for the solvent evaporation, causing increasing resistance after stretched. Conductive polymers composites have attracted significant interest due to their broad applications, such as gaskets, electromagnetic shielding materials, and sensors[130-132]. Flexible conductive elastomers have been prepared through dispersing inorganic conductive materials, such as carbon nanotubes, silver nanowire, or other metal materials, in elastomer matrix [133,134]. However, the conductive materials obtained by above methods have a common issue that is they cannot remain high conductivity under significant strain. The strain ranges of these organic-inorganic materials are below 10%, mostly under 5%. [66]. Polyanilines (PANIs), as typical conductive polymers[67], are drawing great attention for their conductivity, easy preparation and low cost. PANIs were also used as fillers to synthesis conductive elastomer composites using mechanical blending method, but the large strain range and stable conductivity could not be achieved simultaneously[68-70].

Organic soluble PANIs[121] could be prepared in toluene solution. Homogeneous PANI/SEBS composites could be obtained via solution blending method. These conductive elastomers have the same magnitude with carbon-material-filled conductive polymers due to the continuous conductive network formed by percolation theory[101,136], and possess an obvious advantage on strain range and reaction time.

During the dynamic analyzing of the electrical properties of PANI/SEBS composites, we found that the resistivity of material is changing with elongation, which leads to unexpected interesting results. Other researchers' works are showing different trends of resistivity change; both increasing and decreasing were reported, but no theory has been proposed about the principle of changing conductivity. Some conjectures of the relationship between electrical property and structure were carried out to explain the phenomenon. We assumed that the defects clustering and further dispersion caused by stretching were the reason.

The changing conductivity with elongation is not a benefit for the applications as stretchable strain sensors, which can cause unstable signal output while stretching. Still, we found a way to obtain stabilized signals with high reproducibility, which made the PANI/SEBS conductive elastomer a promising material for applications as flexible electrodes and stretchable strain sensors.

4.2 Experiment

Polyaniline toluene solution was prepared in laboratory by following the method reported by Kim et.al [121]. SEBS (YH501T) was provided by China Petroleum & Chemical Corporation of Baling Company. Toluene with purity ≥ 99.7% was purchased from Sinopharm Chemical Reagent Co, Ltd. Aniline, ammonium persulfate(APS), toluene, dodecylbenzenesulfonic acid (DBSA), tetrahydrofuran, acetone were purchased from Sinopharm Chemical Reagent Co, Ltd. All reagents were used as received except as noted.

5.59 g of aniline monomer was added into the emulsion prepared from 200 ml of water mixed with 36.28 g of DBSA and 50 ml of toluene in a cooling bath maintained at 2 ^{o}C for 1 h. 9.13 g of APS dissolved in 50 ml of water was dripped into the polymerization bath for a period of 1 h, and maintained stirring at 0-5 ^{o}C for 17 h. After polymerization was completed, 200 ml of toluene and 200g of acetone was poured into the emulsion and stirred for 1h. The solution was separated into 501.68 g of water layer and 198.36 g of oil layer after being left standing for 1h. The oil layer was vacuum filtrated to remove insoluble and obtained 196.25 g of clarified green oil layer, with a solid content of 4.38%[121].

SEBS was mixed with toluene at 16.5 wt%. in a flask. The flask was heated at 100°C

while stirring till SEBS was completely dissolved, then cooled to room temperature. The 16.5 wt% SEBS toluene solution was added into 3.58 wt% PANI toluene solution at different weight ratio (PANI/SEBS=0,1,2,3,15,25phr), and stirred for 1.5h, then heated in a vacuum oven at 25 ^{o}C -30 ^{o}C afterwards to remove the bubbles in solution. The solution was poured into a self-manufactured PTFE mold and dried at room temperature. Blast drying was proceeded at 30 ^{o}C for 1h to obtain PANI/SEBS conductive elastomer.

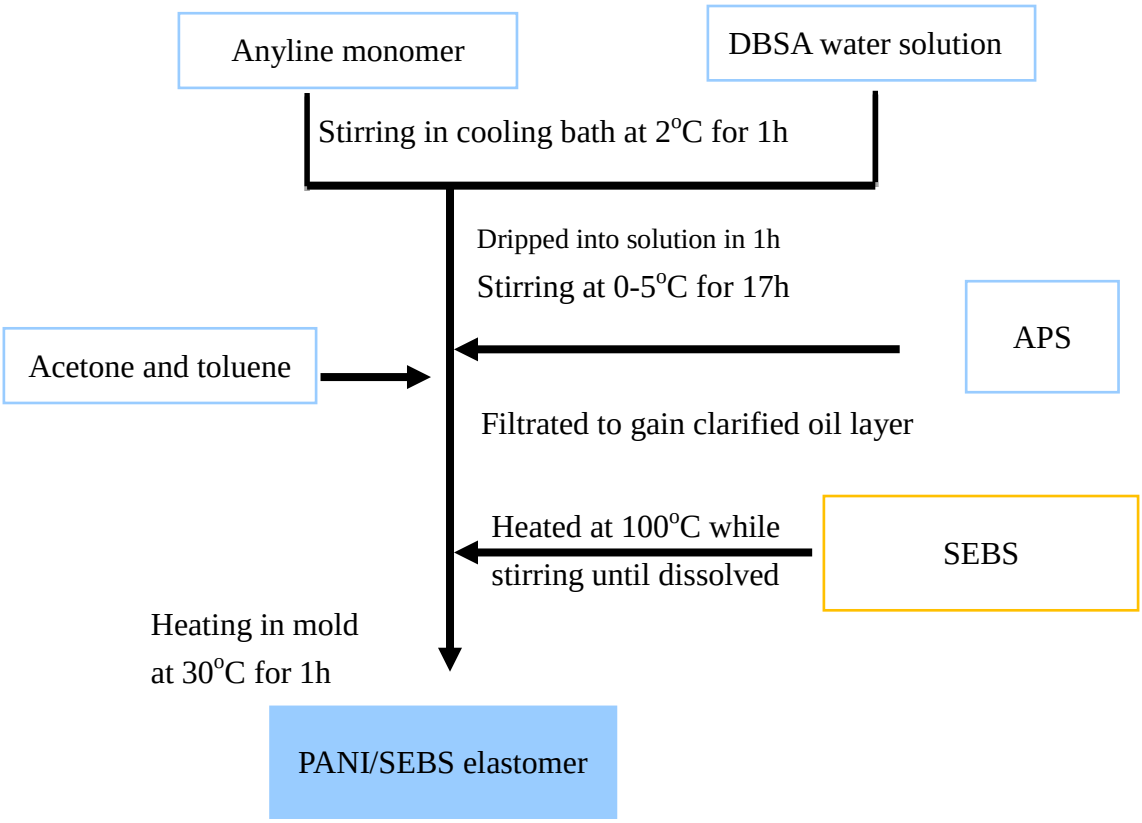

Fig.4-1 Synthesis of PANI/SEBS conductive elastomer

The stress-strain curve was obtained by using a tensile apparatus (Instron Universal Testing Machine, 3367, Instron Engineering Corporation, USA). PANI/SEBS conductive elastomers were characterized by laser-Raman spectrometer (In

Via,Renishaw Corporation, UK). The resistance of PANI/SEBS conductive elastomer was measured by a self-made RVD Circuit and stretch was proceeded by a self-made ball screw slide table.

4.3 Result and discussion

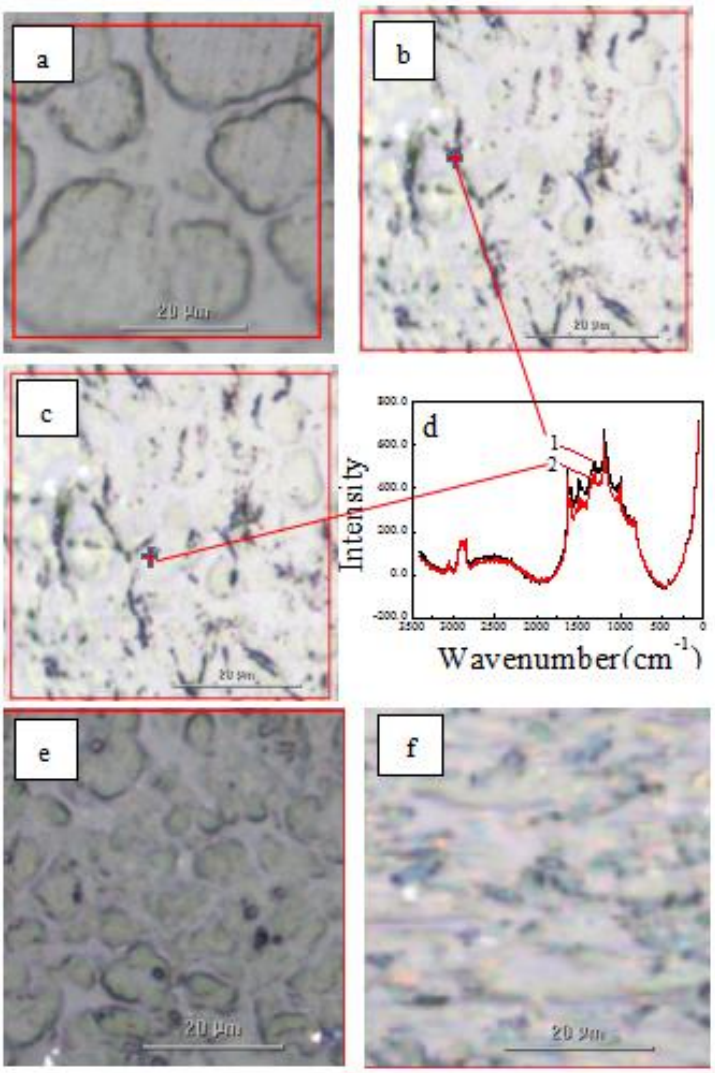

Fig.4-2. the Raman spectra and mapping of material; a: pure SEBS; b; 15 phr SEBS with dot 1; c: 15 phr SEBS with dot 2 d: spectra of dot 1 and 2; e: PANI/SEBS before stretch; f: PANI/SEBS at 100% strain

The Raman spectra showed solid blocks of SEBS formed isolated islands, and soft blocks formed a continuous phase (Fig.4-2-a). After filling with PANI, hard blocks became smaller and the dark PANI parts were located in continuous phase and phase interface, formed a conductive network (Fig.4-2-b). Fig4-2-d showed the raman spectra of dark stripes area resembled blank area which means both area contain similar PANI phase.

The bright dots in Fig,4-3 are the PANI particles dispersed in dark SEBS matrix. Particles in the range of 10 nm to 100 nm were observed. EDS spectra (Fig.4-4) were obtained from the marked spots, confirming these particles contain S and N. As a comparison, EDS spectrum from the black area was obtained as well, where is no S And N detected. We can easily discover that the well dispersed nano-scale PANI particles exist along with the aggregated parts. The conductive network in our system is formed by the nano-scale PANI particles, and aggregated parts cannot contribute to the conductivity.

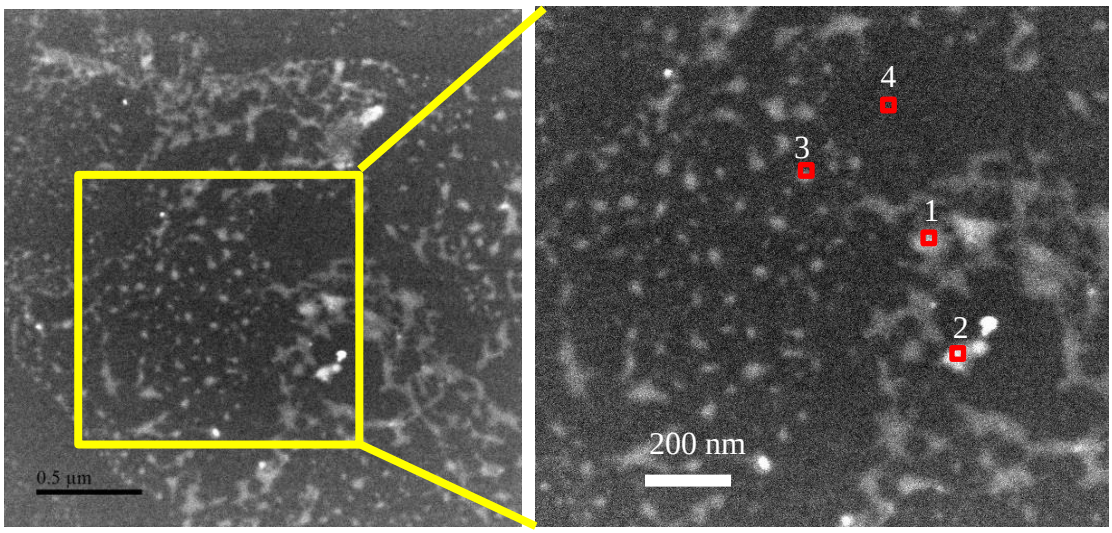

Fig.4-3. The STEM image of PANI/SEBS conductive elastomer

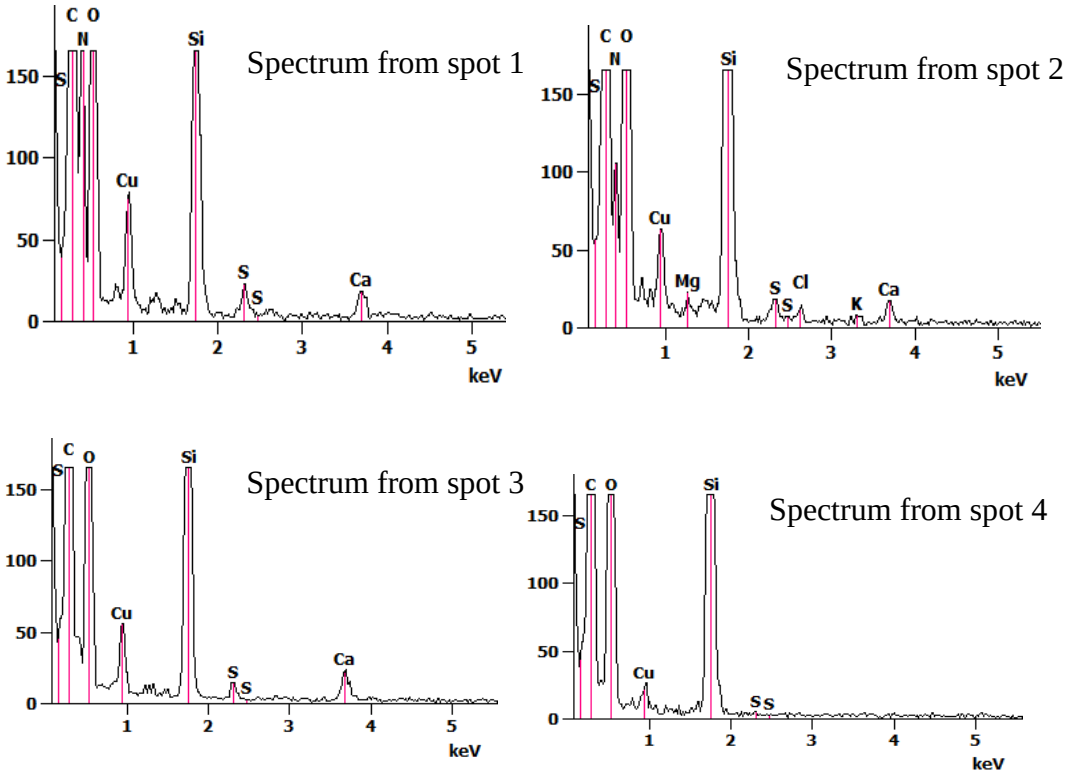

Fig.4-4. The EDS spectra of PANI/SEBS conductive elastomer

Table.4-1 the resistance per centimeter of PANI-SEBS with no stretch compared with PMMA/MWCNT

Charge Amount	**Resistance of PMMA/MWCNT（Ω）**	**Resistance of PANI-SEBS（Ω）**
0phr		$5.75*10^{12}$
1phr	$1.6*10^{7}$	$8.50*10^{11}$
2phr	$6.8*10^{3}$	$2.40*10^{7}$
3phr	$1.6*10^{3}$	$1.35*10^{5}$
25phr		$1.06*10^{3}$

In Fig.4-5 and Table.4-1, the conductive elastomer showed an obvious raise on conductivity with the increasing filling amount of PANI while remaining fine rubber elasticity above the strain of 20%. The material showed a high module below the strain of 20%, but this problem can be fixed by pre-stretch. The conductivity of PANI-SEBS was lower than PMMA/MWCNT reported by Pham et al. at the same charge amount but other advantages was found in later experiments. The resistance was rising before 100% strain and declined afterwards (Fig.4-6). We assume that the elongation of our material lead to a decreasing of resistivity. Before 100% strain, the resistance ascension caused by shape change of sample was dominating, but in large strain, the dropping resistivity

prevailed and resistance started to decrease. The maximum recoverable strain range was up to 100%, that is much higher the composites filled by CNTs with a maximum range less than 5%. Conductive elastomers filled with carbon-based material, especially CNT, needed conductive passages formed with CNT, which requires time to regain former structure or even cannot recover. In our system, due to the evenly dispersed nano-scale PANI conductive phase, the conductive network does not need contacted conductive particles to remain intact, therefore, the conductivity of PANI/SEBS could preserve in large strains.

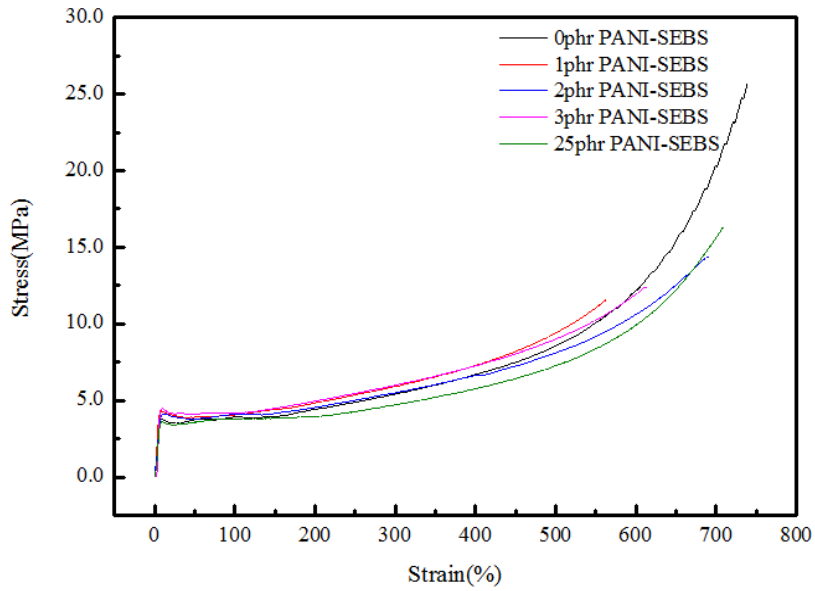

Fig.4-5 stress-strain curve of PANI/SEBS with different filling ratio

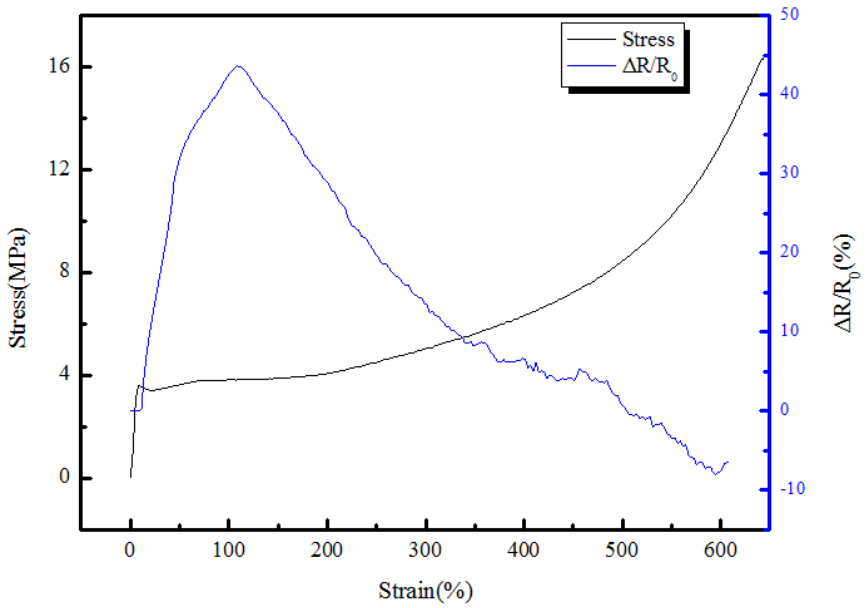

Fig.4-6 stress-strain curve and resistance change of 25 phr PANI/SEBS

The maximum recoverable strain range was up to 100%, that is much higher the composites filled by CNTs with a maximum range less than 5%. We considered the material resumed former structure after stress was removed. Conductive elastomers filled with carbon-based material, especially CNT, needed conductive passages formed with CNT, which need time to regain former structure or even cannot recover. In our system, due to the evenly dispersed nano-scale PANI conductive phase, the conductive network does not need contacted conductive particles to remain intact, therefore, conductivity of PANI/SEBS conductive elastomer could preserve in large strain.

Table. 4-2 Key paraments compared with other reported conductive polymers

Matrix	Filler	Dispersion method	Content	Y[MPa]	ρ[Ω·cm]	Stretchability
SEBS	PANI[137]	Mechanical Blending	31 wt.%	7.4	1.78	< 50%
MA-SEBS	PANI[138]	Grafting	20 vol.%	0.6	6.7e-4	< 300%
PP/MA-SEBS	CNT[139]	Mechanical Blending	10 wt.%	1020	7.1	< 5%
SEBS	PANI	Solution blending	25 phr	15	12.5	> 600%

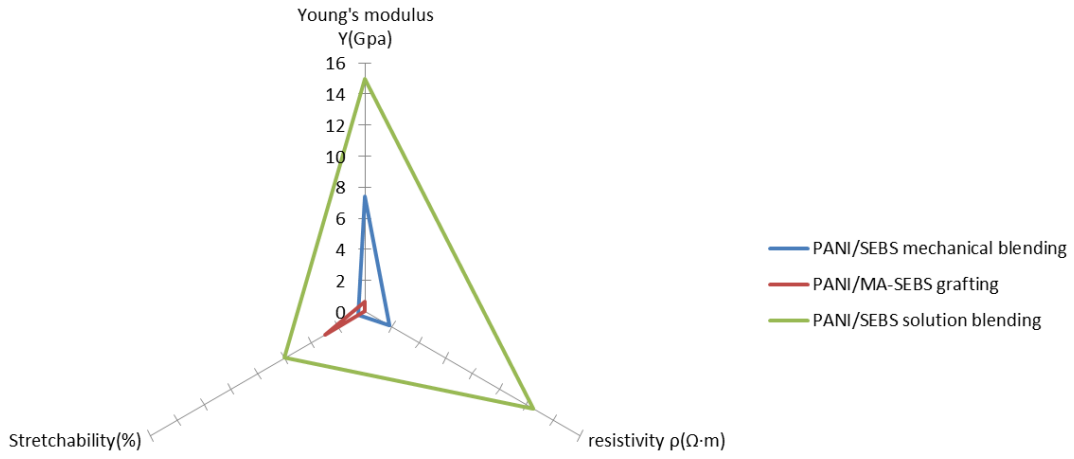

Fig. 4-7 The major parameters of PANI/SEBS conductive elastomer compared with reported materials

From Table.4-2 and 4-7we can see that the conductive elastomer we prepared have

less advantage on conductivity compared with other reported materials, so is the modulus. However, our material can maitain conductive over 600% strain, which can not be achieved by any reported material. The material prepared with PANI grafed to MA-SEBS reported by Stoyanovs[138] showed a very high conductivity, but the grafted PANI can only exist on the surface and shallow of the material, which means only the surface of the material is conductive, the exhibited low volume resistivity is due to the low surface resistivity. Therefore, the material can only be used as thin film. As the thickness of this material grows, the volume resistivity will be increasing greatly. On the other hand, the materials prepared with solution blending method have well dispersed conductive fillers in the whole material, thus our materials can be applied as any shape, such as films or bulk materials.

In Fig4-6 we also found that the resistance of the material is decreasing when stretched. In order to study the electrical properties of the material better, we calculated the resistivity of the material to remove the effect caused by shape changing. The Fig.4-8 is showing that the resistivity of the conductive elastomer is decreasing with elongation as we discussed before. The stretch of sample will cause an increase of the area of the interface between PANI and polymer matrix, and defects might cluster on the phase interfaces. These defects will provide more conductive passages and lead to a

decreasing resistivity [140].

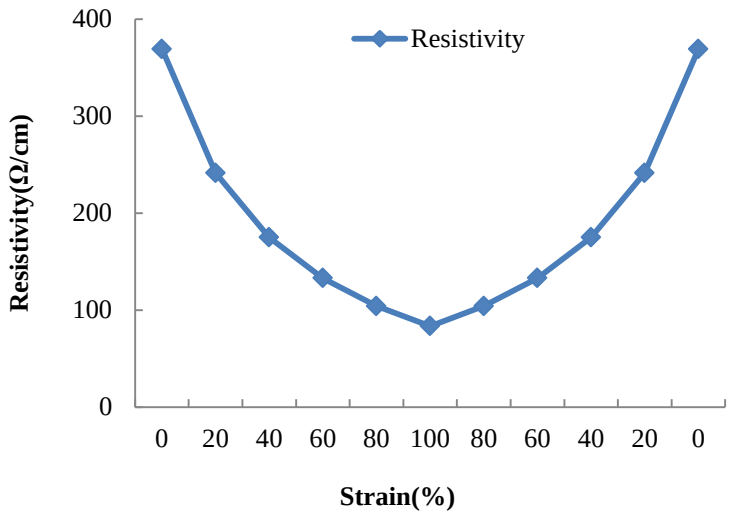

Fig.4-8 Resistivity of PANI/SEBS at different strain ratio

Fig.4-6 is showing that the resistance of PANI/SEBS samples was increasing before 100% strain and decreasing after reaching the peak. We assume that the resistance change of samples was affected by two phenomena. One is the resistance increasing caused by the deformation of samples while stretching, and the other one is the resistivity reducing due to the structural deformation in the material. Before 100% strain, the resistance was increasing for the resistance increasing caused by deformation of samples was dominating. After 100%, the dropping resistivity took over and the resistance started to reduce. The structural deformation is slower than shape change thus the resistance change showed a rising then descending curve. We assume that the slower stretching speed would give the samples longer respond time so the resistance peak

would show earlier. The black and red line in Fig.4-9 confirmed our assumption.

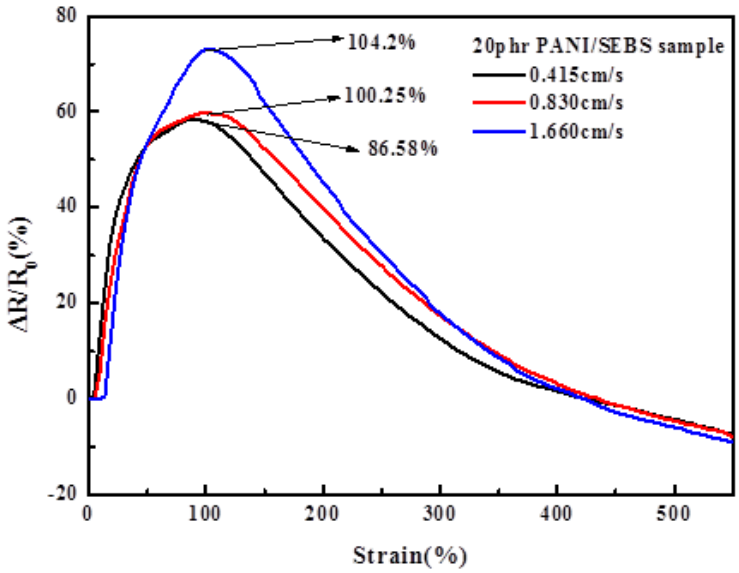

Fig.4-9 The resistances changes with strain of PANI/SEBS conductive elastomer at different stretching speed

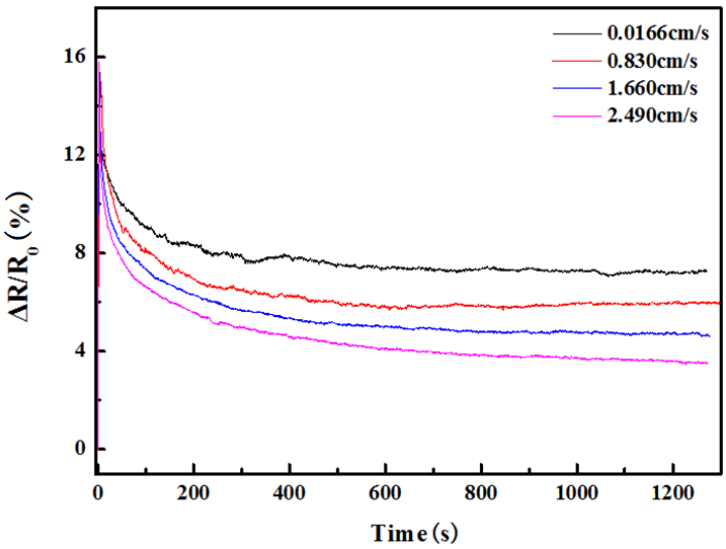

Fig.4-10. The resistance changes with time of PANI/SEBS conductive elastomer at 100% strain with different stretching speed

Fig.4-10 is showing resistance change with time of PANI/SEBS samples stretched by different speed from 0% strain to 100%. As the stretching speed slow down, the samples need less time to recovery to the stabilized condition with a higher resistance. The results are also suggesting that the structure change of the samples is slower than the shape deformation.

The resistance change of material is suggesting that the resistivity of samples is decreasing with elongation. Fig.4-11 shows the decreasing resistance of samples after stretched to a certain strain ratio. The sample was stretched to a certain strain ratio (20, 40, 60, 80, 100, 120 and 140%) and left standing still for several minutes while measuring resistance. The results are showing that the resistances at every strain rate are decreasing obliviously and settled after a while, suggesting a reducing resistivity.

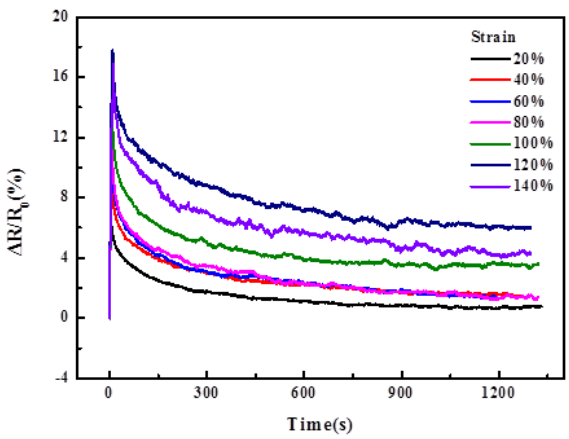

Fig.4-11. The resistance changes with time of PANI/SEBS conductive elastomer at different strain ratio

Unlike carbon nanotubes filled composites, PANI can hardly form a continuous conductive phase in SEBS matrix since PANI and SEBS are incompatible systems. However, the conductivity test showed a different conclusion that continuous conductive network exist in this composite. Therefore we assumed that a nanoscale conductive phase was also dispersed in SEBS matrix coexisting with micron level conductive phase (Fig.4-12). PANI may form a thermoplastic IPN like structure which is not truly IPN structure but a partially interlaced network formed by physical bonds. When the material was stretched, the distance between conductive particles increased. The reason conductive network could remain intact when stretched was because of the existing of nanoscale PANI conductive phase dispersed in SEBS matrix.

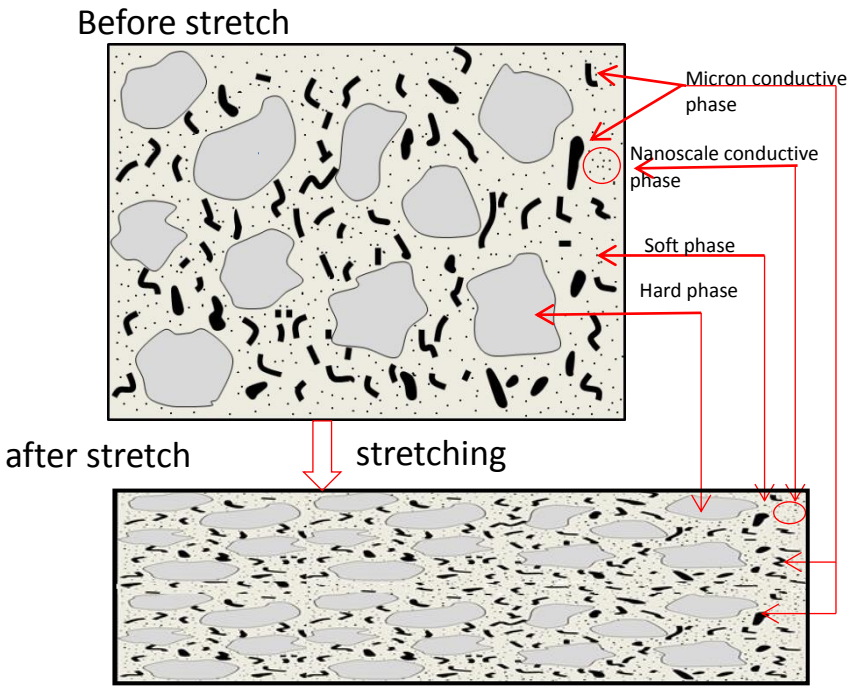

Fig,4-12 Hypothetical structure of PANI/SEBS elastomer

PANI and SEBS are incompatible systems thus PANI cannot form a continuously conductive phase in SEBS matrix. We assume that the conductivity of PANI/SEBS composite is from the conductive network formed by dispersed PANI particles according to percolation theory. One phenomenon affecting the resistivity is that the area of the interfaces between PANI and SEBS polymer matrix will increase during stretching, and causing the defects clustering on the phase interfaces. More conductive passages will form on the defects clusters and leading to a decreasing resistivity.

The Raman spectra (Fig.4-13a) is showing that some of the PANI particles are aggregated and these parts do not contribute to the conductivity of material. As the sample was stretched, the aggregated structure was split and formed with smaller dispersed particles (Fig.4-13b). This phenomenon is also forming more conductive passages and causing higher conductivity.

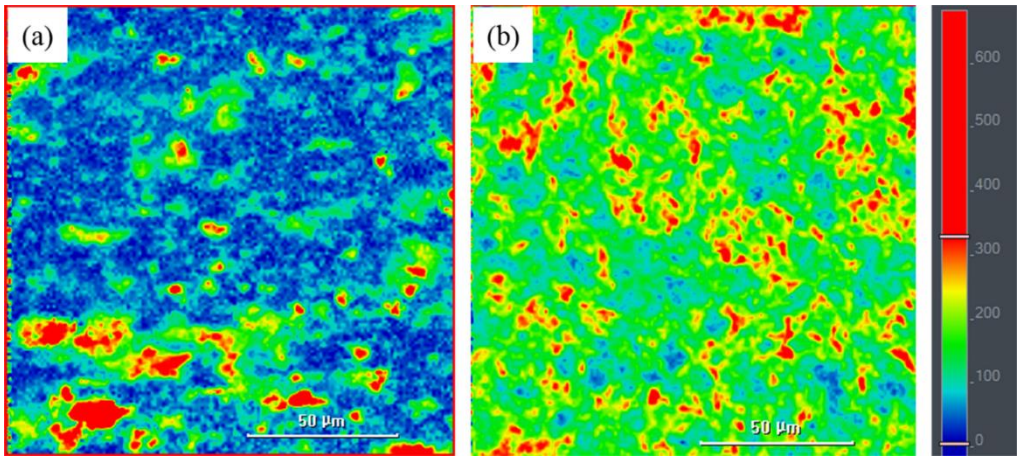

Fig.4-13. The Raman spectra of PANI/SEBS conductive elastomer; a: before stretching, b: stretched to 100% strain

The shape deformation and structure change are not synchronized, which is a big problem if we want to apply the material as a resistance sensor. We tried to minimize the influence of this phenomenon by restrict the strain rate at a small range, for example, 80% to 100%. Fig.4-13 showed that after a few times of stretching, the resistance changes were limited at a very small range and the effect of non-synchronized structure change has been reduced to a certain level.

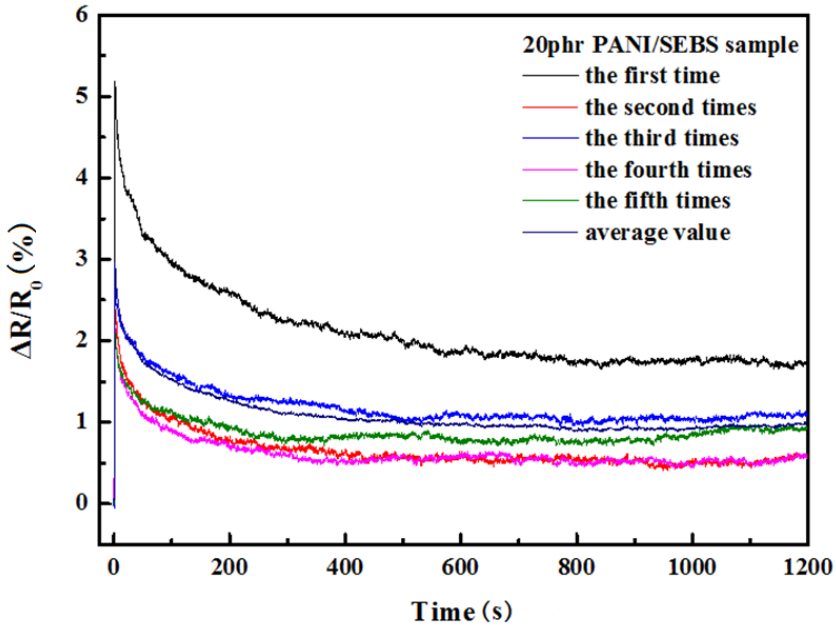

Fig.4-14. The resistance changes with time of PANI/SEBS conductive elastomer stretched from 80% strain to 100%

The resistivity change with elongation has been confirmed and leading to an unpredictable resistance value at different stretching speed. Even though we still found a stable interval at a certain stretching speed. After a few times of stretches the resistance change tend to be settled down (Fig.4-14). Fig.4-15 is showing that the sample is monotonic between strain ratios of 80-100% with high reproducibility. This property could be a very promising application as stretchable strain sensors.

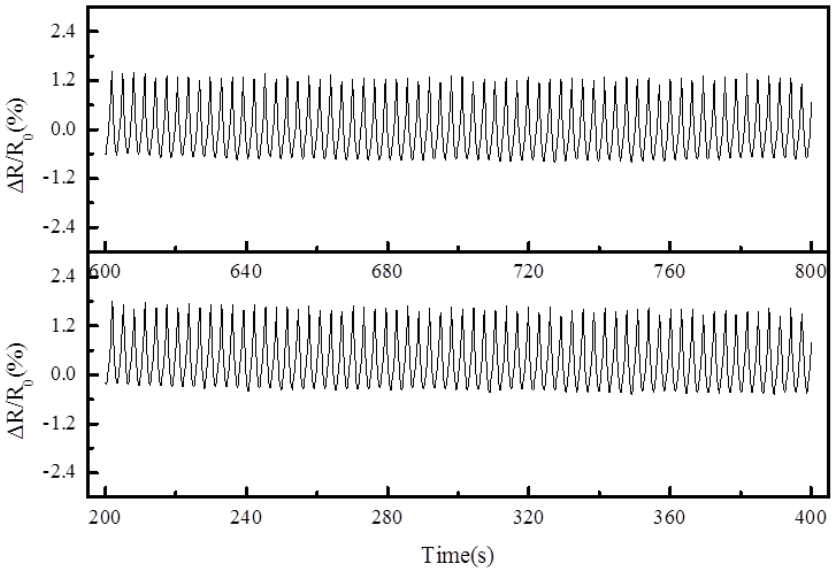

Fig.4-15 The resistance change of PANI/SEBS conductive elastomer while stretching and releasing between 80-100% strain

4.4 Conclusion

PANI/SEBS conductive elastomer is an excellent flexible conductive material with large strain range and relatively good conductivity. The resistivity was found changing with elongation during analyzing, affecting the resistance of material. The structural principles of resistivity change were discussed and reducing resistivity caused by stretching was confirmed. A method of eliminating this effect was discovered for applications as stretchable strain sensors.

Chapter 5 Development and characterizing of CCTO/SEBS dielectric elastomer as capacitive strain sensors

5.1 Introduction

The application of dielectric elastomers as actuators is limited by the high driving voltage. It's impossible to maintain a certain level of modulus with high permittivity at the moment. However, as an electroactive polymer, the dielectric elastomers could be used as materials for strain sensors, which could be applied as soft robots, wearable devices, movements monitoring and virtual reality technologies due to its durability, linear sensing and rapid response [71-74]. Among which, the stretchable strain sensors are drawing attention for their ability of outputting signal while large strain [75, 76]. The stretchable strain sensors could be divided into resistance sensors and capacitive sensors by the sensing mechanism. The resistance sensors are usually fabricated by polymers filled with conductive fillers. The resistance changes during the stretch are decided by both the micro structural deformation and the function between strain and resistance [77]. Capacitive strain sensors were formed with a dielectric layer sandwiched between a pair of stretchable electrodes, the capacitance change are determined by the permittivity and thickness of dielectric layer [71, 78, 79]. Compared with resistance sensors,

the capacitive strain sensors showed linear relationship between strain and capacitance, with fine hysteresis properties [80, 81].

As the key factor of capacitive strain sensors, selecting proper material for dielectric layer can improve the sensing ability [81]. SEBS is a common thermoplastic elastomer with fine elasticity, plasticity [141,142], and low dielectric constant which limited the applications of SEBS as dielectric materials. Calcium copper titanate (CCTO) is a material with huge dielectric constant which could be used as fillers to improve the dielectric properties of composites[143,144]. At 4 MPa pressure the permittivity of CCTO/PDMS of 50 wt.% was improved about three times, but its loss value has been raised by less than twice that of the composites without pressure[145]. Thus we can achieve SEBS composites with higher permittivity by filling CCTO particles.

Electrodes are another key factor for capacitive strain sensors[138,146]. Its very complicated to obtain conductive materials which can maintain conductivity in large strain rate. Existing stretchable conducting materials have been prepared based on organic-inorganic composites such as carbon nanotubes dispersed in rubber matrix[147-149], or metal waves and nets structures like silver nanowire embedded in a soft elastomer matrix[150]. However, the strain range of these kinds of electrodes are normally less than 60% which is hard to applied as electrodes of large-strain

sensor[119,128,129].

In this paper, we synthesized CCTO/SEBS dielectric elastomer as dielectric layer of capacitive sensor, and PANI/SEBS conductive elastomer is also developed for the stretchable electrodes. The XRD, SEM and Raman spectra were processed to characterize the CCTO/SEBS, and dielectric property of material was also tested. We manufactured the capacitive strain sensor through thermoforming process and studied the capacitance change at different conditions, proved CCTO/SEBS a promising material for applications as flexible sensors.

5.2 Experiment

5.2.1 Materials

Aniline, ammonium persulfate(APS), toluene, dodecylbenzenesulfonic acid (DBSA), tetrahydrofuran, acetone were purchased from Sinopharm Chemical Reagent Co, Ltd. SEBS (styrene-ethylene-butylene-styrene block polymer) (YH501T) was provided by China Petroleum & Chemical Corporation of Baling Company. CCTO with particle size of 300nm were provided by ShangHai Dian Yang Industry Co.Ltd, China. Waterborne polyurethane (WPU) was purchased from Bayer AG, Germany. All reagents were used as received except as noted.

5.2.2 Synthesis of CCTO/SEBS dielectric elastomer

SEBS and toluene (weight ratio 5:1) were stirred and condensed at 100 ^{o}C in a flask until SEBS were fully solved, then cooled at room temperature. A certain amount of CCTO was added into the SEBS's toluene solution (CCTO: 0phr, 5phr, 15phr, 25phr; SEBS: 100phr) and ultrasound dispersed for 30 mins, then stirred at room temperature for 1h. Negative pressure (-0.4 MPa) was processed to remove the bubbles in solution, then the mixture was poured into molds and dried at room temperature.

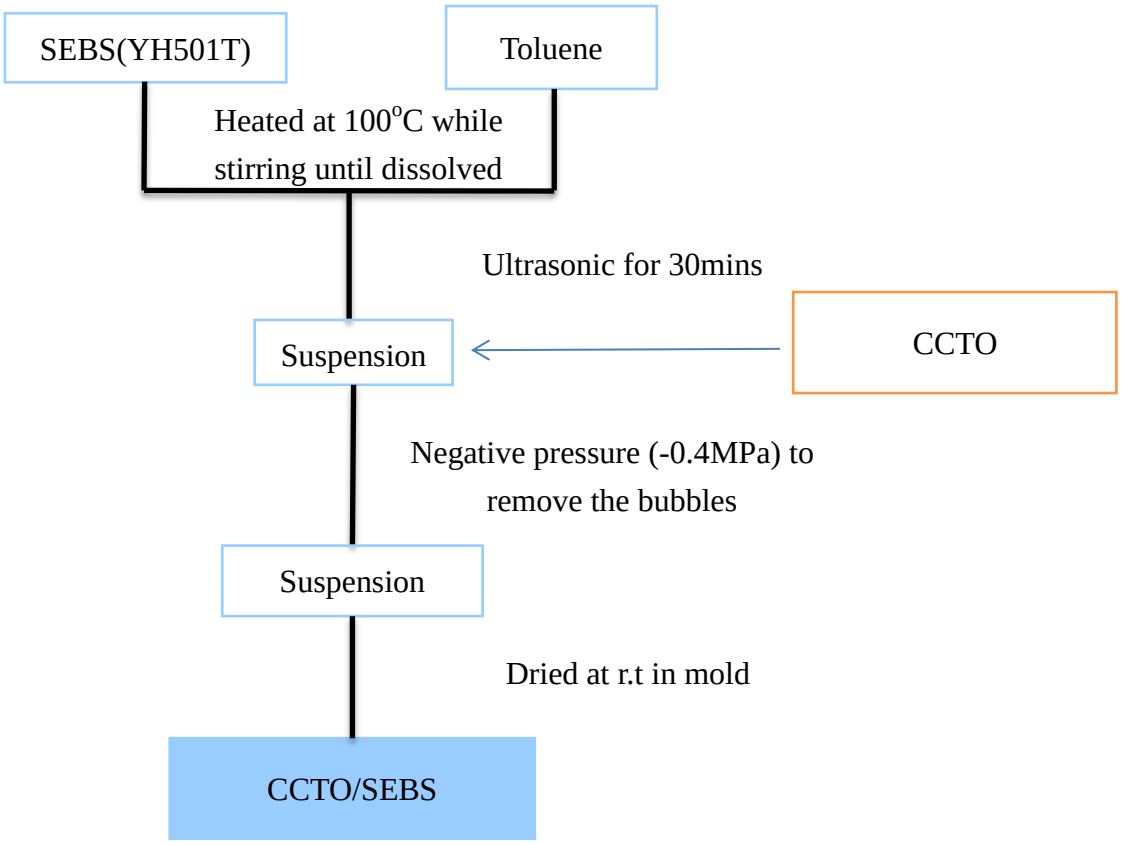

Fig.5-1 Synthesis of CCTO/SEBS

5.2.3 Synthesis of PANI/PDMS composite

5.59 g of aniline monomer was added into the emulsion prepared from 200 ml of water mixed with 36.28 g of DBSA and 50 ml of toluene in a cooling bath maintained at 2°C for 1h. 9.13g of APS dissolved in 50ml of water was dripped into the polymerization bath for a period of 1h, and maintained stirring at 0-5°C for 17h [121]. After polymerization was completed, 200 ml of toluene and 200g of acetone was poured into the emulsion and stirred for 1h. The solution was separated into 501.68 g of water layer and 198.36 g of oil layer after being left standing for 1h. The oil layer was vacuum filtrated to remove insoluble and obtained 196.25 g of clarified green oil layer, with a solid content of 4.38%.

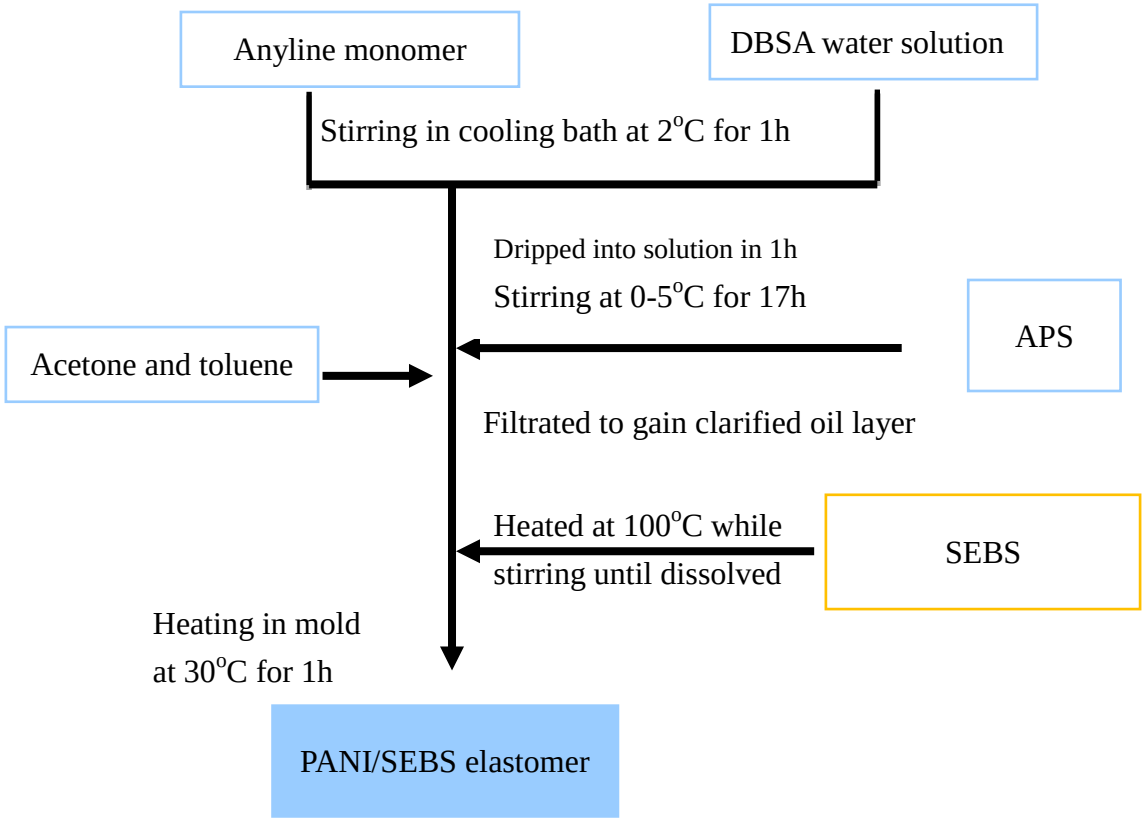

Fig.5-2 Synthesis of PANI/SEBS elastomer

Take an example of filling rate at 0.2wt%, we mixed 0.15g of dodecylbenzenesulfonic acid modified polyaniline in toluene solution, 3.3g of PDMS and 0.17g of curing agent for 20mins, obtaining a homogeneous solution of PANI/PDMS, then poured the above solution into self-made Polytetrafluoroethylene mold and heated at 30°C for 24h. After fully cured, the sample was removed from mold and PANI/PDMS composite with a thickness of 0.5mm was obtained.

5.2.4 Preparing of CCTO/SEBS capacitive strain sensor

PANI/SEBS samples were cut into films of 70x10mm, and CCTO/SEBS samples were cut into films of 120x15mm. The PANI/SEBS and CCTO/SEBS were pasted by

WPU to form a sandwich-like structure, and thermoforming at 80°C for 3h then cooled to room temperature to obtain CCTO/SEBS capacitive strain sensor (Fig.5-1).

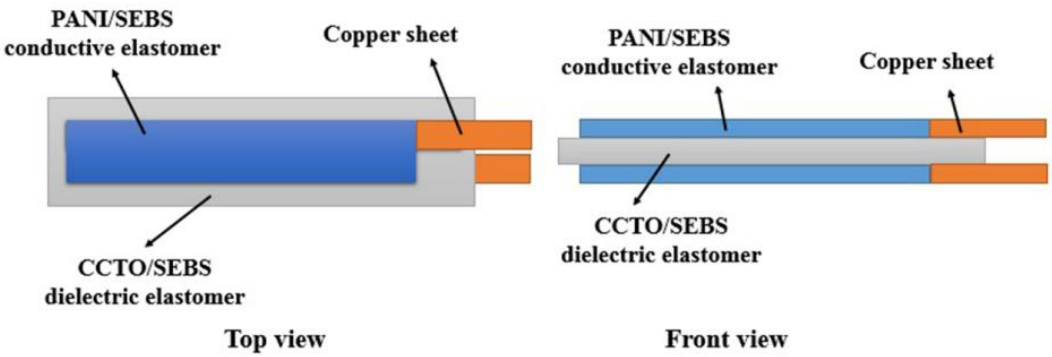

Fig.5-3 The geometric diagram of CCTO/SEBS capacitive strain sensor

5.2.5 Characterizing

DXR Raman spectrometer was provided by Thermo Electron Corporation. Varieties were analyzed after doping magnesium. Sample powders were poured on slides and compacted. Testing range was 4000-400 cm^{-1}, laser wavelength was 532 nm, resolution was less than 2cm^{-1}. Electrically conductive Perfluoropolyether grease was evenly coated on both sides of dielectric elastomer. High voltage of 0-12V/μm was applied on electrodes by a high voltage power supply. The deformation of dielectric elastomer and scale under different voltages were recorded by a digital camera. The image obtained was treated with image enhancement, tilt correction, edge extraction and position recognition in order to retrieve deformation displacement data of dielectric elastomer. XRD data of all samples was obtained at diffraction angle range of 10 to 80°, with

0.600° per steps, processed with a Bruker AXS D8 Advance X-ray diffractometer. The micro structure of samples was analyzed by an S-4800 II FE-SEM, Hitachi. Co.Ltd, Japan, and ThermoFisher DXRxi Raman imaging microscope. The dielectric properties were tested by Concept 80 dielectric spectrometers, Novocontrol Technologies, Germany. The capacitance changes were recorded by C-Stretch system from Bando chemical industries. Ltd, Japan.

5.3 Result and discussion

5.3.1 Structural characterizing

Fig.5-4 is the XRD pattern of pure SEBS and CCTO/SEBS with different filling amount. The pattern is showing that the dielectric elastomer only contain SEBS and CCTO two phases, and the CCTO peaks changes with the filling amount of CCTO.

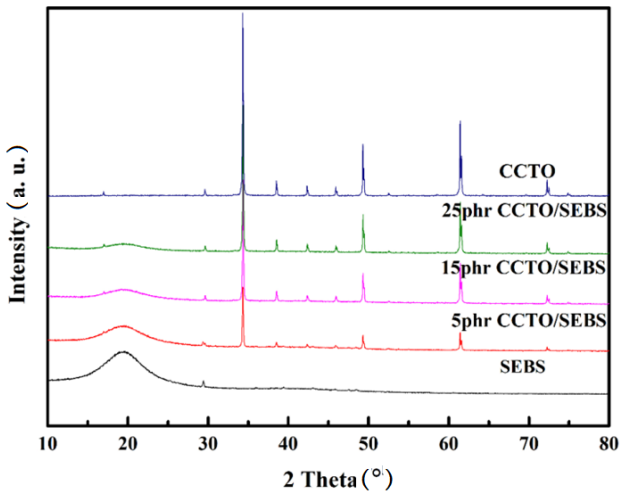

Fig.5-4 The XRD spectrum of pure SEBS and CCTO/SEBS composites filled with different amount of CCTO

The SEM images are showing that the micro structure of SEBS is wave shaped with holes existed (Fig.5-5-a). After the filling of CCTO, the surface of CCTO was smooth and CCTO particles were embedded in the holes without shedding or agglomerating (Fig.5-5-b,c,d).

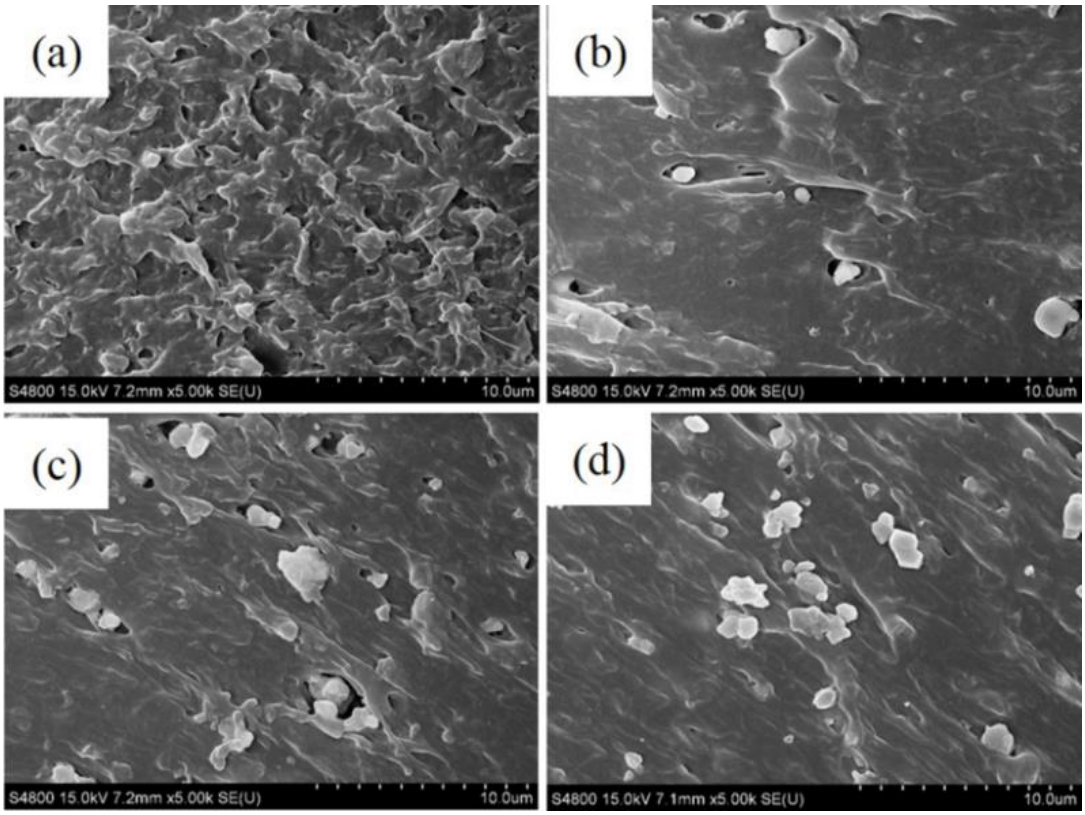

Fig.5-5 The SEM image of SEBS and CCTO/SEBS(a:pure SEBS; b: 4.7 wt% CCTO; c:13wt% CCTO; d: 20wt% CCTO)

Fig.5-6 is the Raman spectra of CCTO/SEBS dielectric elastomer. Fig.5-6-a is imaged at peak intensity ratio of 425cm-1. From Fig.5-6-b we can easily find that the peak intensity of green area is stronger than blue area at wavenumber of 425cm-1 and 510cm-1, which means the green area represents CCTO existence and blue area is

SEBS. Fig.5-6-a is showing that CCTO particles are well dispersed in SEBS matrix under the observing of 100 micrometers scale, perfectly matching the result from 10 micrometers scale's observation by SEM, indicating that the CCTO is well dispersed at submicroscopic and macro scales.

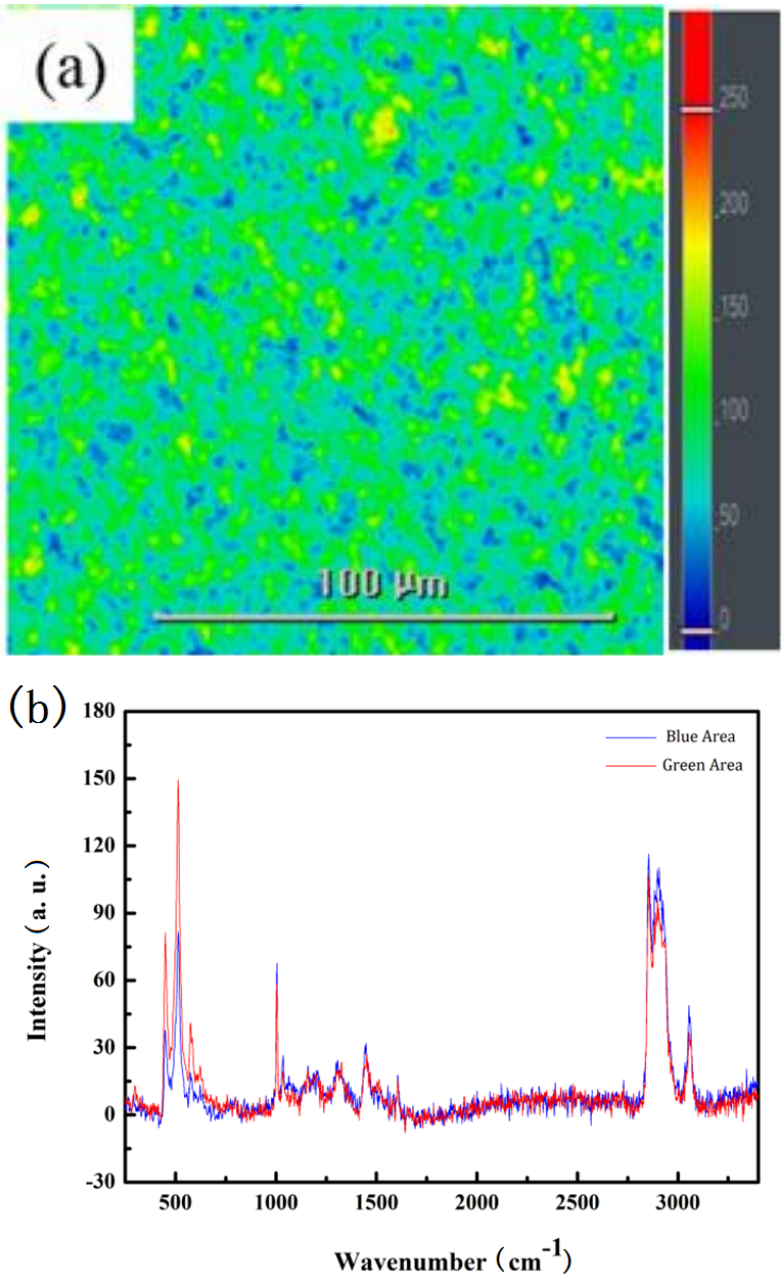

Fig.5-6 Raman image(a) and spectra(b) of 25phr CCTO/SEBS dielectric elastomer

5.3.2 Dielectric properties

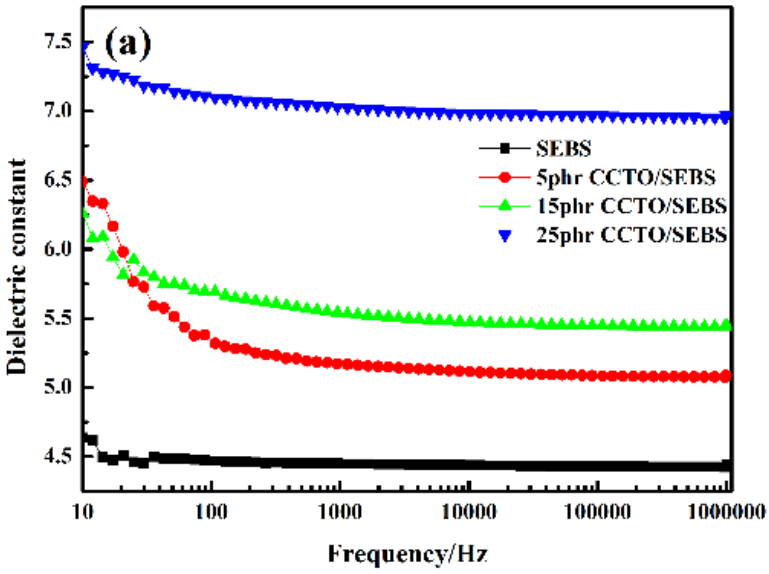

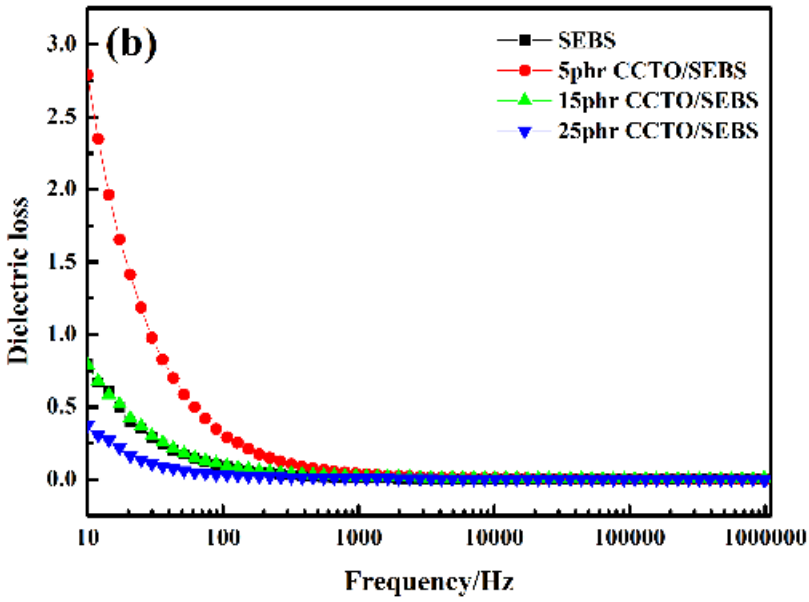

Fig.5-7 The dielectric constant(a) and dielectric loss (b) of CCTO/SEBS dielectric elastomer

Fig.5-7 shows the dielectric constant and dielectric loss of CCTO/SEBS dielectric elastomer. The permittivity of CCTO/SEBS increases as the addition of CCTO particles. The permittivity of composite filled with 25phr CCTO have reached 7.3, which is 70% higher than pure SEBS, while only minor change of dielectric loss have occurred. For the unnormally high dielectric loss and rapid reduce of sample filled with 5 phr CCTO at low frequency, we found that the sample have some aggolomorated clusters of particles at the surface, causing leakage current at low frequency.

5.3.3 Capacitance tests

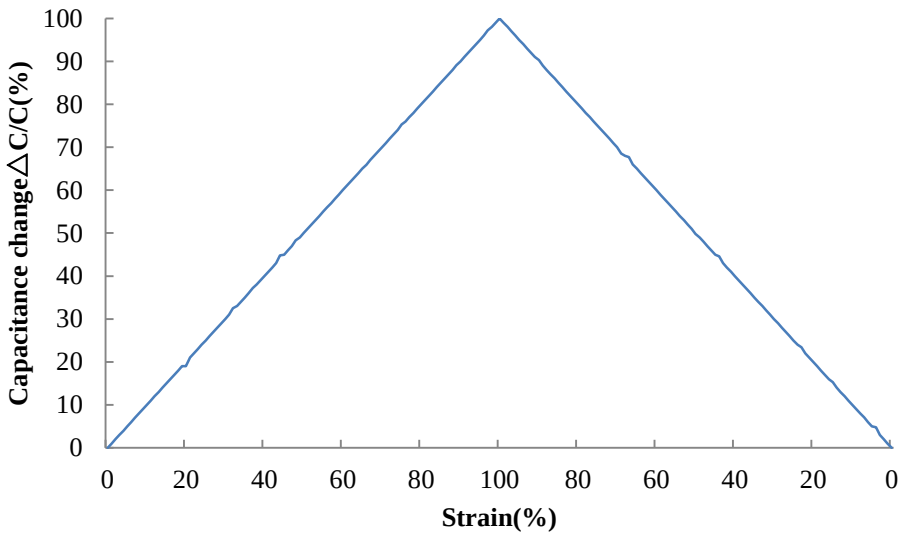

Fig.5-8 The capacitance response to strain

From the Fig.5-8 we can see that the capacitance response to strain was linear. The simple parallel-plate model also predicts a linear capacitive response to the applied strain. In addition, the capacitive gauge factor, defined as $(\Delta C/C_0)/(\Delta l/l_0)$, equals to 1.

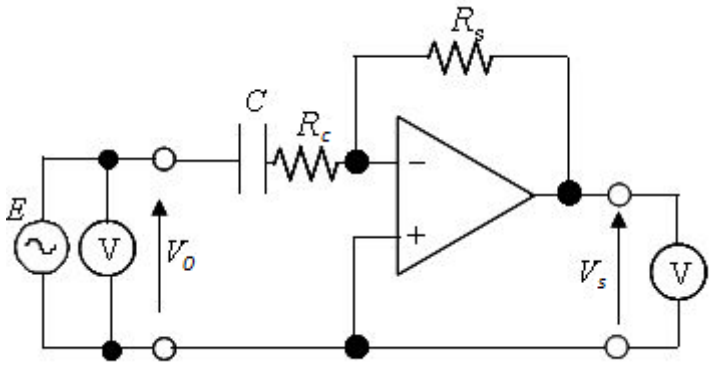

Fig.5-9 circuit diagram of capacitance testing

The circuit diagram of capacitance testing circuit could be described as Fig.5-9, when applied voltage V_0, we have:

$$\frac{V_s}{V_0} = -\frac{R_s}{Z_c} \tag{1}$$

For the capacitive resistance Z_c we have:

$$Z_c^2 = R_c^2 + (\frac{1}{\omega C})^2 \tag{2}$$

Where R_c is the resistance of electrodes we used.

In order to understand the relationship between output signal V_s and strain $\triangle l/l$, we simplified the relationship of resistance and deformation from the blue line in Fig.4-6 to:

$$\begin{cases} \frac{dR}{dl} = 0.45\frac{R_0}{l_0}, \frac{\Delta l}{l_0} < 1 \\ \frac{dR}{dl} = -0.02\frac{R_0}{l_0},, \frac{\Delta l}{l_0} > 1 \end{cases} \tag{3}$$

For capacitance C, from fig.5-8 we have:

$$\frac{dC}{dl} = \frac{C_0}{l_0} \tag{4}$$

From equation (1) and (2), we have:

$$|V_s| = \frac{R_s|V_0|}{|Z|} = \frac{R_s|V_0|}{\sqrt{R^2+\left(\frac{1}{\omega C}\right)^2}} \tag{5}$$

Derivate (5) we have:

$$\frac{d|V_s|}{dl} = \frac{\partial|V_s|}{\partial R}\frac{dR}{dl} + \frac{\partial|V_s|}{\partial C}\frac{dC}{dl} \tag{6}$$

$$\frac{\partial|V_s|}{\partial R}\frac{dR}{dl} = -\frac{\frac{\partial\sqrt{R^2+\left(\frac{1}{\omega C}\right)^2}}{\partial R}R_s|V_0|}{R^2+\left(\frac{1}{\omega C}\right)^2}\frac{dR}{dl} = -\frac{\frac{\frac{\partial R^2+\left(\frac{1}{\omega C}\right)^2}{\partial R}R_s|V_0|}{2\sqrt{R^2+\left(\frac{1}{\omega C}\right)^2}}}{R^2+\left(\frac{1}{\omega C}\right)^2}\frac{dR}{dl} = -\frac{R_s|V_0|R}{\left[R^2+\left(\frac{1}{\omega C}\right)^2\right]^{3/2}}\frac{dR}{dl} \tag{7}$$

$$\frac{\partial|V_s|}{\partial C}\frac{dC}{dl} = -\frac{\frac{\partial\sqrt{R^2+\left(\frac{1}{\omega C}\right)^2}}{\partial C}R_s|V_0|}{R^2+\left(\frac{1}{\omega C}\right)^2}\frac{dC}{dl} = -\frac{\frac{\partial\left(\frac{1}{\omega C}\right)^2+R^2}{2\partial C}R_s|V_0|}{\left[R^2+\left(\frac{1}{\omega C}\right)^2\right]^{\frac{3}{2}}}\frac{dC}{dl} = \frac{R_s|V_0|}{\omega^2\left[C\sqrt{R^2+\left(\frac{1}{\omega C}\right)^2}\right]^3}\frac{dC}{dl} \tag{8}$$

To compare the influence of R and C to the output signal V_s, we compared $\frac{\partial|V_s|}{\partial R}$ and $\frac{\partial|V_s|}{\partial C}$. The capacitance of our sensor is about 100-200pF, and resistance of our electrode is about 1-2 kΩ, length of the samples are about 0.1m and frequency used in the circle was 10 kHz, so here we take $C_0 \approx 100pF$, $R \approx 1000\Omega$, $l_0 \approx 0.1m$, $\omega \approx 2\pi * 10^4 Hz$ to approximately calculate dV_s, then we have

$$\left|\frac{\frac{\partial|V_s|}{\partial R}}{\frac{\partial|V_s|}{\partial C}}\right| = \frac{\frac{R_s|V_0|R}{\left[R^2+\left(\frac{1}{\omega C}\right)^2\right]^{\frac{3}{2}}}}{\frac{R_s|V_0|}{\omega^2\left[C\sqrt{R^2+\left(\frac{1}{\omega C}\right)^2}\right]^3}} = \omega^2 RC^3 \ll 1$$

We can see that the effect of electrode's resistance change is much smaller than the effect of capacitance change. If the applied voltage was higher frequency, the influence

of resistance cannot be ignored.

Fig.5-10 shows the capacitance-time curve of capacitive sensors fabricated with different dielectric layers when stretched for 20 times repeatedly. The capacitance of sensor is increasing with the stretching and decreasing with relaxing, due to the area and thickness changes of dielectric layer. Compared with Cstretch strain sensor purchased from Bando chemistry ltd., our sample is showing higher signal output, means less error caused by noise.

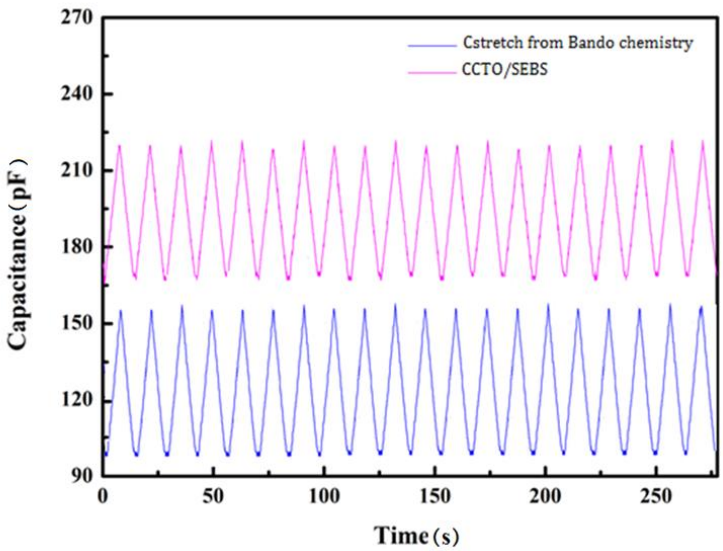

Fig.5-10 The capacitance-time curve of CCTO/SEBS capacitive strain sensor with compared with sensor purchased from bando chemistry ltd.

The capacitance change at different tensile ratio was shown in Fig.5-9. We can clearly observe from the figure that the sensor have a linear relationship between capacitance and strain, and the capacitance change have almost have the same ratio

compared to the strain, suggesting the gauge factor is about 1.

Table.5-1 Performance results compared with other capacitive stretchable strain sensors

Materials	Stretch ability	Gauge factor
CNTs-Dragon-skin[151]	300%	0.97
CNTs-Ecoflex[152]	150%	1
CNTs-silicone[153]	100%	0.99
PANI/SEBS-CCTO/SEBS	600%	0.99

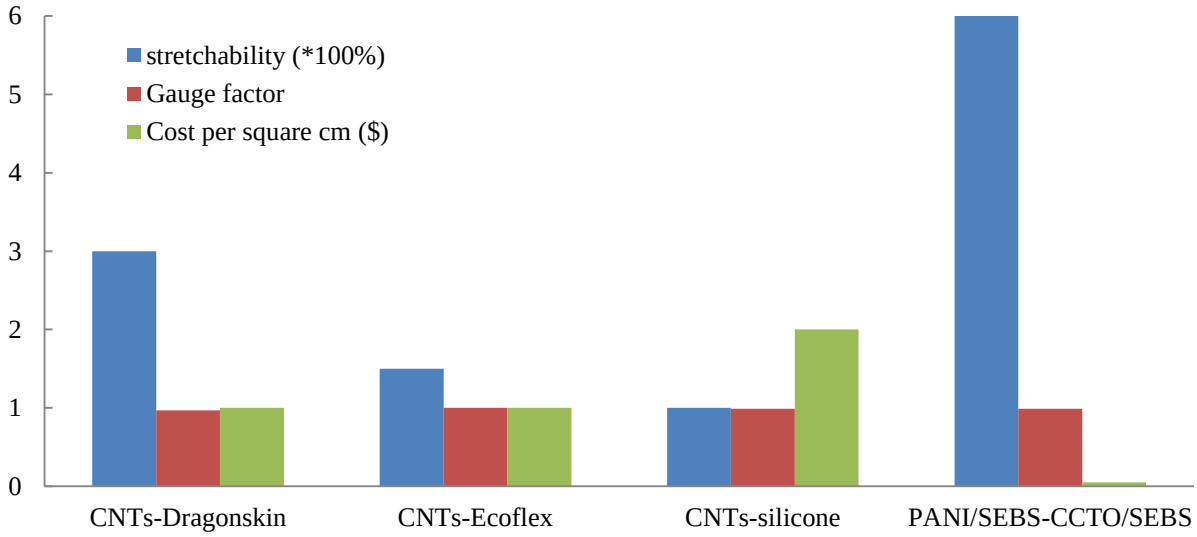

Fig.5-11 The major parameters of PANI/SEBS-CCTO/SEBS strain sensor compared with reported sensors

Compared with other capacitive stretchable strain sensors recently reported listed on Table.5-1, the gauge factors of the materials were almost the same value for the capacitance is linear with strain. The maximum of our material is obviously larger than

any reported sensors. Besides, although nor reported, the signal output of our materials supposed to be larger than other sensors due to the high permittivity of CCTO/SEBS we used as dielectric layer. The electrodes of reported strain sensors are mainly CNTs based, such as CNTs films prepared by CVD method [151], or CNTs solution coated to the surface or elastomer by air-spray [152,153]. The micrometer-sized voids exist in the CNTs films prepared by these methods, and these voids might lead to unpredictable capacitive responses due to the unstable overlap between the opposing CNT films. The large value of deviation of resistance will also lead to unreliable strain gauging performance [153]. In addition, in spite of the other researchers assert that their materials are low cost, the fact is, the long-chain CNTs they used are very expensive precisely. By using PANI/SEBS as electrodes, we genuinely designed a capacitive stretchable strain sensor with easy process and low cost (Fig.5-11).

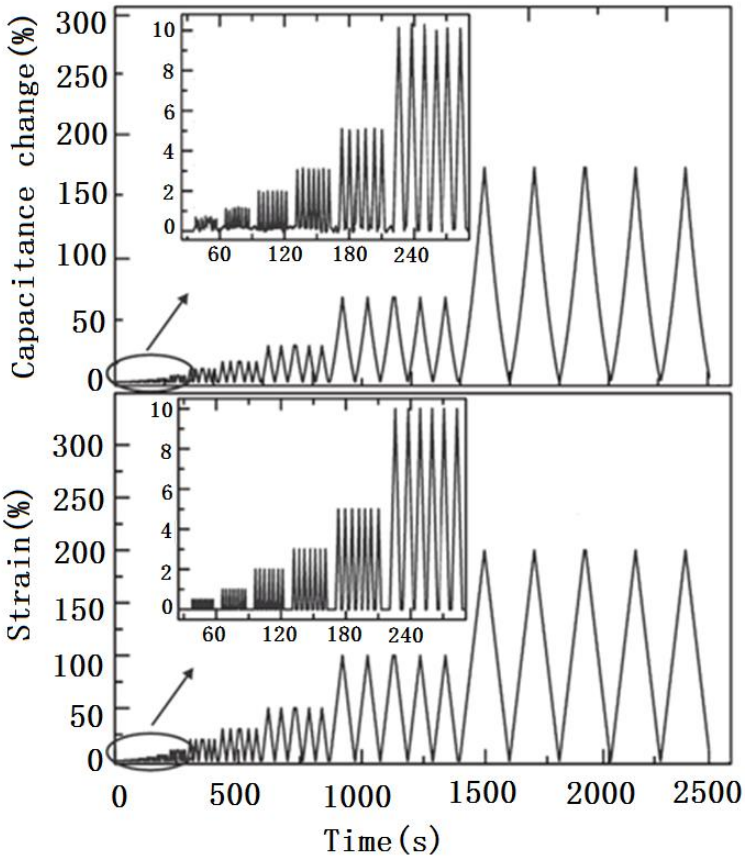

Fig.5-12 The capacitance change with time curve compared with strain-time curve of 25phr CCTO/SEBS capacitive strain sensor

In Fig.5-12 we can observe that the capacitance change with time and strain were synchronous. The capacitance changes was also at the same ratio compared with the strain rate, means the response of the sensor was linear and the gauge factor was about 1, which was mentioned by Cai. et.al in their report [151].

Fig.5-13 is showing the capacitance change of CCTO/SEBS capacitive strain sensor at different stretching rates. When the strain ratio is 100%, the peak to valley value was constantly about 55pF at different stretching rates, meaning the stability of

the sensor is not affected by the stretching rate. Fig.5-14 shows that the sensor could remain a synchronously signal output after 500 times of stretches, showing a fine reliability and reproducibility.

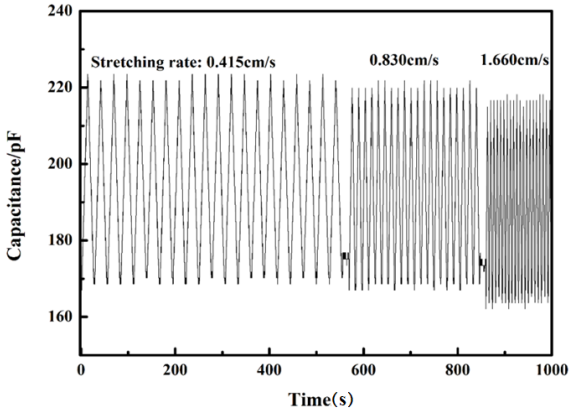

Fig.5-13 The capacitance-time curve of 25phr CCTO/SEBS capacitive strain sensor at different stretching rate

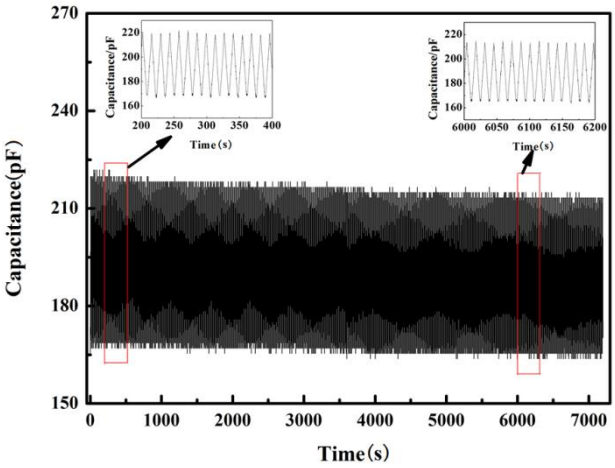

Fig.5-14 The capacitance-time curve of 25phr CCTO/SEBS capacitive strain sensor after 500 times of stretches

5.4 Conclusion

In this chapter, we prepared CCTO/SEBS dielectric elastomer via blending method and find the CCTO particles was well dispersed in composite through SEM and Raman spectra analyzing. The dielectric property tests showed that the composites filled with 25phr of CCTO have the permittivity enhanced by 70% with minor dielectric loss change. A capacitance strain sensor was fabricated by CCTO/SEBS dielectric elastomer and PANI/SEBS conductive elastomer through thermoforming method. The sensor have excellent signal response at different strain ratios and stretching rates, while remain functional after 500 times stretches.

Chapter.6 Conclusions

We focused on seeking a balance of the permittivity and modulus to improve the electrostriction properties of DEs. In order to avoid filling a large amount of dielectric materials, we synthesized high permittivity elastomer CCTO/PDMS via solution blend method.

Agglomeration of particles was observed while increasing the filling amount of CCTO. By modifying the surface of CCTO with organic materials, the particles will disperse better in elastomer matrix, which leads to a lower modulus. We synthesized Core-shell structured calcium copper titanate@polyaniline (CCTO@PANI) using a simple procedure involving in-situ polymerization of aniline in aqueous hydrochloric acid solution. The silicone elastomer (PDMS) filled with self-prepared CCTO@PANI composites had high dielectric constant, low dielectric loss, and actuated strains which was greatly improved at low electric field. Meanwhile, the elastic modulus of CCTO@PANI/PDMS composites was increased slightly only with a good flexibility.

Experiments result showed that sometimes samples filled with agglomerated particles have higher electrostrictive strain than the well dispersed ones. The strategies for designing dielectric elastomers with larger electro-deformations have been probed based on the existing theories and experimental results. The CCTO with smaller particle sizes

showed a larger dielectric parameter. With smaller CCTO particle as the fillings, the fabricated elastomer composite would approach to a low modulus by a proper CCTO phase morphology in the matrix. The result provided aneffective way to design CCTO/PDMS composite as a dielectric elastomer with a higher electro-deformation.

The electrode's flexibility is a main issue that limits the performance of DEs. Carbon grease will become unreliable for the solvent evaporation, causing increasing resistance after stretched. Conductive polymer can be applied as electrode, but CNT based conductive polymer usually can only endure a strain of 5%. Here we present a conductive elastomer using polyaniline (PANI) and styrene-ethylene-butylene-styrene block polymer (SEBS) via solution blending method. The conductive elastomer obtained has excellent conductivity and very good mechanical properties. This is the first conductive elastomer that can maintain conductivity while elongated to 600% strain in the world. Within 0-100% elongation range, the material's resistance showed linear increasing, and could be applied as electrodes for large strains.

Finally, we achieved a CCTO/SEBS dielectric elastomer through blending method and find the CCTO particles was well dispersed in composite through SEM and Raman spectra analyzing. The dielectric property tests showed that the composites filled with 25phr of CCTO have the permittivity enhanced by 70% with minor dielectric loss

change. A capacitance strain sensor was fabricated by CCTO/SEBS dielectric elastomer and PANI/SEBS conductive elastomer through thermoforming method. The sensor have excellent signal response at different strain ratios and stretching rates, while remain functional after 500 times stretches. We genuinely designed a capacitive stretchable strain sensor with easy process and low cost.

Publications

A. Papers

[a] YiYang Zhang, Yang Min, GenLin Wang, ZhiFeng Wang, Jun-Liang Liu, ZhiWei Luo, Ming Zhang*. Design and properties of Calcium Copper Titanate/Poly(dimethylsiloxane) dielectric elastomer composites, Rare Metals, 2017; DOI: 10.1007.(Accepted)

[b] YiYang Zhang, Jie Zhang, GenLin Wang, ZhiFeng Wang, ZhiWei Luo, Ming Zhang*, Manufacturing and characterizing of CCTO/SEBS dielectric elastomer as capacitive strain sensors. Rare Metals, 2017; DOI: 10.1007(Accepted)

[c] Yiyang Zhang*, Genlin Wang, Jie Zhang, Zhifeng Wang, Ming Zhang, Zhiwei Luo, Synthesis and static electrical characterizing of PANI/SEBS conductive polymer via solution blending method Material Letters, under review

[d] Yi Yang Zhang*, Gen Lin Wang, Jie Zhang, Zhi Feng Wang, Ming Zhang, Zhi Wei Luo, Preparation and dynamic analyze of PANI-SEBS conductive elastomer via solution blending method, Micro & Nano Letters, under review

B. International conferences

[e] Yiyang Zhang, Jie Zhang, Genlin Wang, Ming Zhang, Zhiwei Luo, “Preparation and characterizing of PANI/PDMS dielectric elastomer,” 5th Annual International Conference on Material Science and Environmental Engineering(MSEE)

Acknowledgements

Firstly, I would like to express my sincere appreciation to my advisor Prof. Luo Zhiwei for the continuous support of my study and related research, for his patience, motivation, and immense knowledge. I would like to thank you for encouraging my research and for allowing me to grow as a researcher. Your advice on both research as well as on my career have been priceless.

I would also to tank my committee members, Associate Professor Quan Changqin, Professor Zhang Ming, and all members of CS11, for their insightful comments and encouragement, but also for the hard question which incented me to widen my research from various perspectives.

My sincere thanks also goes to the polymer laboratory members in Yangzhou University, who gave access to the laboratory and assistance in experiments. Without their precious support it would be impossible to accomplish this research.

A special thanks to my family. Words cannot express how grateful I am to my mother and father for all of the sacrifices that you've made on my behalf. At the end I would like express appreciation to my beloved wife Ge Meng who spent sleepless nights with and was always my support in the moments when there was no one to answer my queries.

Reference

[1] O'Halloran.A, O'Malley.F, Mchugh.P. A review on dielectric elastomer actuators, technology, applications, and challenges[J]. Journal of Applied Physics, 2008, 104(7): 071101-071110.

[2] Chouinard.P, Plante.J. Bistable Antagonistic dielectric elastomer actuators for binary robotics and mechatronics[J]. IEEE/ASME Transactions on Mechatronics, 2012, 17(99): 1-9.

[3] Rogers.J, Huang.Y. Acurvy,stretchy future for electronics[J]. Proc. Natl. Acad. Sci. U. S.A. 2009, 106: 10875-10880.

[4] Wagner.S, Lacour.S, Jones.J, et al. Electronic skin: architecture and components[J]. Physica E: Low-dimensional Systems and Nanostructures, 2004, 25 (2-3): 326-334.

[5] Koh.S, Zhao.X, Suo.Z. Maximal energy that can be converted by a dielectric elastomer generator[J]. Applied Physics Letters, 2009, 94: 262902-262904.

[6] Brochu.P, Pei.Q.Advances in dielectric elastomers for actuators and artificial muscles[J]. Macromol. Rapid Commun, 2010, 31(1): 10-36.

[7] Zhao.X, Suo.Z. Electrostriction in elastic dielectrics undergoing large deformation[J]. Journal of Applied Physics, 2008, 104(12): 123530-123536.

[8] Liu.Y, Liu.L, Zhang.Z, et al. Analysis and manufacture of an energy harvester based on a Mooney-Rivlin-type dielectric elastomer[J]. Europhysics Letters, 2010, 90(3): 1303-1324.

[9] Anderson.I, Gisby.T, McKay.T, et al. Multifunctional dielectric elastomer artificial muscles for soft and smart machines [J]. Journal of Applied Physics, 2012, 112:041101-041120.

[10] Pelrine.R, Kornbluh.R, Joseph.J, et al. High-strain deformation of elastomeric dielectrics for actuators[J]. Materials Science & Engineering C, 2000, 11(2): 89-100.

[11] Pelrine.R, Kornbluh.R, Pei.Q, et al. High-speed electrically actuated elastomers with strain greater than 100%[J]. Science, 2000, 287(5454):836-839.

[12] Kofod.G, Kornbluh.R.D, Pelrine.R, et al. Actuation response of polyacrylate dielectric elastomers[C]. Spie's, International Symposium on Smart Structures and Materials. International Society for Optics and Photonics, 2001:787-793.

[13] Pelrine.R, Sommerlarsen.P, Kornbluh.R, Heydt.R, et al. Applications of dielectric elastomer actuators[C]. Proceedings of SPIE-The International Society for Optical

Engineering, 2001, 4329: 335-349.
[14] Shankar.R, Ghosh.T, Spontak.R. Dielectric elastomers as next-generation polymeric actuators[J]. Soft Matter, 2007, 3(9): 1116-1129.
[15] Potz.M, Artusi.M, Soleimani.M, et al. Rolling dielectric elastomer actuator with bulged cylindrical shape[J]. Smart Materials and Structures, 2010, 19: 127001-127005.
[16] Bar-Cohen.Y, Heydt.R, Kornbluh.R, et al. Sound radiation properties of dielectric elastomer electroactive polymer loudspeakers[J]. SmartStructures and Materials, 2006, 6168: 61681-61688.
[17] Hochradel.K, Rupitsch.S, Sutor.A, et al. Dynamic performance of dielectric elastomers utilized as acoustic actuators[J]. Applied Physics A, 2012, 107: 531-538.
[18] Aschwanden.M, Stemmer.A. Polymeric, electrically tunable diffraction grating based on artificial muscles[J]. Optics Letters, 2006, 31: 2610-2612.
[19] Biddiss.E, Chau.T. Dielectric elastomers as actuators for upper limb prosthetics: Challenges and opportunities[J]. Medical Engineering & Physics, 2008, 30: 403-418.
[20] Son.S, Goulbourne N. Dynamic response of tubular dielectric elastomertransducers[J]. International Journal of Solids and Structures, 2010, 47: 2672-2679.
[21] Mckay.T, O'Brien.B, Calius.E, et al. An integrated, self-priming dielectric elastomer generator[J]. Applied Physics Letters, 2010, 97(6): 148-155.
[22] Mckay.T, Obrien.B, Calius.E, et al. Soft generators using dielectric elastomers[J]. Applied Physics Letters, 2011, 98(14):142903-142906.
[23] Pelrine.R, Kornbluh.R, Joseph.J. Electrostriction of polymer dielectrics with compliant electrodes as a means of actuation[J]. Sensors & Actuators A Physical, 1998, 64(64): 77-85.
[24] Bar-Cohen.Y, Electroactive Polymer Actuators as Artificial Muscles: Reality, Potential, and challengers[M]. Von Karman Auditorium Lecture Series 2002.
[25] Kim.K, Tadokoro.S. Electroactive Polymers for Robotic Applications: Artificial Muscles and Sensors[M]. London, UK: Springer,2007.
[26] Kornbluh.R. Dielectric elastomer artificial muscle for actuation, sensing, generation, and intelligent structures[J]. 2004, 19(4): 216-224.
[27] Mirfakhrai.T, Madden.J, Baughman.R. Polymer artificial muscles[J]. Materials Today, 2007, 10(4): 30-38.
[28] Pei.Q, Pelrine.R, Stanford.S, et al. Electroelastomer rolls and their application for

biomimetic walking robots[J]. Synthetic Metals, 2003, 135: 129-131.
[29] Löwe.C, Zhang.X, Kovacs.G. Dielectric Elastomers in Actuator Technology[J]. Advanced Engineering Materials, 2010, 7(7): 361-367.
[30] Wissler.M, Mazza.E. Modeling of a pre-strained circular actuator made of dielectric elastomers[J]. Sensors & Actuators A Physical, 2005, 120(1): 184-192.
[31] Choi.H, Jung.K, Chuc.N, et al. Effects of prestrain on behavior of dielectric elastomer actuator[C]. Smart Structures and Materials. International Society for Optics and Photonics, 2005: 283-291.
[32] Li.B, Chen.H, Qiang.J, et al. Effect of mechanical pre-stretch on the stabilization of dielectric elastomer actuation[J]. Journal of Physics D: Applied Physics, 2011,44(15): 155301-155308.
[33] Suo.Z. Theory of dielectric elastomers[J]. Acta Mechanica Solida Sinica, 2010, 23(6): 549-578.
[34] Pharr.M, Sun.J, SuoZ. Rupture of a highly stretchable acrylic dielectric elastomer[J]. Journal of Applied Physics, 2012, 111(10): 104114-104117.
[35] He.T, Zhao.X, Suo.Z. Dielectric elastomer membranes undergoing inhomogeneous deformation[J]. Journal of Applied Physics, 2009, 106(8): 083522-083528.
[36] Zhao.X, Suo.Z. Method to analyze electromechanical stability of dielectric elastomers[J]. Applied Physics Letters, 2007, 91(6): 061921-061922.
[37] Zhao.X, Suo.Z. Theory of dielectric elastomers capable of giant deformation of actuation[J]. Physical Review Letters, 2010, 104(17): 178302-178303.
[38] Park.I, Kim.K, Nam.J, et al. Mechanical, dielectric, and magnetic properties of the silicone elastomer with multi-walled carbon nanotubes as a nanofiller[J]. Polymer Engineering & Science, 2007, 47(9): 1396-1405.
[39] Pötschke.P, Dudkin.S, Alig.I. Dielectric spectroscopy on melt processed polycarbonate-multiwalled carbon nanotube composites[J]. Polymer, 2003, 44(17): 5023-5030.
[40] Dang.Z, Wang.L, Yin.Y, et al. Giant dielectric permittivities in functionalized carbon-nanotube/electroactive-polymer nanocomposites[J]. Advanced Materials, 2007, 19(6): 852-857.
[41] Underhill.R, Michalchuk.B. Carbon nanotube-elastomer composites for use in dielectric polymer actuators[C]. Mems, Nano and Smart Systems, 2005. Proceedings. 2005 International Conference on. IEEE, 2005: 369-370.
[42] Liu.H, Zhang.L, Yang.D, et al. Mechanical, Dielectric, and Actuated Strain of Silicone Elastomer Filled with Various Types of TiO_2[J]. Soft Materials, 2013, 11(3): 363-370.

[43] Yang.D, Tian.M, Kang.H, et al. New polyester dielectric elastomer with large actuated strain at low electric field[J]. Materials Letters, 2012, 76(6): 229-232

[44] Yang.D, Tian.M, Dong.Y, et al. Disclosed dielectric and electromechanical properties of hydrogenated nitrile–butadiene dielectric elastomer[J]. Smart Materials & Structures, 2012, 21(3):035017-035022.

[45] Liu.H, Zhang.L, Yang.D, et al. A new kind of electro-active polymer composite composed of silicone elastomer and polyethylene glycol[J]. Journal of Physics D Applied Physics, 2012, 45(48):485303-485311.

[46] Vucong.T, Jeanmistral.C, Sylvestre.A. Impact of the nature of the compliant electrodes on the dielectric constant of acrylic and silicone electroactive polymers[J]. Smart Materials & Structures, 2012, 21(10): 5036-5045.

[47] Carpi.F, Gallone.G, Galantini.F, et al. Silicone-Poly(hexylthiophene) Blends as Elastomers with Enhanced Electromechanical Transduction Properties[J]. Advanced Functional Materials, 2010, 18(18): 235-241.

[48]Liu.Y, Leng.J, Zhang.Z. New silicone dielectric elastomers with a high dielectric constant[C]. Proc. SPIE, 2008, 6926: 1-8.

[49] Zhao.H, Xia.Y, Dang.Z, et al. Composition dependence of dielectric properties, elastic modulus, and electroactivity in (carbon black-$BaTiO_3$)/silicone rubber nanocomposites[J]. Journal of Applied Polymer Science, 2013, 127(6): 4440-4445.

[50] Dang.Z, Xia.B, Yao.S, et al. High-dielectric-permittivity high-elasticity three-component nanocomposites with low percolation threshold and low dielectric loss[J]. Applied Physics Letters, 2009, 94(4): 042902-042905.

[51] Carpi.F, Rossi.D. Improvement of electromechanical actuating performances of a silicone dielectric elastomer by dispersion of titanium dioxide powder [J]. IEEE Transactions on Dielectrics and Electrical Insulation, , 2005, 12(4): 835-843.

[52] Ouyang.G, Wang.K, Chen.X. TiO_2 nanoparticles modified polydimethylsiloxane with fast response time and increased dielectric constant[J]. Journal of Micromechanics & Microengineering, 2012, 22(7): 74002-74010.

[53] Mathew.G, Rhee.J, Nah.C, et al. Effects of silicone rubber on properties of dielectric acrylate elastomer actuator[J]. Polymer Engineering & Science, 2006, 46(10): 1455-1460.

[54] Tangboriboon.N, Datsanae.S, Onthong.A, et al. Electromechanical responses of dielectric elastomer composite actuators based on natural rubber and alumina[J]. Journal of Elastomers & Plastics, 2013, 45(45): 143-161.

[55] Liu.S, Tian.M, Yan.B, et al. High performance dielectric elastomersby partially reduced graphene oxide and disruption of hydrogen bonding of polyurethanes[J].

Polymer, 2015, 56: 375-384.
[56] Jung.K, Lee.J, Cho.M, et al. Development of enhanced synthetic rubber for energy efficient polymer actuators[J]. Smart Materials & Structures, 2006, 6168(2):61680-61689.
[57] Liu.Y, Liu.L, Zhang.Z, et al. Dielectric elastomer film actuators: characterization, experiment and analysis[J]. Smart Materials & Structures, 2009, 18(9): 95024-95010.
[58] Wingert.A, Lichter.M, Dubowsky.S. On the design of large degree-of-freedom digital mechatronic devices based on bistable dielectric elastomer actuators[J]. IEEE/ASME Transactions on Mechatronics, 2006, 11(4): 448-456.
[59] Lochmatter.P, Kovacs.G, Ermanni.P. Design and characterization of shell-like actuators based on soft dielectric electroactive polymers[J]. Smart Materials and Structures, 2007, 16(4): 1415-1422.
[60] Kovacs.G, Düring.L, Michel.S, et al. Stacked dielectric elastomer actuator for tensile force transmission[J]. Sensors and Actuators A: Physical, 2009, 155(2): 299-307.
[61] Carpi.F, Salaris.C, Derossi.D. Folded dielectric elastomer actuators[J]. Smart Materials & Structures, 2007, 16(2): 300-305.
[62] Kofod.G, Paajanen.M, Bauer.S. Self-organized minimum-energy structures for dielectric elastomer actuators[J]. Applied Physics A, 2006, 85(2): 141-143.
[63] Khodaparast.P, Ghaffarian.S, Khosroshahi.M, et al. Electrode structures in high strain actuator technology[J]. Journal of Optoelectronics and Advanced Materials, 2007, 9(11): 3585-3591.
[64] Benslimane.M, Gravesen.P, Sommer.P. Mechanical properties of dielectric elastomer actuators with smart metallic compliant electrodes[C]. SPIE's 9th Annual International Symposium on Smart Structures and Materials. International Society for Optics and Photonics, 2002: 150-157.
[65] Carpi.F, Chiarelli.P, Mazzoldi.A, et al. Electromechanical characterization of dielectric elastomer planar actuators: comparative evaluation of different electrode materials and different counterloads[J]. Sensors & Actuators A Physical, 2003, 107(1):85-95.
[66] Li.C, Thostenson.E.T, Chou.T, Sensors and actuators based on carbon nanotubes and their composites: A review[J]. Composites Science and Technology, 2008, 68, 1227–1249
[67] Okamoto.Y, Brenner.W, Organic Semiconductors[M], Reinhold 1964.
[68] Cochrane.C, Koncar.V, M.Lewandowski, C.Dufour, Design and Development of a

Flexible Strain Sensor for Textile Structures Based on a Conductive Polymer Composite[J]. Sensors. 2007,7 ,473-492.

[69] Silva.M.J, Sanches.A.O, Malmonge.L.F, Malmonge.J.A. Electrical, Mechanical, and Thermal Analysis of Natural Rubber/Polyaniline-Dbsa Composite[J]. Materials Research, 2014,17 59-63.

[70] Massoumi.B, Farjadbeh.F, Mohammadi.R and Entezami.A.A, Synthesis of conductive adhesives based on epoxy resin/nanopolyaniline and chloroprene rubber/nanopolyaniline: Characterization of thermal, mechanical and electrical properties[J]. Journal of Composite Materials. 2012, 47, 9,1185–1195

[71] Amjadi.M, Kyung.K, Park.I, Sitti.M. Stretchable, skin-mountable, and wearable strain sensors and their potential applications: a review[J]. Advanced Functional Materials. 2016;26,11:1678-1698.

[72] Cohen.D.J, Mitra.D, Peterson.K, Maharbiz.M.M. A highly elastic, capacitive strain gauge based percolating nanotube network[J]. Nano Lett. 2012;12:1821-1845.

[73] Trung.T.Q, Lee.N.E. Flexible and stretchable physical sensor integrated platforms for wearable human-activity monitoring and personal healthcare[J]. Adv.mater. 2016;28:4338-4372.

[74] Shi.G, Zhao.Z, Pai.J, Lee.L, Zhang.L, Stevenson.C, Ishara.K, Zhang.R, Zhu.H, Ma.J. Highly sensitive, wearable, durable strain sensors and stretchable conductors using graphene/silicon rubber composites[J]. Adv.Funct.Mater. 2016;26:7614-7625.

[75] Zheng.Y, Li.Y, Dai.K, Liu.M, Zhou.M, Zheng.G, Liu.C, Shen.C. Conductive thermoplastic polyurethane composites with tunable piezoresistivity by modulating the filler dimensionality for flexible strain sensors[J]. Composites: Part A. 2017;101:41-49.

[76] Gong.X, Fei.G, Fu.W, Fang.M, Gao.X, Zhong.B, Zhang.L. Flexible strain sensor with high performance based on PANI/PDMS films[J]. Organic Electronics. 2017;47:51-56.

[77] Amjadi.M, Pichitpajongkit.A, Ryu.S, Korea.I. Piezoresistivity of Ag NWS-PDMS nanocomposite[C]. In 2014 IEEE 27th International Conference on Micro Electro Mechanical Systems (MEMS) 26-30 Jan 2014:785-788.

[78] Kollosche.M, Stoyanov.H, Laflamme.S, Kofod.G. Strongly enhanced sensitivity in elastic capacitive strain sensors[J]. J Mater Chem. 2011;21:8292-8294.

[79] Babu.S, Singh.K, Govindan.A. Dielctric properties of CaCu3Ti4O12-silicone resin composites[J]. Appl Phys A. 2012;107:697-700.

[80] Goel P, Singh JP. Fabrication of silver nanorods embedded in PDMS film and its application for strain sensing[J]. J Phys D: Appl Phys. 2015;48,44:445303.

[81] Amjadi.M, Pichitpajongkit.A, Lee.S, Ryu.S, Park.I. Highly stretchable and sensitive strain sensor based on silver nanowire-elastomer nanocomposite. ACS Nano. 2014;8:5154.

[82] Froulich.H Theory of Dielectrics: Dielectric Constant and Dielectric Loss[M]. Clarendon Pr, 1987.

[83] Illingworth.V, The Penguin Dictionary of Physics[M], Penguin Books, London, 1991

[84] Lines.M.E, Glass.A.M, Principles and Applications of Ferroelectrics and Related Materials[M].Clarendon, Oxford, 1977

[85] Wallace.D.C, Thermodynamics of Crystals[M], Wiley, New York, 1972,Chap. 1.

[86] D.Sun, A.Wu, S.Yin. Structure, Properties, and Impedance Spectroscopy of $CaCu_3Ti_4O_{12}$ Ceramics Prepared by Sol–Gel Process [J].Am. Ceram.Soc. 2008, 91,(1) 169-173

[87] Carpi.F, Rossi.D. Dielectric elastomer cylindrical actuators: electromechanical modelling and experimental evaluation[J]. Materials Science & Engineering C, 2004, 24(4):555-562.

[88] Zhang.Q, Su.J, Kim.C, et al. An experimental investigation of electromechanical responses in a polyurethane elastomer[J]. Journal of Applied Physics, 1997, 81(6): 2770-2776.

[89] Ueda.T, Kasazaki.T, Kunitake.N, et.al. Polyurethane elastomer actuator[J]. Synthetic Metals, 1997, 85(1-3): 1415-1416.

[90] Fukuda.T, Luo, Ito.A. Development of Dielectric Elastomer Actuators Part I : Performance of Polyurethane Film Actuators with Dangling Chains and Network Structures[J]. Advanced Materials Research. Vol. 557. Trans Tech Publications, 2012.1852-1856

[91] Fukuda.T, Luo, Ito.A. Development of Dielectric Elastomer Actuators Part II : Preparation of the High Dielectric Constant Film Actuators Containing $BaTiO_3$ Particles[J]. Advanced Materials Research. Vol. 557. Trans Tech Publications, 2012.1869-1874

[92] Park.E et.al. Morphology, mechanical, and dielectric breakdown properties of PBT/PET/TPE, PBT/PET/PA66, PBT/PET/LMPE, and PBT/PET/TiO_2 blends[J]. Polymer Composites, 2008, 29(10): 1111-1118.

[93] Sengers.W, Wübbenhorst.M, Picken.S, et al. Distribution of oil in olefinic thermoplastic elastomer blends[J]. Polymer, 2005, 46(17): 6391-6401.

[94] Ha.S, Yuan.W, Pei.Q, et al. Interpenetrating networks of elastomers exhibiting 300% electrically-induced area strain[J]. Smart Materials and Structures, 2007,

16(2): S280-S287.
[95] Kornbluh.R, Pelrine.R, Pei.Q, et al. Ultrahigh strain response of field-actuated elastomeric polymers[C]. SPIE's 7th Annual International Symposium on Smart Structures and Materials. International Society for Optics and Photonics, 2000: 51-64.
[96] Plante.J, Dubowsky.S. On the performance mechanisms of dielectric elastomer actuators[J]. Sensors and Actuators A: Physical, 2007, 137(1): 96-109.
[97] Ha.S, Park.I, Wissler.M, et al. High electromechanical performance of electroelastomers based on interpenetrating polymer networks[C]. The 15th International Symposium on: Smart Structures and Materials & Nondestructive Evaluation and Health Monitoring. International Society for Optics and Photonics, 2008: 69272-69280.
[98] Zhang.X, Wissler.M, Jaehne.B, et.al. Effects of crosslinking, prestrain, and dielectric filler on the electromechanical response of a new silicone and comparison with acrylic elastomer[C]. Smart Structures and Materials. International Society for Optics and Photonics, 2004: 78-86
[99] Kornbluh.R, Pelrine.R, Prahlad.H, et al. Silicon to silicone: stretching the capabilities of micromachines with electroactive polymers[J]. IEEE Transactions on Sensors & Micromachines, 2004, 124(8):266-271.
[100] Johansson.C, Robertsson.M. Broadband dielectric characterization of a silicone elastomer[J]. Journal of Electronic Materials, 2007, 36(9): 1206-1210.
[101] Efros,A.L, Shklovskii.B.I, Critical Behaviour of Conductivity and Dielectric Constant near the Metal-Non-Metal Transition Threshold[J]. Phys. Status Solidi B.1976, 76: 475–485.
[102] Zhang.Q, Bharti.V, Zhao.X, Giant electrostriction and relaxor ferroelectric behavior in electron-irradiated poly(vinylidene fluoride-trifluoroethylene) copolymer[J] Science. 1998, 280(5372), pp.2101-2104.
[103] Sarban.R, Jones.R.W, Mace.B.R, Rustighi.E, A tubular dielectric elastomer actuator: Fabrication, characterization and active vibration isolation, M.S.S.P. 2011, Vol.25, pp.2879-2891,.
[104] Choi.H.R, Jung.K, Ryew.S, Nam.J.D, Jeon.J, Koo.J.C, Tanie.K, Biomimetic soft actuator: design, modeling, control, and applications, IEEE/ASME Trans. Mechatron. 2005,10,6, pp581-593,.
[105] F.Carpi, D.Rossi, D.Kornbluh, R.Pelrine, R.E.Sommer-Larsen.P, Dielectric elastomer as electromechanical transducers: Fundamentals, materials, devices, models and applications of an emerging electroactive polymer technology,

2011,Elsevier.
[106] G. Wang, Y. Zhang, L. Duan, K. Ding, Z. Wang, M. Zhang, Property reinforcement of silicone dielectric elastomers filled with self-prepared calcium copper titanate particles, J.Appl.Polym.Sci. 2015,132,42613(6pp).
[107] L. Duan, G. Wang, Y. Zhang, Y. Zhang, Y. Wei, Z. Wang, M. Zhang, High Dielectric and Actuated Properties of Silicone Dielectric Elastomers Filled with Magnesium-Doped Calcium Copper Titanate Particles, Polymer Composites. 2016, Vol.10, 1002,(7pp)
[108] G. Wang, Y. Zhang, L. Duan, K. Ding, Z. Wang, M. Zhang, Preparation of π–conjugated truxene/silicone dielectric elastomers with large actuated strain at low electric field, Mater. Lett. 2016,Vol.169, pp.157-159.
[109]Zhang C H, Hu Z, Gao G, et al. Damping behavior and acoustic performance of polyurethane/lead zirconate titanate ceramic composites[J]. Materials & Design, 2013, 46(4):503-510.
[110] Davtyan S P, Tonoyan A O, Hayrapetyan S M, et al. A note on the peculiarities of producing of high-temperature super-conducting polymer–ceramic composites[J]. Journal of Materials Processing Technology, 2005, 160(3):306-312.
[111]Chen. Q, Hong. R.Y. Fabrication and characterization of Ba0.5Sr0.5TiO3-PANI/PS three-phase composites [J]. Ceramics International, 2015, 41(2):2533-2542.
[112] Chen. Q, He Q, Lv M, et al. The vital role of PANI for the enhanced photocatalytic activity of magnetically recyclable N–K2Ti4O9/MnFe2O4/PANI composites[J]. Applied Surface Science,2014,311(9):230-238.
[113] Shen.Y, Zhao.Q, Li.X, et.al. Enhanced visible-light induced degradation of benzene on Mg-ferrite/hematite/PANI nanospheres: In situ, FTIR investigation[J]. Journal of Hazardous Materials, 2012, 241–242(1):472-477.
[114] Thomas.P, Dwarakanath.K, Varma.K.B.R. In situ synthesis and characterization of polyaniline-$CaCu_3Ti_4O_{12}$,nanocrystal composites[J]. Synthetic Metals, 2013, 159:2128-2134.
[115] Witt.N, Tang.Y, Ye L, et al. Silicone rubber nanocomposites containing a small amount of hybrid fillers with enhanced electrical sensitivity[J]. Materials & Design, 2013, 45:548-554.
[116] Sharma.S.K, Gaur.H, Kulkarni.M, et.al. PZT–PDMS composite for active damping of vibrations[J]. Composites Science & Technology, 2013, 77:42-51.
[117] Li.Y, Verbiest.T, Vankelecom.I. Improving the flux of PDMS membranes via localized heating through incorporation of gold nanoparticles[J]. Journal of

Membrane Science, 2013, 428:63–69.
[118] Yang.D, Zhang.L, Liu.H, et.al. Lead magnesium niobate-filled silicone dielectric elastomer with large actuated strain[J]. Journal of Applied Polymer Science, 2012, 125(3):2196–2201.
[119]Romasanta.L.J, Leret.P, Casaban.L, Hernández.M, Rubia.M.A, Fernández.J.M, Kenny.J.M, Lopez-Manchado.M.A, Verdejo.R, J. Towards materials with enhanced electro-mechanical response: $CaCu_3Ti_4O_{12}$–polydimethylsiloxane composites[J]. Mater. Chem. 2012, 22, 24705-24712.
[120] Xie.G, Xi.P, Liu.H, Chen.F, Huang.L, Shi.Y, Wang.J. A facile chemical method to produce superparamagnetic graphene oxide–Fe_3O_4 hybrid composite and its application in the removal of dyes from aqueous solution[J]. Journal of Materials Chemistry, . 2012.22(3), 1033-1039.
[121] Kim.J, Kwon.S, Ihm.D, Synthesis and characterization of organic soluble polyaniline prepared by one-step emulsion polymerization[J]，Current Applied Physics. 2007,7, 205–210
[122] Stroud.D, Generalized effective-medium approach to the conductivity of an inhomogeneous material[J]. 1975, Phys. Rev. B. 12, 8: 3368-3373
[123] Weiglhofer.W.S., Lakhtakia,A., Michel.B, Maxwell Garnett and Bruggeman formalisms for a particulate composite with bianisotropic host medium[J]., Microw. Opt. Thechnol. Lett. 1998,15,4: 263-266
[124] Tian.M, Li.M, Li.J Effect of size on dielectric constant for low dimension materials[J]. Physica B 2011; 406, 541–544
[125] Almeida.A.F.L, Fechine.P, Góes.J.C, et al. Dielectric properties of BaTiO3, (BTO)–$CaCu_3Ti_4O$~~12~~, (CCTO) composite screen-printed thick films for high dielectric constant devices in the medium frequency (MF) range[J]. Materials Science & Engineering B, 2004, 111(2-3):113-123.
[126] Yang.C, Song.H, Liu.D. Effect of coupling agents on the dielectric properties of $CaCu_3Ti_4O_{12}$/PVDF composites[J].Composites Part B Engineering, 2013, 50(1):180–186.
[127] Xuan.S, Wang.Y, Leung.C, et.al. Synthesis of Fe_3O_4@Polyaniline Core/Shell Microspheres with Well-Defined Blackberry-Like Morphology[J]. Journal of Physical Chemistry C, 2013, 112(48):18804-18809.
[128] Zhao.H, Zhang.L, Yang.M, Dang.Z, Temperature-dependent electro-mechanical actuation sensitivity in stiffness-tunable $BaTiO_3$/polydimethylsiloxane dielectric elastomer nanocomposites[J].Appl. Phys. Lett. 2015, 106, 092904.
[129]Böse.H, Uhl.D, Flittner.L, Schlaak.H, Dielectric elastomer actuators with

enhanced permittivity and strain[J] Proc. SPIE 2011, 7976, 79762 J

[130]Yang.Y, Gupta.M.C, Dudley.K.L, Lawrence.R.W, Novel Carbon Nanotube Polystyrene Foam Composites for Electromagnetic Interference Shieldin[J]., Nano Lett.2005, 5,11, 2131–2134

[131]Isaji.S, Bin.Y, Matsuo.M, Electrical and self-heating properties of UHMWPE-EMMA-NiCF composite films[J], Journal of Polymer Science. 2009, 47, 1253–1266

[132]Yamada.S, Hayamizu.Y, Yamamoto.Y, Yomogida.Y, Najafabadi.A.I, Futaba.D.N, Hata.K, A stretchable carbon nanotube strain sensor for human-motion detection[J], Nature Nanotechnology. 2011, 6 296–301

[133]Pham.G.T, Park.Y, Liang.Z, Zhang.C, Wang.B, Processing and modeling of conductive thermoplastic/carbon nanotube films for strain sensing[J], Composites,2008, Part B 39,209–216

[134]Zhang.Z, Liao.Q,Zhang.X,Zhang.G, Li.P, Lu.S, Liua.S, Zhang.Y, Highly efficient piezotronic strain sensors with symmetrical Schottky contacts on the monopolar surface of ZnO nanobelts[J], Nanoscale. 2015, **7** ,1796-1801

[135] Dietrich.S; Anthony.A, Introduction to Percolation Theory[M] , CRC Press, 1994.

[136] Kollosche.M, Stoyanov.H, Laflamme.S,Kofod.G. Strongly enhanced sensitivity in elastic capacitive strain sensors[J]. Journal of Materials Chemistry, 2011;21(23), 8292-8294.

[137] Barra.G.M, Jacques.L.B., Oréfice.R.L., Carneiro.J.R. Processing, characterization and properties of conducting polyaniline-sulfonated SEBS block copolymers[J]. European polymer journal, 2004;40(9), 2017-2023.

[138] Stoyanov.H, Kollosche.M, Risse.S, Wache.R, Kofod.G. Soft conductive elastomer materials for stretchable electronics and voltage controlled artificial muscles. Advanced Materials. 2013;25:578.

[139] Zhou.X, Xie.X, Zeng,F, Li.R,, Mai.Y. Properties of polypropylene/carbon nanotube composites compatibilized by maleic anhydride grafted SEBS[J]. Key Engineering Materials, Trans Tech Publications 2006,312, 223-228..

[140] Rana.U, Nambissan.P.M, Malik,S, Chakrabati.K, Effects of process parameters on the defects in graphene oxide-polyaniline composites investigated by positron annihilation spectroscopy[J], Phys.Chem.Chem.Phys., 2014,16, 3292-3298

[141] Xia.W, Pang.S, Yang.J, Fan.Y. Structure and properties of SEBS/PP/OMMT nanocomposites[M]. Transactions of Nonferrous Metals Society of China. 2006;16:s524-s528.

[142] Calisi.N, Giuliani.A, Alderighi.M, Schnorr.J.M, Swager.T.M, Francesco.F.D,

Pucci.A. Factors affecting he dispersion of MWCNTs in electrically conducting SEBS nanocomposites[J]. European Polymer Jouranl. 2013;46,6,1471-1478.

[143] Kim.M, Hong.S, Koo.C. Electric actuation properties of SEBS/CB and SEBS/SWCNT nanocomposite films with different conductive fillers[J]. Macromol Res. 2012;20,1:59-65.

[144] Duan.L, Wang.G, Zhang.Y, Zhang.Y, Wei.Y, Wang.Z, Zhang.. High dielectric and actuated properties of silicone dielectric elastomers filled with magnesium-doped calcium copper titanate particles[J]. Polymer composites. 2016; doi:10.1002 pc.2398.

[145] Li.T, Chen.J, Dai.H, Liu.D, Xiang.H, Chen.Z. Dielectric properties of $CaCu_3Ti_4O_{12}$-silicone rubber composites[J]. J Mater Sci: Mater Electron. 2015;26:312.

[146] Torabi.S, Cherry.M, Duijnstee.E, Corre.V.M.L, Qiu.L, Hummelen.J.C, Palasantzas.G, Koster.L.J.A. Rough electrode creates excess capacitance in thin-film capacitors[J]. ACS Apple Mater Interfaces. 2017;9:27290-27297.

[147] Pham.G.T, Park.Y, Liang.Z, Zhang.Z, Wang.B, Processing and modeling of conductive thermoplastic/carbon nanotube films for strain sensing[J], Composites, Part B. 2008;39:209-216.

[148] Rogers.J, Someya.T, Huang.Y. Materials and mechanics for stretchable electronics[J]. Science. 2010;327: 1603-1607

[149] Rogers.J , Huang.Y. A curvy, stretchy future for electronics[J]. Proc. Natl. Acad. Sci. USA 2009; 106:10875-10876.

[150] Yu.Z, Zhang.Q , Li.L, Chen.Q , Niu.X , Liu.J , Pei.Q, Highly flexible silver nanowire electrodes for shape-memory polymer light-emitting diodes[J]. Adv. Mater. 2011; 23: 664-668.

[151] Cai.L, Song.L, Luan.P, Zhang.Q, Zhang.N, Gao.Q, Zhao.D, Zhang.X, Tu.M, Yang.F, Super-stretchable, transparent carbon nanotube-based capacitive strain sensors for human motion detection[J] .Sci. Rep.2013,3,3048

[152] Shin.U, Jeong.D, Park.S, Kim.S, Lee.H, Kim.J, Highly stretchable conductors and piezocapacitive strain gauges based on simple contact-transfer patterning of carbon nanotube forests[J]. Carbon 2014,80,396-404 .

[153] Cohen.D.J, Mitra.D, Peterson.K, Maharbiz.M, A Highly Elastic, Capacitive Strain Gauge Based on Percolating Nanotube Networks[J]. Nano Lett.2012,12,1821-1825.

Doctor Thesis, Kobe University
“Development of Electroactive Polymers and It’s Applications”, 126 pages
Submitted on January, 26th, 2018
The date of publication is printed in cover of repository version published in Kobe University Repository Kernel.